• TECHNICAL REPORTS NO. 1 •

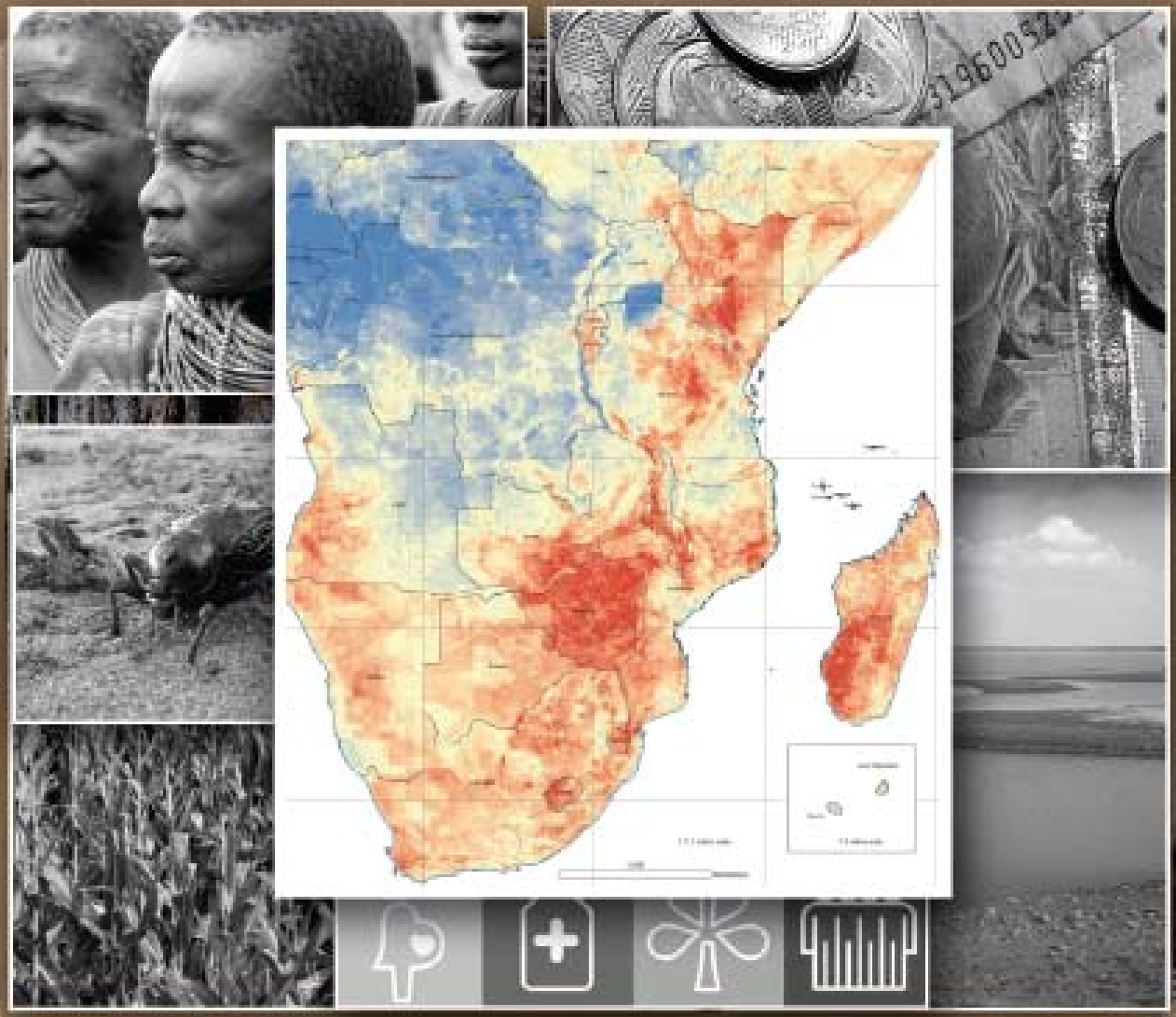

Climate Risk and Vulnerability Mapping for Southern Africa

STATUS QUO (2008) AND FUTURE (2050)

December 2010

SOUTHERN AFRICA
REGIONAL CLIMATE CHANGE PROGRAMME
Building resilience. Securing equity.

Climate Risk and Vulnerability Mapping for Southern Africa

STATUS QUO (2008) AND FUTURE (2050)

DECEMBER 2010

R.A.G. DAVIES, S.J.E. MIDGLEY AND S. CHESTERMAN

TECHNICAL REPORTS NO. 1

oneWORLD
We build resilient futures

Regional Climate Change Programme: Southern Africa
For the Department for International Development
CNTR 200607514

Cape Town, South Africa, November 2010
info@oneworldgroup.co.za
www.rccp.org.za
www.oneworldgroup.co.za

DISCLAIMER: This material has been funded by UKaid from the Department for International Development. However, the views expressed do not necessarily reflect the Department's official policies.

AUTHORS: R.A.G. Davies, S.J.E. Midgley and S. Chesterman

ACKNOWLEDGEMENTS:
For Phase 1, the following people are thanked: Michelle Wienhold completed metadata on all the data sources for the geodatabase. Andy Nelson and Uwe Deichmann kindly directed us to the best available datasets on human population density in Africa, and access to markets (traveltime) data. Nishadi Eriyagama of the International Water Management Institute in Sri Lanka (IWMI) very kindly supplied the summarised data for the coefficient of variation in inter-annual rainfall and this saved us many grid manipulations. Theo Kleynhans and Anton Kunneke from the Faculty of AgriSciences at Stellenbosch University helped us with useful contact information and data sources.

For Phase 2, the following people are thanked: Data for irrigation potential were kindly supplied by Liang You of IFPRI. Copenhagen University provided a dataset showing taxa richness patterns for 4144 vertebrate species across Sub-Saharan Africa. Neil Burgess of WWF kindly provided comparable data on vertebrate taxa richness in Madagascar and other unrepresented areas. For the forest loss analysis, we thank Dr Valerie Kapos at WCMC and Dr Matthew Hansen at Geographic Information Science Center of Excellence – SDSU for their assistance.

Advice on the choice of GCMs and scenario used for the rainfall projections was given by Dr Guy Midgley (SANBI, South Africa), Dr Carlo Buontempo (Meteorological Office Hadley Centre, UK) and Dr Geert Jan van Oldenborgh (Royal Netherlands Meteorological Institute KNMI). Dr van Oldenborgh also generously provided advice on the extraction of datasets from the Climate Explorer website. We are very grateful to Drs Philip Thornton, Peter Jones and colleagues (ILRI, Kenya) for allowing us to incorporate their findings on projected losses in crop production areas.

Table of Contents

1. Executive Summary

As part of the Regional Climate Change Programme (RCCP) for Southern Africa, we carried out a geographic climate change risk and vulnerability 'hotspot' analysis. This GIS-based project set out to explore where current and future climate stressors have the greatest impact within the SADC (Southern Africa Development Community) region, and how adaptive capacity could shape the vulnerability of communities.

We gathered the best available geo-referenced data for 51 variables within the following three categories: Adaptive Capacity (19 data layers), Sensitivity (16 data layers), and Exposure to climate risk. The Exposure and Sensitivity categories together comprise the potential impact of such risks ('problem areas'), and this combined with the capacity to manage and respond to those risks (Adaptive Capacity) comprises vulnerability, with the most vulnerable areas termed 'hotspots'.

We conducted a two-phased analysis, the first for the current situation ('status quo', ca. 2008) and the second for the mid-term future (ca. 2050). For the former, we developed an Exposure category (8 data layers) reflecting current and recent historical exposure to climate-related stressors. We conducted weighted overlay analyses of the three category layers at 1km^2 resolution across the SADC region and extending outward with transboundary drainage basins. We present the results as summary layers for each category and, once identified, by hotspot location.

For the futures (2050) analysis, we added projected climate and population changes (8 new data layers) to the existing Exposure category (thus giving 16 data layers) which was combined with the other categories as previously to identify problem areas and vulnerability.

We found that the most sensitive regions follow the Afro-montane belt and include the smaller countries of Lesotho, Zimbabwe, Swaziland and Malawi, followed by South Africa, Tanzania, Zambia and parts of Madagascar. Areas currently (2008) most exposed to climate risk follow the eastern seaboard where droughts, floods and cyclones occur regularly, but more arid regions towards the west are also exposed to risk. This results in a broad latitudinal band of high exposure across the sub-tropics (ca. 12-25°S). When sensitivity is combined with exposure in a single layer, Swaziland, Lesotho, Zimbabwe and Malawi contain the 'highest impact' areas, followed by parts of Madagascar, Mozambique, Zambia and Tanzania. By contrast, stable and humid environments translate into lower impact in the Congo Basin (Democratic Republic of the Congo) extending into eastern Angola.

SADC countries vary greatly in their capacity for adaptation to climate variability and change, and when we applied this factor (to give an indication of vulnerability) there was clear separation between areas where countries have higher capacity (particularly Mauritius, South Africa, Botswana and Namibia), and others with much lower adaptive capacity. Mozambique, Madagascar, Malawi emerged as the 'hotspots' in this vulnerability analysis, in addition to Zimbabwe, Lesotho and Swaziland. Zambia, Angola and DRC emerged as intermediate. Some countries, for example Zambia, Angola, DRC and Tanzania display highly differential results at a sub-national level, with some parts of the country showing high vulnerability and others lower vulnerability.

After the addition of the future climate and population data layers to the Exposure category, the patterns generally remained similar but with some significant additions to the hotspot areas. The future Exposure category showed a broadening of the high exposure latitudinal band up to 30°S, and also extending into northern Angola and the DRC. When combined with Sensitivity, the resulting Impacts layer then included greater portions of Angola and the DRC, with an intensification over the South African Highveld, southern and western Zambia, Malawi and south-western Madagascar. Reductions in intensity were seen in northern Mozambique, central Tanzania and south-western South Africa. Finally, with Adaptive Capacity included, new and intensive vulnerability hotspots emerged over large parts of the DRC and Angola, as well as Madagascar. These countries share the combination of increased exposure to climate risk and thus new and intensified problem areas, and weaker adaptive capacity. Countries such as Zambia, South Africa and Malawi also show

intensification of problem areas, but their better adaptive capacity results in little change to this 'hotspot' outcome.

In summary, five major clusters of vulnerability 'hotspots' emerge in southern Africa. These are (1) central Tanzania; (2) a large area incorporating southern and central Mozambique, Malawi, Zimbabwe and southern Zambia; (3) most of Madagascar; (4) southern and north-western Angola; (5) southern and particularly western DRC. Centres of resilience are identified for the northern Congo Basin, north-eastern Angola, northern Zambia, north-western and south-eastern Tanzania, and northern Mozambique. The south-west block (South Africa, Botswana, Namibia) and Mauritius are less vulnerable on account of their higher adaptive capacity, at a national level. This is also the case, to a smaller degree, for Lesotho and Swaziland. This does not diminish the fact that highly vulnerable communities also exist in these regions, who will be in need of assistance in dealing with increased climate-related risk brought about by climate change.

2. Background

The purpose of the Regional Climate Change Programme (RCCP) is 'to enable transboundary adaptation to climate change, with equitable access to climate funding, in southern Africa' (OneWorld Sustainable Investments 2009). In particular, the RCCP is designed to address how the climate changes anticipated for the SADC (Southern African Development Community) region will impact on food security, water resources and related services, hydro- and biomass-based energy supply, ecosystem services, and health objectives, and where these impacts are most likely to be felt. The region is considered to be highly vulnerable to climate-related challenges (IPCC 2007a): it is over-reliant on rainfed agriculture for food production, it has a large poor rural population, relatively undiversified economies and poorly developed infrastructure. Most of the SADC region is expected to become warmer and drier with climate change (Hulme et al. 2001).

A core component of the RCCP is to collate, generate and disseminate high quality and relevant information that will allow policy makers and planners to make informed choices on how they might respond to the way climate change will impact on local populations and livelihoods. There is a need for this response to be greatest in areas likely to be most hard hit by climate change. Despite the above-mentioned shared vulnerabilities, the SADC region is not uniform: it is characterised by widely divergent climate systems, natural resources (soils, water), plant and animal life and ecosystems, farming and other land use systems, social systems (including population demographics) and economic strengths and weaknesses. Assessing the vulnerability of this vast region to climate change must take into account these spatial differences in an evidence-based and integrated manner. For example, arid environments are not necessarily vulnerable if social and economic factors are strong, whereas climatically conducive environments can be highly sensitive to rapidly increasing population pressures and detrimental land management, rendering them vulnerable to climate change. Adaptation planning should be as spatially explicit as possible, thus ensuring that the focus is trained on natural and human systems most in need of strengthening.

The Risk and Vulnerability Mapping element of the RCCP set out to explore where current and future climate stressors have the greatest impact within the SADC region, and how adaptive capacity could shape the vulnerability of communities.

3. Approach and methods

Various conceptual understandings of vulnerability to climate change exist; we have chosen to use the widely accepted model employed by the Intergovernmental Panel on Climate Change (IPCC). The IPCC (2007b) defines vulnerability to climate change as "the degree to which a system is susceptible to, and unable to cope with, adverse effects of climate change, including climate variability and extremes. Vulnerability is a function of the character, magnitude, and rate of climate change and variation to which a system is exposed, its sensitivity, and its adaptive capacity." The assessment of vulnerability then includes a measure of exposure to the risk factors and sensitivity to the factors, together comprising the potential impact of such risks, and the capacity to manage and respond to those risks (Fig. 1):

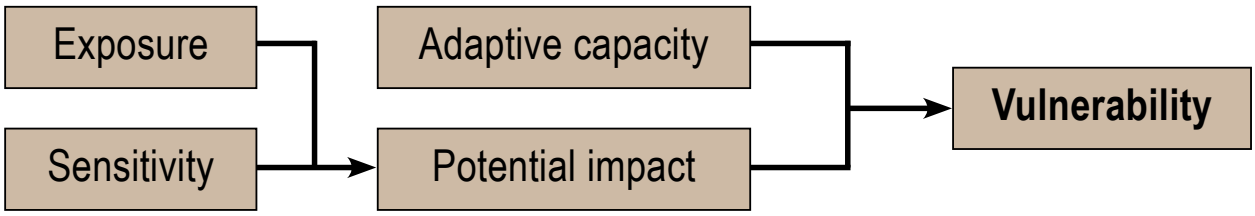

Fig. 1: Vulnerability and its components

We conducted a two-phased analysis, the first for the current situation ('status quo', ca. 2008) and the second for the mid-term future (ca. 2050). For the former, we developed an Exposure category reflecting current and recent historical exposure to climate-related stressors. These were overlaid with Sensitivity and Adaptive Capacity categories to depict current vulnerability to climate. For the futures analysis, we added projected climate and population changes to the year 2050 to the existing Exposure category which was combined with the other categories as previously.

The assumption is that current exposure to climate-related stressors will remain, but will be exacerbated by additional pressures arising from population growth, future climate change (rainfall and temperature), resulting loss of cropland, and sea level rise. We also make the assumption (for now) that current Adaptive Capacity and Sensitivity will remain the same over this time period. Further iterations of the mapping could conceivably analyse how these categories may change (e.g. through rapid socio-economic development of some countries) and in themselves become responsive to climate and population change, particularly the components of the Sensitivity category.

Multiple datasets were chosen within each of the categories Exposure, Sensitivity and Adaptive capacity, on the basis of their statistical reliability (high quality) and their geographic representation, and preferably at sub-national scale. Fourteen of the fifteen SADC states are represented, excluding only Seychelles for which data are difficult to source due to the high resolution required for the very small sizes of the nation's numerous islands.

Because many of the risks are closely bound to water supplies and how we use them, we took cognizance of water basins and catchment areas, some of which are transboundary and if not carefully and cooperatively managed may give rise to conflicts. Certain catchment areas of SADC extend beyond the political boundary of SADC (notably into Congo, Central African Republic, Sudan, Uganda, Rwanda, Burundi and Kenya). Efforts were made to collate all indicator data including demography and economics for the full extent of all SADC catchment regions, including adjoining countries.

Other similar investigations have used Principal Components Analysis to quantify the influence of independent variables on a dependent variable. As we had multiple dependent variables that we wished to consider, and in order to preserve accountability of the respective variables in

understanding the resulting patterns, we used a simple overlay approach in which we could control the respective influences of those variables we considered to be most relevant to the futures of people influenced by climate change. We combined the datasets in weighted overlay models for each category to produce a summary layer of each. We applied weightings varying from *1 to *3 in accordance with the confidence we held that each dataset was reliable and truly represented the detailed geographical distribution of the variable in question.

In order to combine multiple different GIS layers in the analysis it was necessary, firstly, that all layers followed the same scale of values and that all revealed at this scale the pertinent variation held within the dataset. We chose an integer scale from 1-9 to facilitate the handling of the grid layers. For certain GIS layers, data were highly clustered. Population density, for instance, had extremely high values for urban areas which masked the important variation in lower density rural areas. Data values were most often reclassified on a 1-9 scale using the Jenks natural breaks classification and in extreme cases, where the variation between regions was still not clearly portrayed, we used a logarithmic scale. Thus the differences between the regions in most final layers used represent a geographic ranking of pertinent differences rather than absolute scale.

For each of the status quo and futures analyses, we combined the values from the Sensitivity analysis with those of the Exposure analysis to produce a single layer which represents Problem Areas (Impact) of climate-related stressors. This can be taken to represent our best estimate for the geographic distribution of the 'problems' that people are likely to face across southern Africa with climate change in the forthcoming four decades. We then combined this layer with the values from the Adaptive Capacity analysis in order to reveal vulnerability Hotspots where local people are going to be in greatest need of assistance in dealing with these problems.

We ran a smoothing analysis to calculate average values for the data within a search radius of 50km, to identify locations for centres of hotspots or centres of resilience.

All metadata were systematically documented and are available separately from this report. Key metadata was sought for each layer in the geodatabase in the event that ISO 19139 or FGCD metadata has not been populated.

- Originator of the data set;
- Publication date;
- Title of the data set;
- Format of the data set;
- Description of the data set;
- Purpose of the data set;
- Date of completion;
- Status of data set (e.g. complete);
- Contact details of custodian;
- Accuracy of attributes;
- Accuracy of spatial data;
- Scale of maps;
- Projection/coordinate system;
- Datum, ellipsoid;
- Access constraints;
- Use constraints and Distribution information;
- Spatial boundary extent.

4. Status quo (2008) Risk and Vulnerability

4.1 Adaptive capacity category layers

4.1.1 Infrastructure Poverty Layer

weighting * 2

A good statistical relationship has been demonstrated between the night-time lights dataset (DMSP) and economic activity (Doll et al. 2000; Sutton et al. 2007). We used the NOAA Earth Observation Group global poverty dataset which is derived from the ratio of the radiance of the nightlights dataset to the human population density dataset (Landscan 2004) at 30 arc second (1km^2) resolution (Elvidge et al., 2009). Landscan 2004 is not derived from night-time lights so the ratio is a legitimate index of poverty. The estimates were calibrated using national level poverty data from the World Development Indicators (World Bank 2006). We are confident that this layer represents poverty at the highest resolution possible at point of writing, but it represents 'infrastructure' poverty. High densities of people can inhabit productive tropical climates without being short of food and other essentials so 'hunger' poverty needs to be addressed in other layers. We experimented with a combination of poverty layers but it was considered more sensible to keep them apart for separate weighting. This layer is considered a very valuable component of the hotspots analysis because it inputs to the project a very high resolution population dataset.

Data were clipped to the analysis area. The pixel values were highly fragmented and at 30 arc seconds may have contained fine-scale artifacts at urban edges due to data mismatch between the population and night-lights datasets. So we used instead a focal statistics grid which calculated the mean value within 5 cells (5km) of each grid cell. All cell values were re-classified to a scale of 1-9 using Jenks natural breaks method to be comparable with other layers (missing values were converted to zeros). We reversed the scale so that high values of poverty corresponded to low values of adaptive capacity. This layer is shown in the figure. Red areas represent areas of high infrastructure poverty. Full detail in metadata.

web-link:
http://www.ngdc.noaa.gov/dmsp/download_poverty.html

(NOAA websites are provided as a public service by the U.S. Department of Commerce, National Oceanic and Atmospheric Administration, National Environmental Satellite, Data and Information Service. Information presented on these web pages is considered public information and may be distributed or copied.)

4.1.2 Economic Wealth Layer

weighting * 3

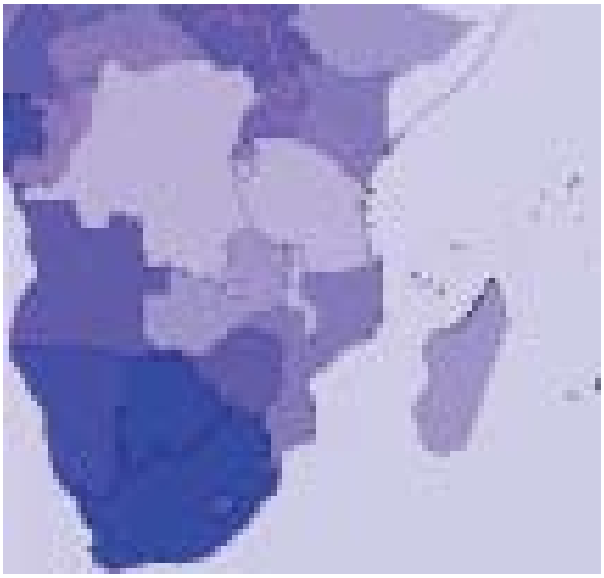

We used the indicator GDP per capita (in purchasing power parity terms in US dollars) from the 2007/2008 UNDP Human Development Report (data for this indicator from 2005), to indicate the relative economic wealth of each country

in the SADC region. The indicator is obtained by dividing the Gross Domestic Product by the midyear population.

Data were linked by country to the national boundaries shapefile (Digital Chart of the World) and then converted into raster format (1km^2 resolution) and cropped to the analysis area. All cell values were reclassified to a scale of 1-9 using Jenks natural breaks method to be comparable with other layers (missing values were converted to zeros). This layer is shown in the figure. Dark blue areas represent areas of high per capita GDP. Full detail in metadata.

web-link:
http://hdr.undp.org/en/reports/global/hdr2007-2008/

United Nations Development Programme (2007)

4.1.3 Malnourishment in Children under 5 years old

weighting * 3

Considered to be one of the best indicators of human poverty, the proportion of children under 5 years old that are below normal weight is also available at a sub-national scale. Unlike the 'infrastructure' poverty dataset above, this layer should indicate balance or imbalance between people and their food supplies.

The Global Sub-national Prevalence of Child Malnutrition dataset (CIESIN 2005) consists of estimates of the percentage of children with weight-for-age z-scores that are more than two standard deviations below the median of the NCHS/CDC/WHO International Reference Population. Data are reported for the most recent year with subnational information available at the time of development. This dataset is produced by the Columbia University Center for International Earth Science Information Network (CIESIN).

We used the shapefile version of the dataset, converted this into a raster format (1km^2 resolution) and cropped to the analysis area. All cell values were reclassified to a scale of 1-9 using Jenks natural breaks method to be comparable with other layers (missing values were converted to zeros). We inverted the scale so that high levels of child malnutrition indicated low levels of adaptive capacity. This layer is shown in the figure. Dark blue areas represent areas of low malnourishment. Full detail in metadata.

web-link:
http://sedac.ciesin.org/povmap/ds_global.jsp

Center for International Earth Science Information Network (CIESIN), Columbia University (2005)

4.1.4 Education Index

weighting * 2

We used the indicator Education Index from the 2007/2008 UNDP Human Development Report (data for this indicator from 2005), to indicate the relative education levels of each country in the SADC region. This is one of the three indices on which the human

development index is built. It is based on the adult literacy rate and the combined gross enrolment ratio for primary, secondary and tertiary schools.

Data were linked by country to the national boundaries shapefile (Digital Chart of the World) and then converted into raster format (1km^2 resolution) and cropped to the analysis area. All cell values were reclassified to a scale of 1-9 using Jenks natural breaks method to be comparable with other layers (missing values were converted to zeros). This layer is shown in the figure. Dark blue areas represent areas of high education levels. Full detail in metadata.

web-link:
http://hdr.undp.org/en/reports/global/hdr2007-2008/

United Nations Development Programme (2007)

4.1.5 Health Expenditure

weighting * 2

We used the indicator Health Expenditure per capita

from the 2007/2008 UNDP Human Development Report (data for this indicator from 2005), to indicate the relative health levels of each country in the SADC region. This is derived as the sum of public and private expenditure (in purchasing power parity terms in US dollars), divided by the mid-year population. Health expenditure includes the provision of health services (preventive and curative), family planning activities, nutrition activities and emergency aid designated for health, but excludes the provision of water and sanitation.

Data were linked by country to the national boundaries shapefile (Digital Chart of the World) and then converted into raster format (1km^2 resolution) and cropped to the analysis area. All cell values were reclassified to a scale of 1-9 using Jenks natural breaks method to be comparable with other layers (missing values were converted to zeros). This layer is shown in the figure. Dark blue areas represent areas of high per capita health expenditure. Full detail in metadata.

web-link:
http://hdr.undp.org/en/reports/global/hdr2007-2008/

United Nations Development Programme (2007)

4.1.6 Malaria Incidence

weighting * 1

We used epidemiological data based on empirical field evidence of the disease from the Malaria

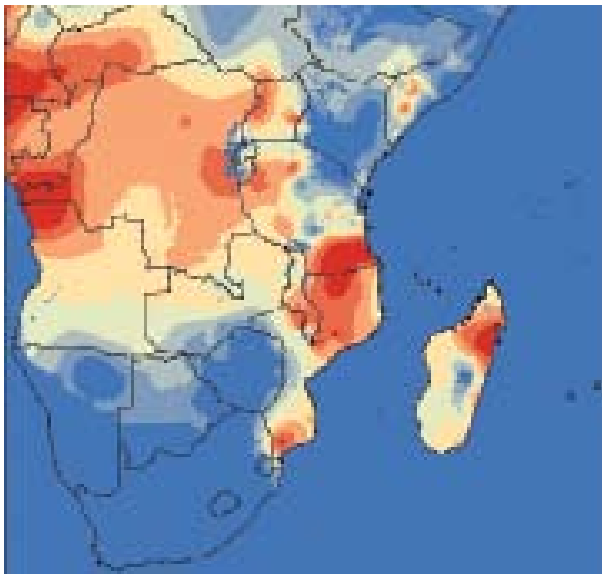

Atlas Project or MAP (Hay et al. 2010). This is a global database at 5km^2 resolution derived from 24,492 parasite rate surveys.

Data were cropped to the analysis area. All cell values (at 1km^2 resolution) were reclassified to a scale of 1-9 using Jenks natural breaks method to be comparable with other layers (missing values were converted to zeros). We reversed the values so that high malaria incidence corresponded to low adaptive capacity. This layer is shown in the figure with red areas corresponding to high incidence of malaria. Full detail in metadata.

web-link:
http://www.map.ox.ac.uk/

Hay SI, Okiro EA, Gething PW, Patil AP, Tatem AJ, et al. (2010) Estimating the Global Clinical Burden of Plasmodium falciparum Malaria in 2007. PLoSMed 7(6): e1000290. doi:10.1371/journal.pmed.1000290.

4.1.7 Tsetse Fly Habitat Suitability

weighting * 1

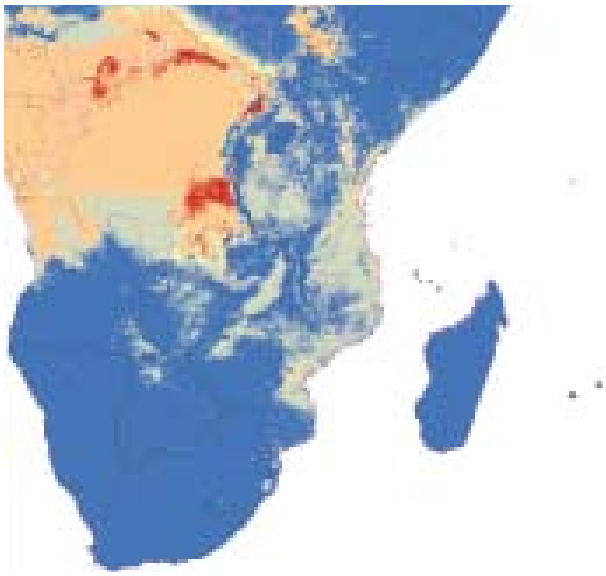

Tsetse flies are an important vector for diseases in rural Africa. This dataset contains the predicted areas of suitability for the three tsetse fly groups (Fusca, Palpalis and Morsitans) and for 24 tsetse species. The predictor variables include remotely sensed (satellite image) surrogates of climate – vegetation, temperature, moisture. Demographic, topographic and agroecological predictors are also used. The models are applied to the predictor imagery to determine the probability of fly distributions. Data are provided at 5km^2 resolution for the whole sub-Saharan Africa.

We reclassified each grid to a scale 1-9, took the sum of the three grids for the three fly groups and then reclassified again to a scale of 1-9 using Jenks natural breaks method to be comparable with other layers (missing values were converted to zeros). We reversed the values so that high values of suitability corresponded to low values of adaptive capacity. This layer is shown in the figure with red and orange areas showing low values i.e. highly suitable for this vector. Full detail in metadata.

web-link:
http://www.fao.org/geonetwork/

(The maps were produced in November 1999 for FAO Animal Health and Production Division and DFID Animal Health Programme by Environmental Research Group Oxford (ERGO Ltd) in collaboration with the Trypanosomosis and Land Use in Africa (TALA) research group at the Department of Zoology, University of Oxford)

4.1.8 HIV Prevalence

weighting * 2

We used the indicator HIV prevalence from the 2007/2008 UNDP Human Development Report (data for this indicator from 2005), to indicate the relative influence of the disease among SADC countries. The indicator gives the percentage of people aged 15-49 years who are infected with HIV.

Data were linked by country to the national boundaries shapefile (Digital Chart of the World) and then converted into raster format (1km^2 resolution) and cropped to the analysis area. Values were reversed to represent % HIV negative rather than % HIV positive. All cell values were reclassified to a scale of 1-9 using Jenks natural breaks method to be comparable with other layers (missing values were converted to zeros). This layer is shown in the figure with pale areas representing low values and thus high impact areas. Full detail in metadata.

web-link:
http://hdr.undp.org/en/reports/global/hdr2007-2008/

United Nations Development Programme (2007)

4.1.9 Access to Improved Water

weighting * 3

We used the indicator Access to Improved Water from the 2007/2008 UNDP Human Development Report (data for this indicator from 2005), to indicate the relative influence of the disease among SADC countries. This indicator gives the share of the population with reasonable access to any of

the following types of water supply for drinking: household connections, public standpipes, boreholes, protected dug wells, protected springs and rainwater collection. *Reasonable access* is defined as the availability of at least 20 litres a person per day from a source within one kilometre of the user's dwelling.

Data were linked by country to the national boundaries shapefile (Digital Chart of the World) and then converted into raster format (1km^2 resolution) and cropped to the analysis area. All cell values were reclassified to a scale of 1-9 using Jenks natural breaks method to be comparable with other layers (missing values were converted to zeros). This layer is shown in the figure with dark blue areas representing good access. Full detail in metadata.

web-link:
http://hdr.undp.org/en/reports/global/hdr2007-2008/

United Nations Development Programme (2007)

4.1.10 Subscribers to a Cellular Network

weighting * 1

We used the indicator Cellular Subscribers from the 2007/2008 UNDP Human Development Report (data for this indicator from 2005), to indicate the relative influence of cellular connectivity among SADC countries. The indicator provides the number of subscribers (per thousand of the population) to an automatic public mobile telephone service that provides access to the public switched telephone network using cellular technology. Systems can be analogue or digital.

Data were linked by country to the national boundaries shapefile (Digital Chart of the World) and then converted into raster format (1km^2 resolution) and cropped to the analysis area. All cell values were reclassified to a scale of 1-9 using Jenks natural breaks method to be comparable with other layers (missing values were converted to zeros). This layer is shown in the figure with dark blue areas representing good access. Full detail in metadata.

web-link:
http://hdr.undp.org/en/reports/global/hdr2007-2008/

United Nations Development Programme (2007)

4.1.11 Travel Time to Nearest City

weighting * 2

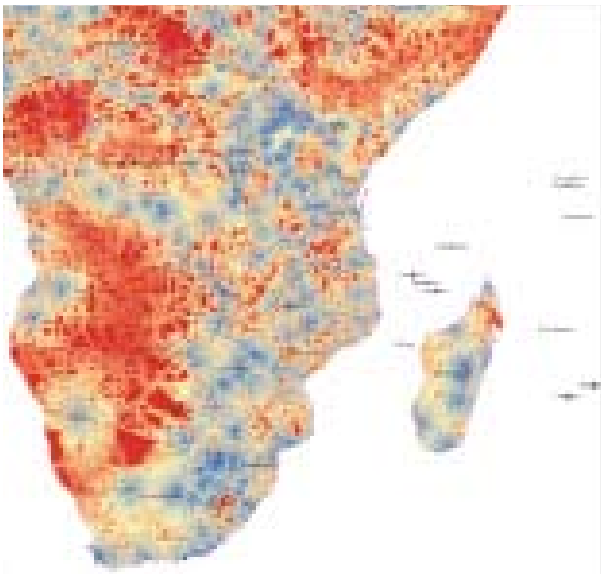

We used a new map of Travel Time to Major Cities – developed by the European Commission and the World Bank to represent access to markets, schools, hospitals, water etc. The map captures connectivity and the concentration of economic activity. The data are fine resolution (30 arc seconds or 1km^2). Values represent minutes of land based travel time to the nearest city of 50,000 people (year 2000).

Data were cropped to the analysis area. All cell values were reclassified to a scale of 1-9 using Jenks natural breaks method to be comparable with other layers (missing values were converted to zeros). This layer is shown in the figure with dark blue areas representing good access. Full detail in metadata.

web-link:
http://bioval.jrc.ec.europa.eu/products/gam/download.htm

This map was made for the World Bank's World Development Report 2009 Reshaping Economic Geography – see Nelson (2008) Global Environment Monitoring Unit – Joint Research Centre of the European Commission, Ispra Italy.

4.1.12 Night Lights Dataset

weighting * 3

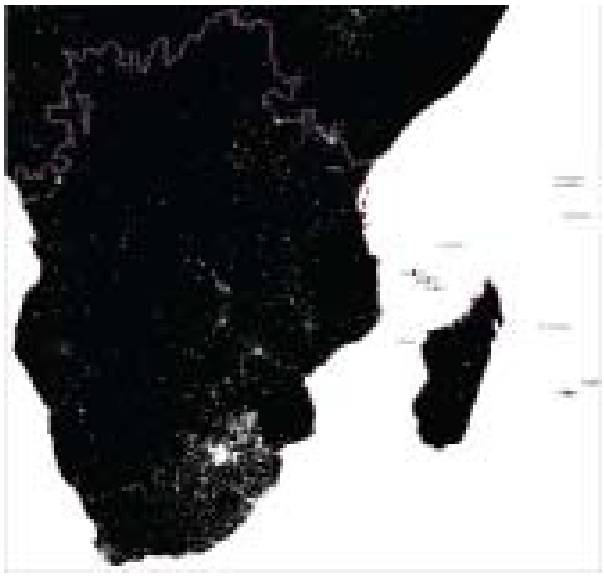

Given the demonstrated relationship between night-time lights and economic activity (Doll et al. 2000; Sutton et al. 2006), we used radiance calibrated lights from F162006 (courtesy of NOAA National Geophysical Data Center) to indicate concentrations of economic activity across southern Africa. These data are cloud-free composites at 30 arc second grids and have benefited from various algorithms to remove unwanted light, glare and reflection from various sources.

We cropped the data to the analysis area and ran a focal statistics analysis to determine mean values within 10km of each grid cell. This had a smoothing effect and represents some of the extended influence of intense economic activity for local people. All cell values were reclassified to a scale of 1-9 to be comparable with other layers (missing values were converted to zeros). We did a manual reclassification in order to discern the pertinent variation. This layer is shown in the figure. Full detail in metadata.

web-link:
http://www.ngdc.noaa.gov/dmsp/download.html

Image and data processing by NOAA's National Geophysical Data Center. DMSP data collected by US Air Force Weather Agency.

4.1.13 Contribution of Agriculture to Gross Domestic Product

weighting * 2

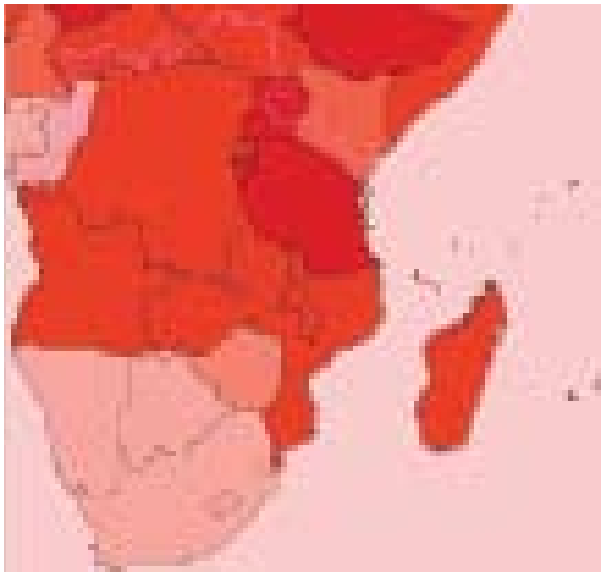

We used the indicator Percent Contribution of Agriculture to GDP from *World Development Indicators* (World Bank, 2007) to indicate the relative dependency of SADC countries on this income. The assumption is that countries with a low reliance on agriculture will have other resources available during a climate shock and have more capability to adapt.

Tabular data were linked by country to the

national boundaries shapefile (Digital Chart of the World) and then converted into raster format (1km^2 resolution) and cropped to the analysis area. There was no data for Somalia so we used the average of adjoining countries (23%). All cell values were reclassified to a scale of 1-9 using Jenks natural breaks method to be comparable with other layers (missing values were converted to zeros). This layer is shown in the figure with dark red areas representing heavy reliance on agriculture. Full detail in metadata.

web-link:
http://web.worldbank.org/WBSITE/EXTERNAL/DATASTATISTICS/0,,contentMDK:21298138~pagePK:64133150~piPK:64133175~theSitePK:239419,00.html

World Bank (2007). World Development Indicators 2007. World Bank, Washington. 432pp.

4.1.14 Water Discharge

weighting * 1

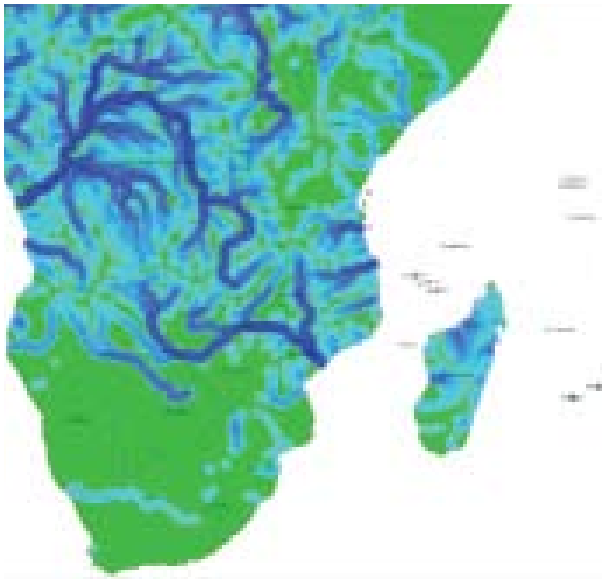

People living close to major rivers have a renewable resource at hand which may help them adapt to climate change through storage developments and irrigation. People living far from major rivers are at a relative disadvantage in this regard. To differentiate these regions we used the mean annual discharge grid (km^3/yr) from the African Water Stress Study (Vörösmarty et al. 2005). This study produced hydrological model outputs at 8km^2 resolution.

We cropped the data to the analysis area and ran a focal statistics analysis to determine the sum of values within 50km of each grid cell. This had a smoothing effect and represents some of the extended influence of major rivers as a resource for local people. All cell values were reclassified to a scale of 1-9 to be comparable with other layers (missing values were converted to zeros). After a log transformation, cell values were reclassified to a scale of 1-9 using Jenks natural breaks method to be comparable with other layers (missing values were converted to zeros). This layer is shown in the figure with dark blue areas representing high values of discharge. Full detail in metadata.

web-link:
http://wwdrii.sr.unh.edu/download.html

Vörösmarty et al. 2005. Geospatial indicators of emerging water stress: An application to Africa. *Ambio* 34 (3): 230-236.

4.1.15 Irrigation Potential

weighting * 2

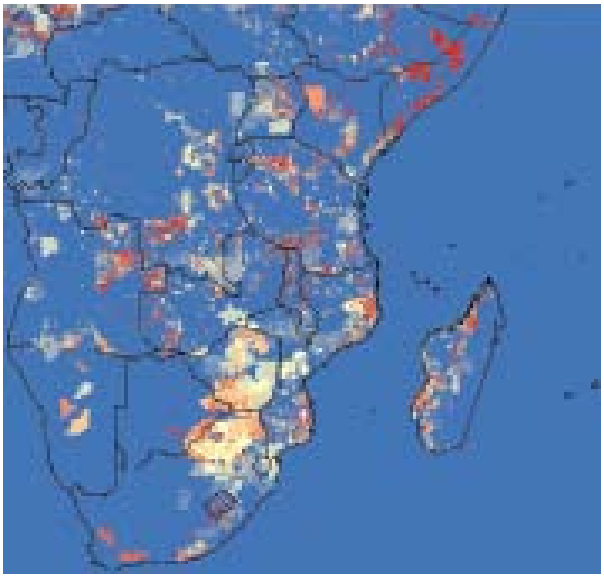

Only 6% of cultivated land in Africa is managed for irrigation compared with 37% for Asia. This layer represents, should funds be available, where in southern Africa there is potential to economically develop irrigation schemes for capturing and utilising expected run-off. Most attention is currently given to expected water stress arising from climate change. But this layer shows the benefical potential of water in the future if available and managed correctly. By overlay onto the hotspots map or other drought layers this layer could be used to establish priorities for these irrigation solutions to future

climate stress. However, it should be noted that the underlying analysis does not factor in the possible changes in water availability under scenarios of climate change.

Data were kindly supplied by Liang You. Values represent internal rate of return i.e. profitability. This analysis was carried out separately for small and large schemes but we combined these two datasets by addition after consultation with Liang You (pers. comm.) The Access database was loaded into the GIS using the Harvest Choice grid format reference system that may be found at *http://gislnxserver.irri.org/hc/grids.html*

After combination, 1km^2 cell values were reclassified on a scale of 1 to 9 with 9 representing maximum capacity for adaptation and missing values were set to zero. Full detail in metadata.

web-link:
http://www.ifpri.org/publication/what-irrigation-potential-africa

4.1.16 Conflicts

weighting * 1

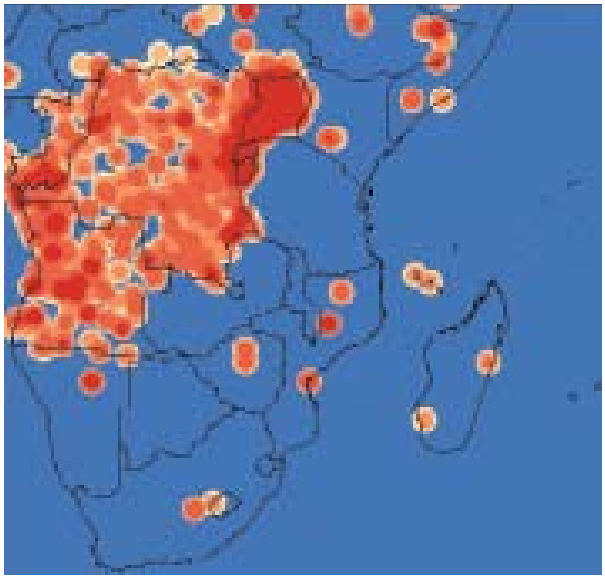

In addition to governance, we examined two datasets on armed conflicts to obtain a sub-national layer which indicates density of unrest.

The ACLED dataset (1960 – 2004) codes exact locations, dates, and additional characteristics of individual battle events in eight countries across Central and West Africa affected with civil war (Raleigh et al. 2005). There is a specific focus on tracking rebel activity and distinguishing between territorial transfers of military control from governments to rebel groups and vice versa, and the location of rebel group bases, headquarters, strongholds and presence. The dataset also records one-sided violence on civilians by both government or rebel actors and conflicts between rebel groups. ACLED provides comprehensive coverage in Central African countries for the period but does not present comparable data for other regions notably Mozambique over the same time period. The conflicts coded for in the dataset are in general compatible with the Uppsala/PRIO armed conflicts dataset.

Our second dataset is the Uppsala Conflict Data Programme (UCDP) which is not restricted to any specific countries. Since 1979, UCDP has recorded ongoing violent conflicts. This effort continues to the present day, now coupled with the collection of information on an ever-broadening scope of aspects pertaining to organised violence. UCDP provides one of the most accurate and well-used data-sources on global armed conflicts and its definition of armed conflict is becoming a standard in how conflicts are systematically defined and studied.

These two points datasets showed separate events for Sub-Saharan Africa so we combined the datasets and gave every event a score of 3 for battles and 1 for other events. We then carried out a kernel density analysis of the data using the score as the population field and with a search radius of one decimal degree (approx 111 km). This analysis reveals high concentrations of conflicts around Uganda, Rwanda, Burundi and the Albertine Rift, plus widespread conflicts through DRC and Angola and sporadic conflict events elsewhere. Red areas on the graphic denote high conflict density but we inverted the scale and reclassified on our scale of 1 to 9 in order to provide a layer where high values of adaptive capacity corresponded to the lowest densities of conflict. Full detail in metadata.

web-links:
http://www.prio.no/CSCW/Datasets/Armed-Conflict/Armed-Conflict-Location-and-Event-Data/; http://www.ucdp.uu.se/gpdatabase/search.php

Raleigh, Clionadh & Håvard Hegre, 2005. 'Introducing ACLED: An Armed Conflict Location and Event Dataset'. Paper presented to the conference on 'Disaggregating the Study of Civil War and Transnational Violence', University of California Institute of Global Conflict and Cooperation, San Diego, CA, 7–8 March.

4.1.17 Governance

weighting * 2

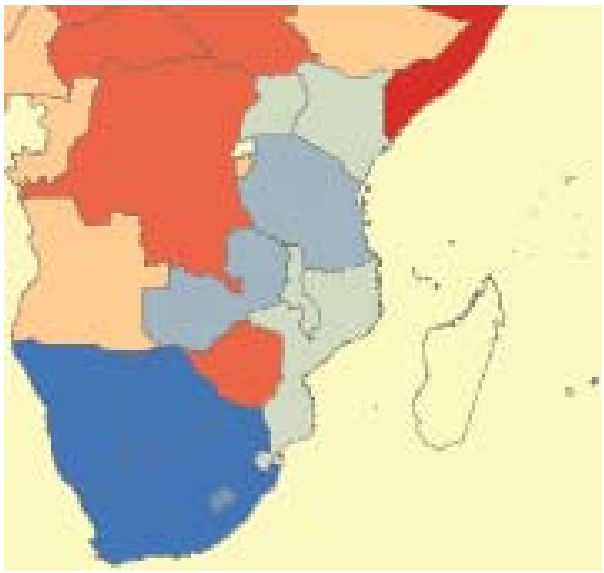

Adaptive capacity is also considered to be influenced by governance. We expect that citizens would receive better help in coping with climate stressors and disaster events in situations with good governance. We use the Ibrahim Index which measures the delivery of public goods and services to citizens by government and non-state actors. This index uses indicators across four main categories: Safety and Rule of Law; Participation and Human Rights; Sustainable Economic Opportunity; and Human Development as proxies for the quality of the processes and outcomes of governance. It is a comprehensive collection of qualitative and quantitative data that assess governance in Africa, is funded and led by an African institution and is considered to be a progressive and consultative assessment of governance. There are alternative indicators e.g. the World Bank's World Governance Indicator (WGI) which we are also evaluating.

We used the national indicators for 2008/9 and reclassified the values on our scale of 1 to 9. On the graphic red areas indicate poor governance. Full details in metadata.

web-link:
http://www.moibrahimfoundation.org/en/section/the-ibrahim-index

4.1.18 Forest Resources

weighting * 1

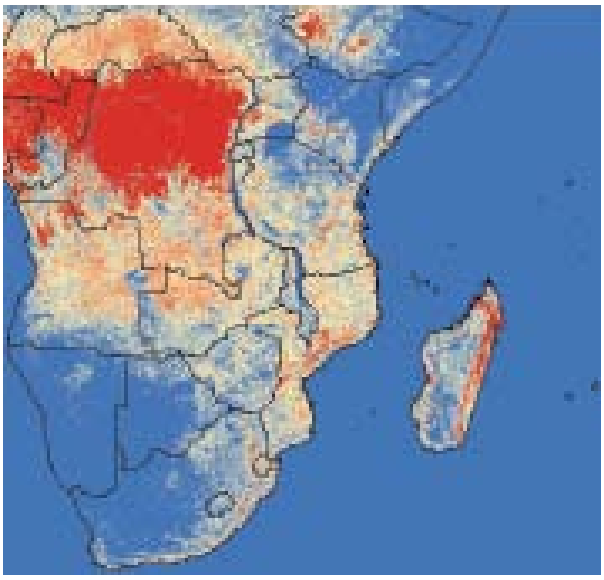

As a first component layer representing ecosystem services we include here the MODIS Vegetation Continuous Fields Dataset (% woody vegetation with a start point of 5% woody vegetation cover in agreement with FGGD classification of woodlands and forest). Afrotropical forest resources, much of which occurs in DRC represents 67 Pg $C_{biomass + soil}$ (Scharlemann et al. 2010). Globally, forests act as a major store for carbon, a significant service in the context of CO_2 emissions. There are other localized services, notably beneficial effects on the water cycle. We consider that areas of southern Africa which are rich in forest are wealthier in terms of adaptive capacity as a result of this significant natural asset.

The product is derived from all seven bands of the MODerate-resolution Imaging Spectroradiometer (MODIS) sensor onboard NASA's Terra satellite. The continuous classification scheme of the VCF product may depict areas of heterogeneous land cover better than traditional discrete classification schemes. While traditional classification schemes indicate where land cover types are concentrated, this VCF product is ideal for showing how much of a land cover such as 'forest' exists anywhere on a land surface. Full detail in metadata.

web-link:
http://glcf.umiacs.umd.edu/data/vcf/

4.1.19 Biodiversity

weighting * 2

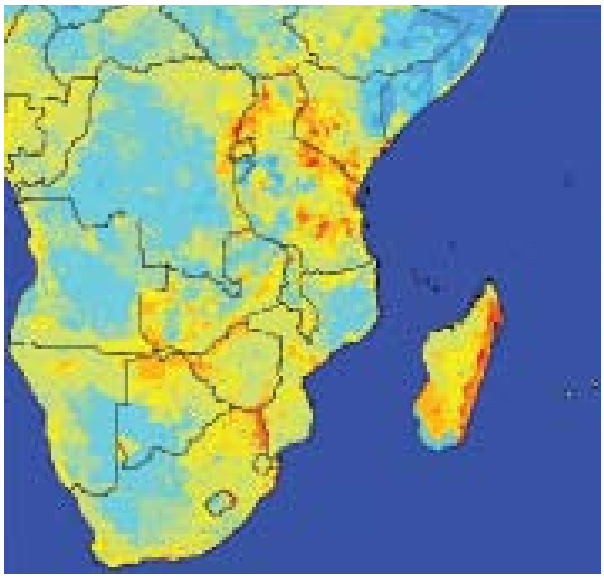

Biodiversity could be placed in either the adaptive capacity group or the sensitivity group. Areas rich in biodiversity are more resilient to perturbations and provide more help to people in the delivery of healthy ecosystem services. Areas depleted of biodiversity by contrast can be considered more prone to perturbations e.g. locust irruptions, and more sensitive to climatic extremes.

There are two ways of viewing biodiversity value: either in terms of innate value and what needs to be protected (what is rare and vulnerable); or in terms of what biodiversity provides for people by way of ecosystem services. There must be overlap in these two measures of biodiversity value but within the time frame of this project we focus initially on the innate value of biodiversity represented in this layer, while the following layer (Forest Resources) offers our first representation of biodiversity value in terms of ecosystem service provision.

To assess the innate value of biodiversity across SADC we developed three component layers: a species value layer, a habitats value layer, and a protection or security layer. These three are combined in equal influence.

For the species value layer there are insufficient data across Africa as yet on the exact occurrence of species, particularly rare and protected species. Instead, as a proxy, we use a one degree grid from Copenhagen University showing taxa richness patterns for 4144 vertebrate species across Sub-Saharan Africa (mammals, birds, snakes and amphibians), which has been derived from overlays of range of occurrence maps.

web-link:
http://www.zmuc.dk/CommonWeb/research/biodata.htm

The vertebrate taxa grid only covers mainland Sub-Saharan Africa. For Madagascar and other unrepresented areas we filled in using comparable data on vertebrate taxa richness in WWF Ecoregions kindly provided by Neil Burgess of WWF.

For the habitats layer we considered White's Phytechoria but chose to use instead WWF Ecoregions being more contemporary and with units distinct on mainland Africa from island (Madagascar) equivalents. We carried out two analyses of WWF Ecoregions across SADC to measure their extent and their level of anthropogenic transformation. We considered smaller ecoregions to be more vulnerable than very expansive ones and valued this on a scale of 1-9. We developed a separate layer based on the Globcover landcover dataset and for each landcover class we ascribed an estimate of the degree of transformation of the pristine habitat that once occurred there (see table), this value could then be transposed to each 300m x 300m grid cell in the Globcover dataset and an index of % transformation be deducted for each ecoregion in Africa. We reclassified % transformation on a scale of 1-9 and then computed a final habitats value layer by simply adding the two value layers together such that small, transformed habitats carried the highest values.

For assessing overall biodiversity value across the SADC region we also wanted a layer which represented how secure or how protected biodiversity is. We obtained this from three data subsets: WDPA (protected areas database); GRUMP human population density; and travel-time to cities. The assumption is that biodiversity is safer into the long term and thus has more value if it is contained in a well-managed protected area, with low human population density and far from infrastructure. To assess the efficacy of management of protected areas we derived a national figure for annual spend per km^2 on protected areas from data provided in James et al. (1999). This publication provides data on many African countries. For a few

VALUE	% TRANSFORMATION	LAND COVER TYPE
11	80	Post-flooding or irrigated croplands (or aquatic)
14	60	Rainfed croplands
20	40	Mosaic cropland (50-70%) / vegetation (grassland/shrubland/forest) (20-50%)
30	30	Mosaic vegetation (grassland/shrubland/forest) (50-70%) / cropland (20-50%)
40	15	Closed to open (>15%) broadleaved evergreen or semi-deciduous forest (>5m)
50	10	Closed (>40%) broadleaved deciduous forest (>5m)
60	20	Open (15-40%) broadleaved deciduous forest/woodland (>5m)
70	35	Closed (>40%) needleleaved evergreen forest (>5m)
90	30	Open (15-40%) needleleaved deciduous or evergreen forest (>5m)
100	20	Closed to open (>15%) mixed broadleaved and needleleaved forest (>5m)
110	20	Mosaic forest or shrubland (50-70%) / grassland (20-50%)
120	20	Mosaic grassland (50-70%) / forest or shrubland (20-50%)
130	20	Closed to open (>15%) (broadleaved or needleleaved, evergreen or deciduous) shrubland (<5m)
140	20	Closed to open (>15%) herbaceous vegetation (grassland, savannas or lichens/mosses)
150	20	Sparse (<15%) vegetation
160	10	Closed to open (>15%) broadleaved forest regularly flooded (semi-permanently or temporarily) – Fresh or brackish water
170	10	Closed (>40%) broadleaved forest or shrubland permanently flooded – Saline or brackish water
180	20	Closed to open (>15%) grassland or woody vegetation on regularly flooded or waterlogged soil – Fresh, brackish or saline water
190	90	Artificial surfaces and associated areas (Urban areas >50%)
200	10	Bare areas
210	10	Water bodies
220	5	Permanent snow and ice
230	10	No data (burnt areas, clouds,à)

African countries with missing values, values were estimated from the known values of neighbouring states with comparable economies. The values showed extreme variation from 28c/km^2 per annum in Angola to over $3000/km^2 in Mauritius. So we took a logarithm of the expenditure per km^2 per annum to assemble the budgets on a comparable scale and reclassified this to a scale of 1-9.

We chose to use the GRUMP population density dataset as this is considered the best contemporary dataset for contrasting population density in Africa between urban and rural areas. Again there is extreme variation in this value across grid cells so we used the logarithm to shorten the scale and reclassified it to values between 1 and 9.

The GRUMP dataset allocates population density according to administration district and urban areas. It does not contain an algorithm as do other datasets for the distance from settlements, roads and other infrastructure. Instead we introduced a third dataset, Travel time to Cities (4.1.11) from EC and the World Bank. Again we computed the logarithm scale to shorten the extreme variation and reclassified on a scale 1-9.

We then combined these three layers by summing efficacy of protection with travel time to cities, and then subtracting population density (where high values afford low protection). The output is a dataset which makes sense at fine resolution across the region as a representation of the future security of biodiversity.

Our final biodiversity layer is derived simply as the sum of the species value layer plus the ecoregions value layer plus the 'biosecurity' layer.

4.2 Sensitivity category layers

4.2.1 Percent Land under Irrigation

weighting * 3

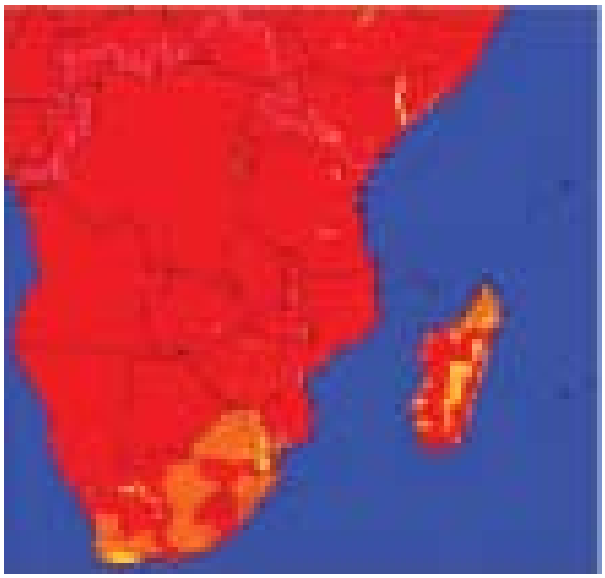

The FGGD irrigated areas map is a global raster datalayer with a resolution of 5 arc-minutes. Each pixel in the map contains a value representing the percentage of the area equipped for irrigation.

We cropped the data to the analysis area and calculated the inverse proportion of the values, i.e. the percent area not under irrigation to represent areas more sensitive to climate change stressors. All cell values were reclassified to a scale of 1-9 using Jenks natural breaks method to be comparable with other layers (missing values were converted to zeros). This layer is shown in the figure with dark red areas representing more sensitive areas. Full detail in metadata.

web-link:
www.fao.org/ag/agl/aglw/aquastat/irrigationmap/index10.stm

The data are a IIASA modification of FAO and University of Kassel (2002), Digital Global Map of Irrigated Areas v. 2.1.

4.2.2 Human Appropriation of Net Primary Productivity

weighting * 2

The Human Appropriation of Net Primary Productivity (HANPP) as a Percentage of Net Primary Product (NPP) highlights regions in which human consumption of NPP is greatly in excess of production by local ecosystems (Imhoff et al. 2004). It currently provides our only subnational (quarter degree square raster) indication of food balance / imbalance. HANPP is derived from FAO national statistics on consumption and allocated geographically in accordance with the gridded population of the world (SEDAC). NPP is derived from satellite information. Humans appropriate net primary productivity through the consumption of food, paper, wood and fiber.

We cropped the data to the analysis area and calculated the inverse proportion of the values, i.e. the percent area not under irrigation to represent areas more sensitive to climate change stressors. The variability in rural areas was masked by the very high values in urban areas. A log transformation enabled geographic differentiation of values in rural areas. All cell values were then reclassified to a scale of 1-9 using Jenks natural breaks method to be comparable with other layers (missing values were converted to zeros). This layer is shown in the figure with red areas representing high consumption (more sensitive). Full detail in metadata.

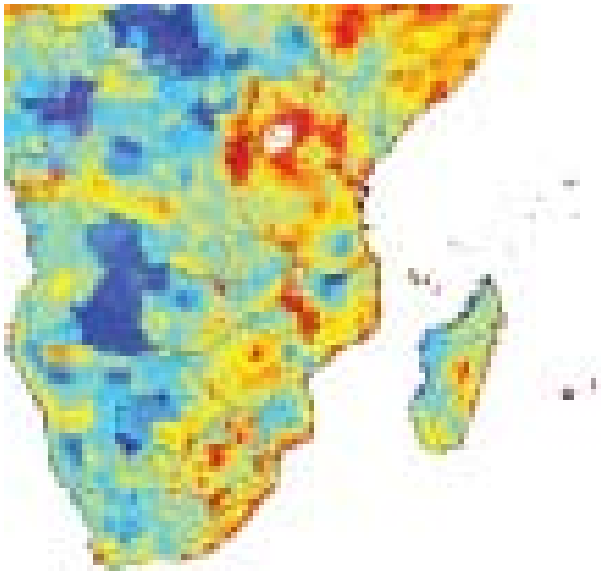

web-link:
http://sedac.ciesin.columbia.edu/es/hanpp.html

This dataset is distributed by the Columbia University Center for International Earth Science Information Network (CIESIN).

4.2.3 Volume of Rainfall per Person on Agricultural Land

weighting * 3

We estimated density of people ‘farming’, by multiplying the UNEP Africa population database by the proportion of each grid cell allocated to cropland (rainfed or irrigated; source: FAO/

IIASA GAEZ). So we assume that if a grid square of the cropland dataset (10km^2 resolution) has a value of 25%, then a quarter of the population estimates for each of the four grid cells it covers (5km^2 resolution) will be living on cropland. This is a simplistic assumption but it provides a measure for comparing areas especially where population density is consistently high or low across many grid cells. To obtain an indication of water balance within rural areas we used the Worldclim (Hijmans et al. 2005) precipitation data to calculate cubic meters of rainfall per 'farmer' at 1km^2 resolution.

We cropped the data to the analysis area. The variability in rural areas was masked by the very extremely low values in extremely densely populated areas. A log transformation enabled geographic differentiation of values among rural areas. All cell values were reclassified to a scale of 1-9 using Jenks natural breaks method to be comparable with other layers (missing values were converted to zeros). We reversed the values so that low rainfall corresponded to high sensitivity. There were a lot of areas, outside cropland, where there were no values so we allocated the lowest sensitivity score to these areas. This analysis therefore only indicates rainfall stress for agriculturalists, not for livestock farmers. This layer is shown in the figure with red areas representing sensitive areas of low rainfall per person on cropland. Full detail in metadata.

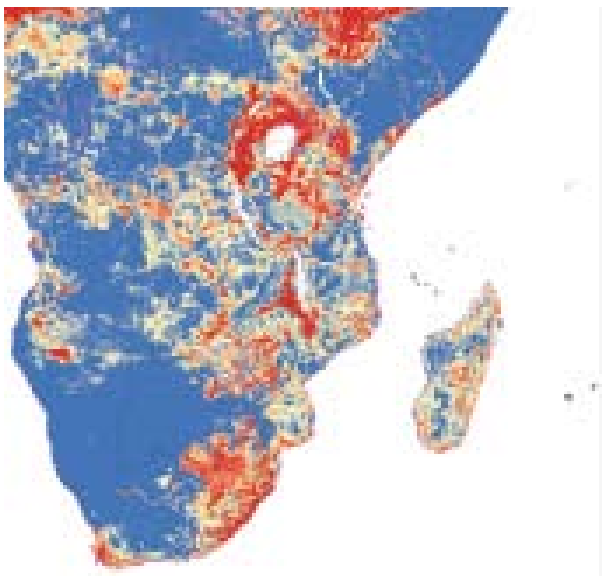

web-links:
http://www.worldclim.org/
http://na.unep.net/globalpop/africa/
http://www.fao.org:80/geonetwork/srv/en/resources.get?id=14067&fname=Map5_2.zip&access=private

4.2.4 Crowding on Agricultural Land

weighting * 2

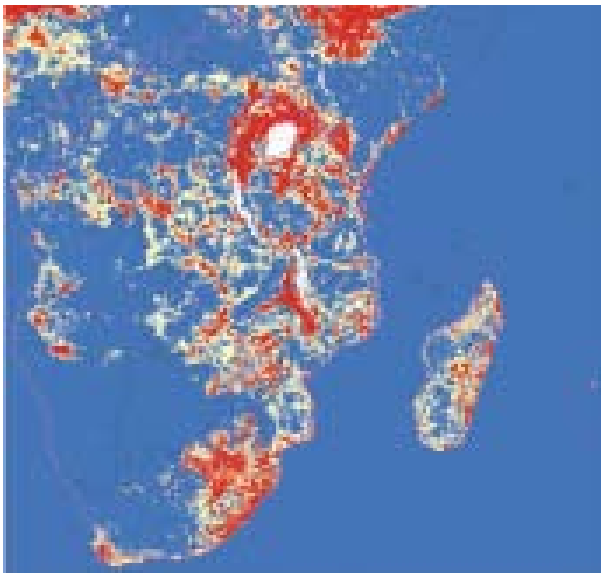

In addition to the above indicator of rainfall supplies we also used the simple estimate for density of 'farmers', people inhabiting arable land, by multiplying the UNEP Africa population database by the proportion of each grid cell allocated to cropland (rainfed or irrigated; source: FAO/IIASA GAEZ).

We cropped the data to the analysis area. All cell values were reclassified to a scale of 1-9 using Jenks natural breaks method to be comparable with other layers (missing values were converted to zeros). This layer is shown in the figure with red areas representing sensitive areas of high densities of people on agricultural land. Full detail in metadata.

web-links:
http://na.unep.net/globalpop/africa/ http://www.fao.org:80/geonetwork/srv/en/resources.get?id=14067&fname=Map5_2.zip&access=private

4.2.5 Length of Growing Period

weighting * 2

The length of the growing period is crucial for crop production and studies indicate that significant areas will fail for crop production as climate change progresses (ILRI 2006). While we await specific data from these studies we use the Length of Growing Period (LGP) zones of the world to indicate sensitivity. The FGGD LGP zone map is a global raster datalayer with a resolution of 5 arc-minutes. Each pixel contains a class value for the dominant LGP zone found in the pixel.

We cropped the data to the analysis area. Values were inverted so that shorter growing periods corresponded to higher sensitivity. All cell values were reclassified to a scale of 1-9 using Jenks natural breaks method to be comparable with other layers (missing values were converted to zeros). This layer is shown in the figure with dark areas representing sensitive areas. Full detail in metadata.

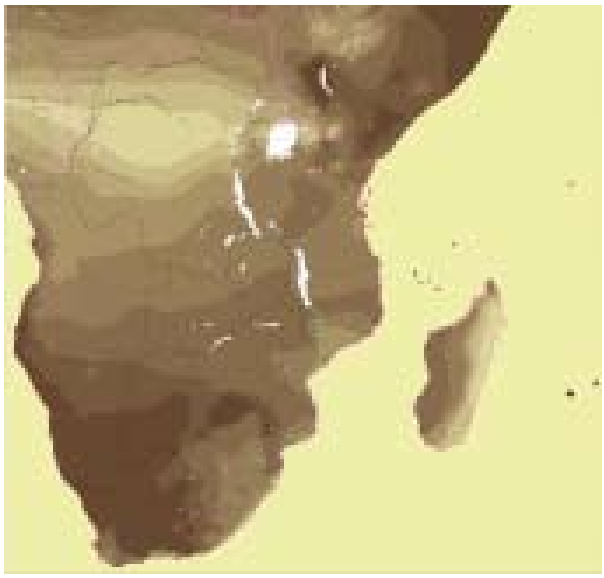

web-links:
http://www.fao.org/geonetwork/srv/en/main.home

The FGGD Digital Atlas: This dataset is contained in Module 4 "Environmental conditions" of Food Insecurity, Poverty and Environment Global GIS Database (FGGD) (FAO and IIASA 2007).

4.2.6 Easily Available Soil Moisture

weighting * 3

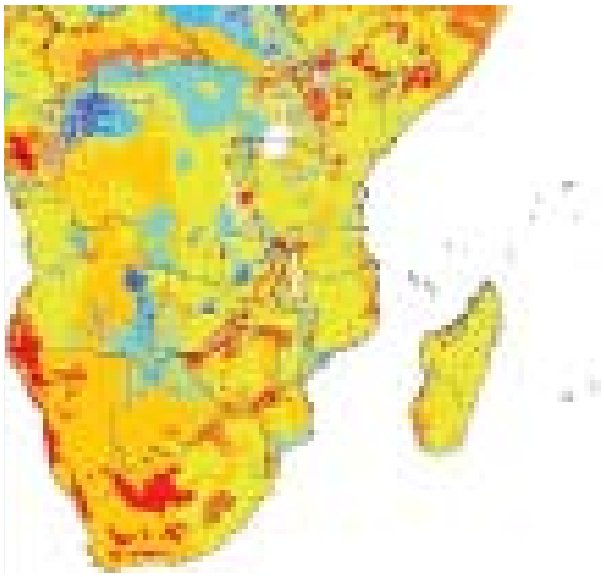

This grid from FAO offers an estimate of easily available soil moisture in mm/m with a spatial resolution of 5 * 5 arc minutes. Information with regard to easily available soil moisture was calculated from the 'Derived Soil Properties' of the 'Digital Soil Map of the World' which contains raster information on soil moisture in different classes.

We cropped the data to the analysis area. Values were inverted so that low soil moisture corresponded to higher sensitivity. All cell values were reclassified to a scale of 1-9 using Jenks natural breaks method to be comparable with other layers (missing values were converted to zeros). This layer is shown in the figure with red areas representing sensitive areas. Full detail in metadata.

web-links:
http://www.fao.org/geonetwork/srv/en/main.home

Derived from Digital Soil Map of the World

4.2.7 Soil Degradation

weighting * 2

The Global Assessment of Human Induced Soil Degradation (GLASOD) was conducted by the International Soil Reference and Information Centre (ISRIC) at Wageningen, The Netherlands, as commissioned by the United Nations Environment Programme (UNEP). ISRIC produced a 1:10 million scale wall chart in 1990 and subsequently produced a digital data set. In essence, the GLASOD data base contains information on soil degradation within map units as reported by numerous soil experts around the world through a questionnaire. It includes the type, degree, extent, cause and

rate of soil degradation. From these data, GRID produced digital and hardcopy maps and made area calculations (Oldeman et al. 1990).

We cropped the data to the analysis area. We used the degree of soil degradation to indicate sensitivity which varies 1,2,3,4. We converted these values to 3,5,7,9 (missing values were converted to zeros). This layer is shown in the figure with orange and red areas representing sensitive areas. Full detail in metadata.

web-links:
http://www.fao.org/geonetwork/srv/en/main.home

4.2.8 Slope

weighting * 2

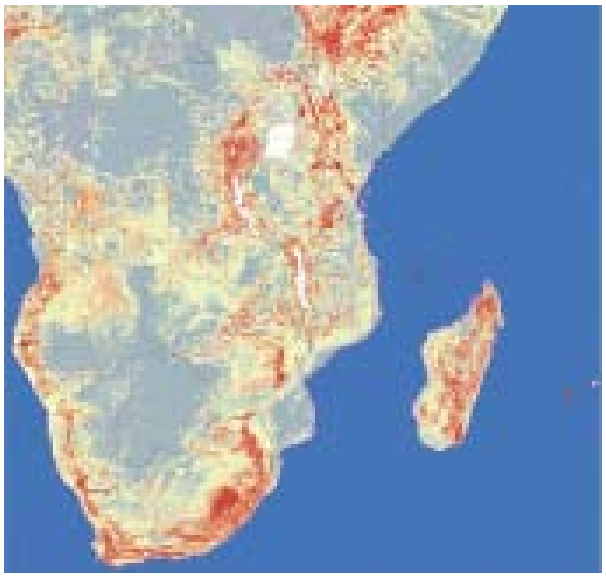

To derive slope we used the Shuttle Radar Topography Mission DTED® Level 1 (3-arc second) Data. The resolution is 3 arc seconds (90 meters). The pixel value represents the elevation in meters. For the RCCP we used spatial analyst extension in ArcMAP to derive slope from this DEM.

We cropped the data to the analysis area. All cell values were reclassified to a scale of 1-9 using Jenks natural breaks method to be comparable with other layers (missing values were converted to zeros). This layer is shown in the figure with orange and red areas representing sensitive areas. Full detail in metadata.

web-links:
http://edcsns17.cr.usgs.gov/srtmdted/

U.S. Geological Survey Center for Earth Resource Observation and Science (EROS), National Aeronautics and Space Administration (NASA), National Geospatial-Intelligence Agency (NGA), ESRI

4.2.9 Net Primary Productivity

weighting * 2

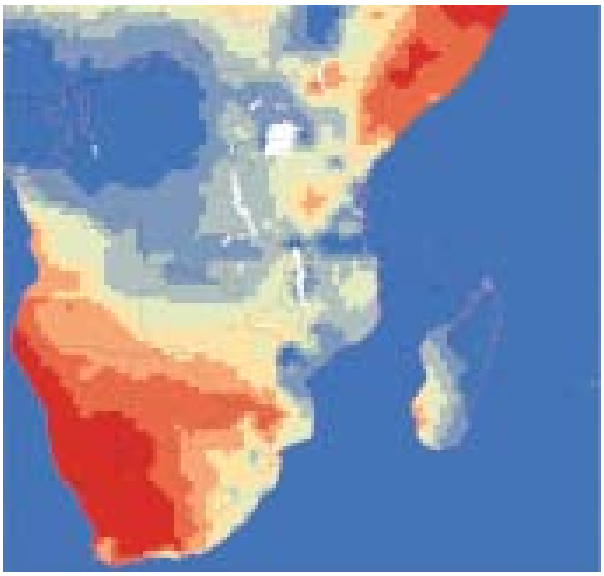

We considered areas of low productivity to be marginal and more sensitive to the effects of climate change than very productive areas. We used the Global Climatological Net Primary Production of Biomass dataset from CLIMPAG at five degree resolution as an indicator. This is calculated from climate data (GPCC VASClimO) for the period 1951-2000.

We cropped the data to the analysis area. All cell values were reclassified to a scale of 1-9 using Jenks natural breaks method to be comparable with other layers (missing values were converted to zeros). This layer is shown in the figure with orange and red areas representing sensitive areas. Full detail in metadata.

web-links:
http://www.fao.org/nr/climpag/globgrids/NPP_en.asp

FAO: CLIMPAG; Lieth (1972)

4.2.10 Major Agricultural Systems

weighting * 1

We used the World Bank / FAO Major farming systems of Sub-Saharan Africa dataset to indicate livelihoods which could be considered more sensitive to climate change. In this shapefile, farming systems are defined as populations of farms that have broadly similar resource bases, enterprise patterns, household livelihoods and constraints, and for which similar development strategies and interventions would be appropriate. The biophysical, economic and human elements of

NO.	MAJOR FARMING SYSTEM	PREVALENCE OF POVERTY (FAO) – PROXY FOR CURRENT SENSITIVITY	TEMPERATURE INCREASE 2°C, NO CHANGE IN RAINFALL	TEMPERATURE INCREASE 2°C, RAINFALL 10% DECREASE	TEMPERATURE INCREASE 2°C, RAINFALL 10% INCREASE	OVERALL
1	Irrigated	low	1	1	1	1
2	Tree crop	low	2	3	2	2
3	Forest based	moderate	2	3	2	2
4	Rice-tree crop	moderate	2	3	2	2
5	Highland perennial	moderate	1	2	1	1
6	Highland temperate mixed	high	2	2	1	2
7	Root crop	moderate	2	2	1	2
8	Cereal-root crop mixed	high	3	3	2	3
9	Cereal-based	high	3	3	2	3
10	Large commercial & smallholder	low	2	2	1	2
11	Agro-pastoral millet/sorghum	high	3	3	2	3
12	Pastoral	high	3	3	2	3
13	Sparse (arid)	low	2	2	1	2
14	Coastal artisanal fishing	low	1	1	1	1

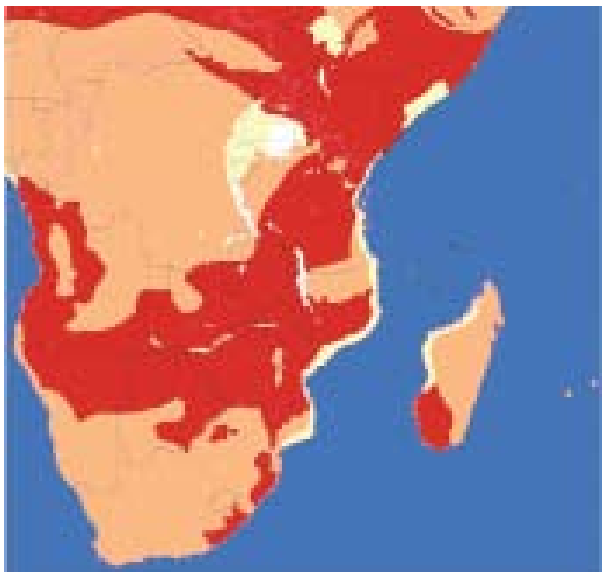

a farm are interdependent, and thus farms can be analysed as systems from various points of view. In this study, farm activities and household livelihoods embrace fishing, pastoralism, farm forestry, hunting and gathering, as well as cropping and intensive animal husbandry.

We joined the farming system values in the shapefile to the following table with scores where 1 represents low sensitivity and 3 represents high sensitivity. We used the overall score.

We then converted the shapefile to a grid and cropped the data to the analysis area. We changed the score values 1,2,3 to 3,6,9 respectively to be comparable with other layers (missing values were converted to zeros). This layer is shown in the figure with red areas representing the most sensitive areas. Full detail in metadata.

web-links:
http://www.fao.org/geonetwork/srv/en/main.home

World Bank, FAO

4.2.11 Own Food Production

weighting * 1

We consider countries which are able to produce a lot of food per person to be less sensitive to the effects of climate change. We used values of own food production in g/pp/day derived from the RCCP Food Economy Analysis for SADC countries for the period 2003-2005. Neighbouring countries to SADC in the north were given an average value (531g).

Tabular data were linked by country to the national boundaries shapefile (Digital Chart of the World) and then converted into raster format (1km^2 resolution) and cropped to the analysis area. All cell values were reclassified to a scale of 1-9 using Jenks natural breaks method to be comparable with other layers (missing values were converted to zeros). This layer is shown in the figure with red areas representing sensitive areas. Full detail in metadata.

web-links:
http://www.rccp.org.za

RCCP Food Economy Analysis for 2003-05, based on FAO data

4.2.12 Protein Consumption

weighting * 1

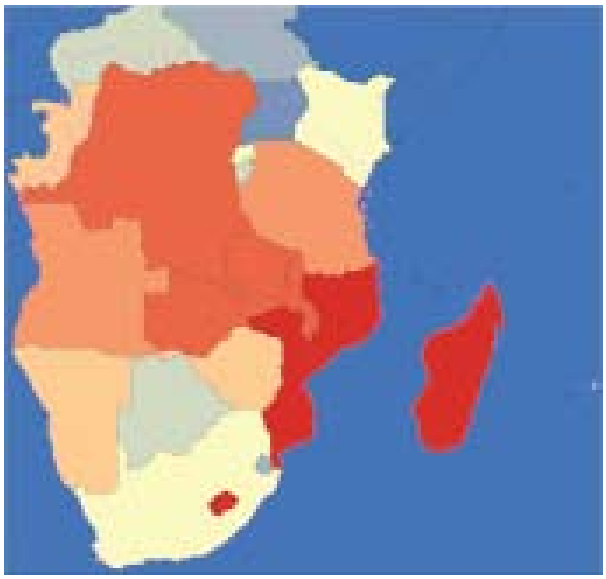

We consider countries which have better diet parameters to be less sensitive to the effects of climate change. We used values of Dietary Protein Consumption in g/person/day derived from the RCCP Food Economy Analysis for SADC countries for the period 2003-2005. Neighbouring countries to SADC in the north were given an average value (55g).

Tabular data were linked by country to the national boundaries shapefile (Digital Chart of the World) and then converted into raster format (1km^2 resolution) and cropped to the analysis area. All cell values were reclassified to a scale of 1-9 using Jenks natural breaks method to be comparable with other layers (missing values were converted to zeros). This layer is shown in the figure with red areas representing sensitive areas. Full detail in metadata.

web-links:
http://www.rccp.org.za

RCCP Food Economy Analysis for 2003-05, based on FAO data

4.2.13 Dietary Diversity

weighting * 1

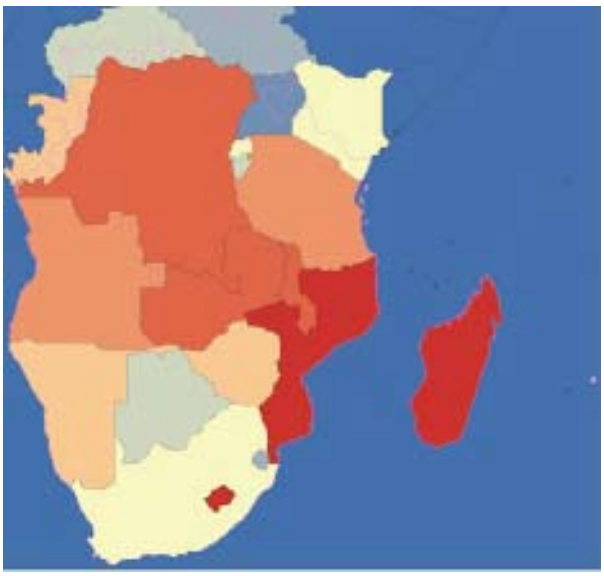

We consider countries which have better diet parameters to be less sensitive to the effects of climate change. We used values of Diet Diversification Index from FAO Food Security Statistics for African countries for the period 2003-2005.

Tabular data were linked by country to the national boundaries shapefile (Digital Chart of the World) and then converted into raster format (1km^2 resolution) and cropped to the analysis area. Values were inverted so that high diet diversification corresponded to low sensitivity. All cell values were reclassified to a scale of 1-9 using Jenks natural breaks method to be comparable with other layers (missing values were converted to zeros). This layer is shown in the figure with red areas representing sensitive areas. Full detail in metadata.

web-links:
http://www.fao.org

FAO Food Security Statistics for African countries for the period 2003-2005

4.2.14 Water Withdrawals

weighting * 2

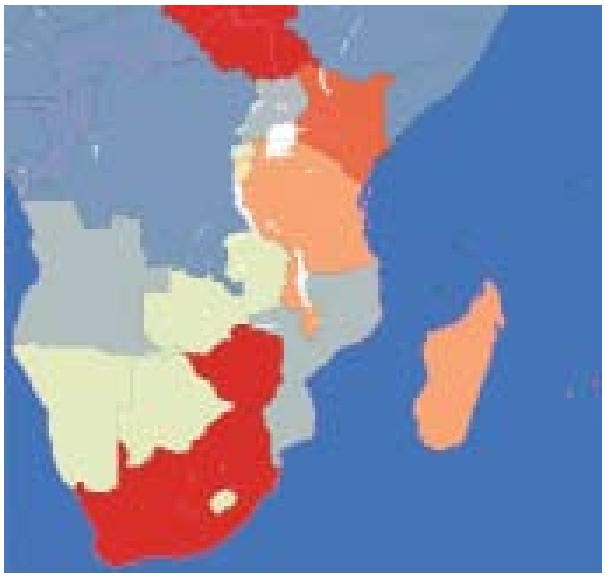

We consider countries which have higher rates of water withdrawals at present to be more sensitive to the effects of climate change. We used data from AQUASTAT on the intensity of freshwater withdrawals from total renewable resources.

Tabular data were linked by country to the national boundaries shapefile (Digital Chart of the World) and then converted into raster format (1km^2 resolution) and cropped to the analysis area. Values were inverted so that high diet diversification corresponded to low sensitivity. All cell values were reclassified to a scale of 1-9 using Jenks natural breaks method to be comparable with other layers (missing values were converted to zeros). This layer is shown in the figure with red areas representing sensitive areas. Full detail in metadata.

web-links:
http://www.fao.org/nr/water/aquastat/main/index.stm

AQUASTAT

4.2.15 People Living in Water Stress

weighting * 2

People living in water stress in today's conditions may be considered more sensitive to future climate change. We used a dataset showing thousands of people living in water stress from the African Water Stress Study (Vörösmarty et al. 2005). This provides the density of human population living above or below the relative water use threshold of 40%, presumed to indicate severe stress, under the 30-year recurrence drought.

These data are at reasonable resolution (12km^2) but there are many cell values missing because the model did not detect renewable resources. To smooth the data we ran a focal statistics analysis to determine the mean of values within 100km of each 1km^2 grid cell. All cell values were reclassified to a scale of 1-9 to be comparable with other layers (missing values were converted to zeros). This layer is shown in the figure with red areas representing high values of water stress / sensitivity. Full detail in metadata.

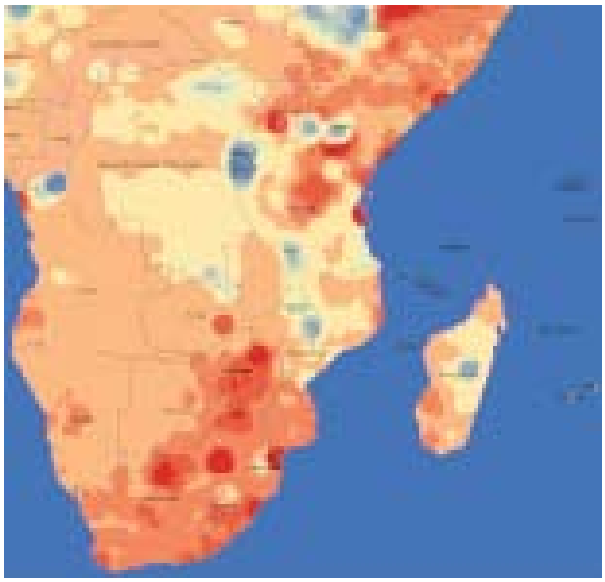

web-link:
http://wwdrii.sr.unh.edu/download.html

4.2.16 Forest loss

weighting * 2

We assume that deforestation has rendered certain areas of southern Africa more sensitive to climate stressors on account of the loss of normal vegetation cover, the slash and burn land use that often ensues, the depletion of biodiversity, the reduction in ecosystem services and significant loss of beneficial assets. Forest loss and degradation in the tropics is also considered responsible for 6-17% of all greenhouse gas emissions.

In this layer we combine three datasets: the Global Gross Forest Loss, the disturbed forest component of the WCMC Global Forests Dataset and a third dataset derived by comparing the historic extent of forests (WCMC) with the current extent of forest cover based on the MODIS Vegetation Continuous Fields product: *http://glcf.umiacs.umd.edu/data/vcf/*

Our start point is the Global Gross Forest Loss dataset which is widely considered to be the best available dataset on forest loss based on satellite interpretation (MODIS, Landsat), so this dataset takes precedence over the others in our aggregation. It represents the period 2000 – 2005 so is not a full account of historic forest loss. The grid resolution is quite large (approx. 20km x 20km) so it is unlikely that single grid cells exhibit 100% loss. Values between 0 and 100% were interpolated on our scale of 1-9. Source: *http://globalmonitoring.sdstate.edu/projects/gfm/index.html* Hansen et al. (2010).

The second component dataset is the 'disturbed' forest category within the Global Forests Dataset from WCMC. We chose to include this dataset because it revealed deforestation impact in lowland Africa (DRC) not shown in the previous dataset. This dataset represents historic status quo pre 1997, and is not now maintained. Because of caveats described for both datasets (Kapos pers. comm.; Hansen pers. comm.) we chose to give grid cells where disturbed forest was recorded a relatively low score of 3.

These two datasets still do not provide a full account of historic forest loss. To gain a representation of this we used the historic forest extent dataset at WCMC which is based on White's phytechoria. We added in areas of current forest from the Continuous Fields dataset that were missing in the historic extent (notably Cape forests). This historic dataset does not reveal forest density or treecover, it simply gives a representation of the full extent of vegetation classes considered forest and woodland. In order to obtain an estimate of % forest cover in the historic dataset we looked at current forest cover values from the Continuous Fields dataset and for each grid cell in the historic dataset we interpolated a % cover value from the closest values in the current forest extent dataset (Inverse Distance Weighting method based on closest 12 values). We could then subtract current % cover values from the interpolated historic % cover values to obtain a considered estimate of overall % cover loss through history. This derived dataset effectively filled gaps in our knowledge for forest that may have been depleted in past centuries. We validated the derived loss dataset by comparing it to current land cover (Globcover) and we found that areas indicated as forest loss corresponded well with anthropogenic transformation classes e.g. crop cultivation (Sahel) or areas of very high livestock density (northern Namibia and Botswana). Because estimates of tree cover or forest cover are low in these peripheral regions (5-10% treecover) the derived estimate of loss which is the absolute difference between historical cover and current cover is mostly very low too. We interpolated the figure of % cover loss to our chosen scale of 1-9. The derived dataset only includes high values of loss in areas considered to have been once closed forest but is now cleared e.g. along the Congo River.

These three datasets were then combined by taking the maximum value after consultation with Dr Valerie Kapos at WCMC and Dr Matthew Hansen at Geographic Information Science Center of Excellence – SDSU.

4.3 Exposure category layers: status quo (2008)

4.3.1 Coefficient of Variation for Inter-annual Rainfall

weighting * 2

Droughts and floods are more likely to occur in areas where rainfall is unpredictable and inconsistent. It is anticipated that variability of climate and the amplitude of extreme climate events will increase in the future (IPCC 2007c) but again it is not possible to be certain about where these effects will most be felt. We looked at the past patterns of unpredictable climate in southern Africa by using the coefficient of variation in mean annual precipitation.

The local variation of rainfall between years gives a good indicator of where droughts are most often experienced. However, where organizations use these data to indicate drought they often make the assumption that truly arid desert regions never experience drought because they are in a permanent state of drought, and filter out the data for those regions. This leads to an abrupt change in values where you move, for instance, from the semi-arid Pro-Namib to the truly arid Namib Desert. We felt that this abrupt change in exposure to drought along the border of semi-arid areas was not real in terms of drought experience for farmers either side of this arbitrary cut-off. For this reason we decided to combine two datasets, both derived from reliable long-term rainfall datasets: The first dataset makes no assumptions about drought incidence and purely presents rainfall variability so is complete for desert regions as well; the second dataset includes filters on drought incidence.

1. These data were calculated by the International Water Management Institute (IWMI) using the 100 year gridded precipitation dataset (CRU TS 2.0) developed by the University of East Anglia (Eriyagama et al. 2009). The latest version of this data set is available for download at the CRU web link below. All cell values were reclassified to a scale of 1-9 using the Jenks natural breaks method to be comparable with other layers (missing values were converted to zeros). This layer is shown in the figure with brown areas representing high values of exposure to unpredictable climate. Full detail in metadata.

web-links, sources, credits:
www.iwmi.org;
http://www.cru.uea.ac.uk/cru/data/hrg.htm

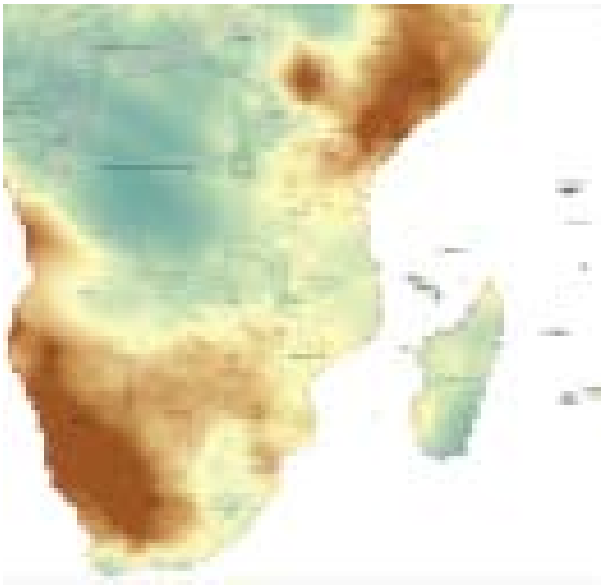

We are very grateful to Nishadi Eriyagama, Water Resources Engineer, International Water Management Institute (IWMI), P.O. Box 2075, Colombo, Sri Lanka, who forwarded the summary data on c.v. rainfall to the RCCP.

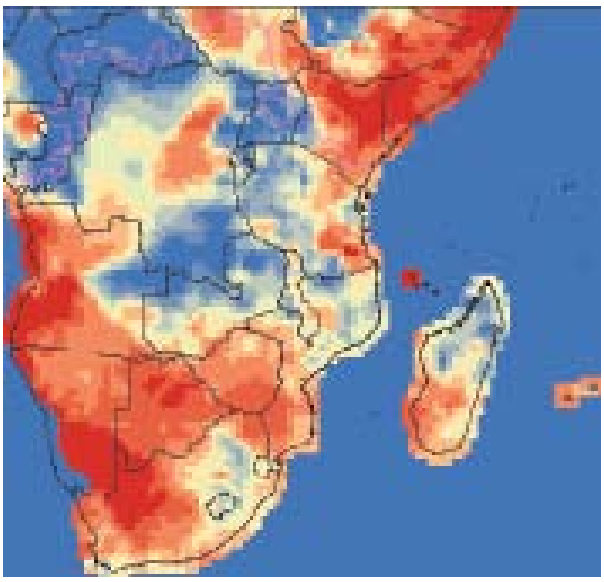

2. These data include an estimate of the Coefficient of variation (measure of precipitation variability relative to the climatological mean precipitation). It is based on two sources: 1) A global monthly gridded precipitation dataset obtained from the Global Precipitation Climatology Center (GPCC). 2) A GIS modeling of global Standardized Precipitation Index based on McKee et al. (1993) methodology. Unit is CV index multiplied x 100. This product

was designed by IRI and CIESIN (Columbia University) for the Global Assessment Report on Risk Reduction (GAR). It was modeled using global data. All cell values were reclassified to a scale of 1-9 using Jenks natural breaks method to be comparable with other layers (missing values were converted to zeros). This layer is shown in the figure with red areas representing exposed areas. Full detail in metadata.

web-links, sources, credits:
http://preview.grid.unep.ch/

Global Risk Data Platform (PreventionWeb), World Bank, UNEP, UNDP, UN/ISDR. Credit: IRI and CIESIN (Columbia University).

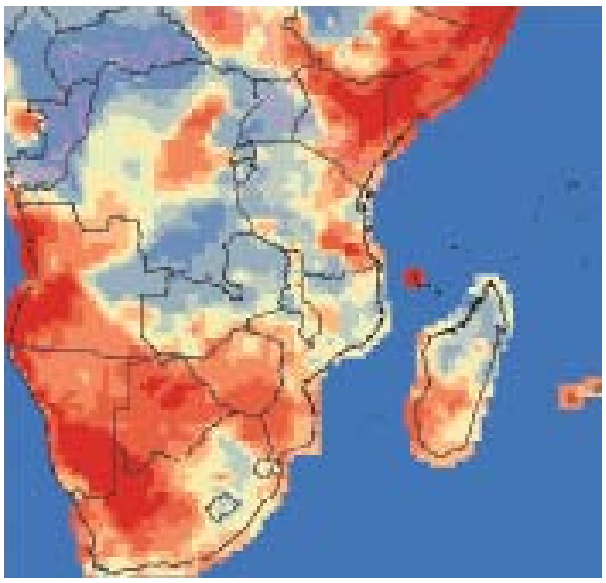

Both datasets reveal interesting patterns of interannual variation in rainfall across southern Africa with some subtle differences, and both are based on reliable long-term climate data. So we decided to use a maximum value of variability from the two datasets and in this way preserved the 'difficult' areas that were identified by both treatments while at the same time avoiding the unrealistic boundary effect around the true deserts. This layer is shown in the figure with red areas representing exposed areas. This was the final dataset we used with credits as above. Full detail in metadata.

4.3.2 Coefficient of Variation for Monthly Rainfall

weighting * 2

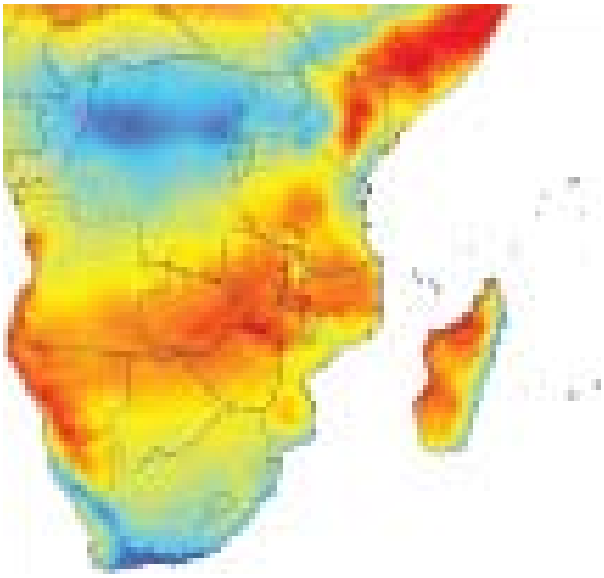

Unpredictability of rainfall over longer periods (between years) is probably our best indicator for likelihood of drought but we also considered that areas which experience high seasonality of rainfall would be exposed to more risk of climate change stressors than areas which received their rainfall consistently throughout the year. We used the Worldclim (Hijmans et al. 2005) Bioclimatic variable 'Bio15' which presents the coefficient of variation in rainfall across monthly intervals for the period 1950 – 2000 and represents a good indicator of seasonality at a high resolution (1km^2). This provides a good means for contrasting the seasonal rainfall across most of southern Africa with the consistent rainfall of the tropics. However, we do not feel that the low seasonality of rainfall experienced in the Karoo which falls between summer and winter rainfall regimes renders this very arid area less exposed to the stressors of climate change (rainfall in this region is unpredictable both across months and across years), consequently we gave this layer a lower weighting in the anlaysis.

We cropped the data to the analysis area. All cell values were reclassified to a scale of 1-9 using Jenks natural breaks method to be comparable with other layers (missing values were converted to zeros). This layer is shown in the figure with red areas representing exposed areas. Full detail in metadata.

web-links, sources, credits:
http://www.worldclim.org/

4.3.3 Risk of Cyclones

weighting * 2

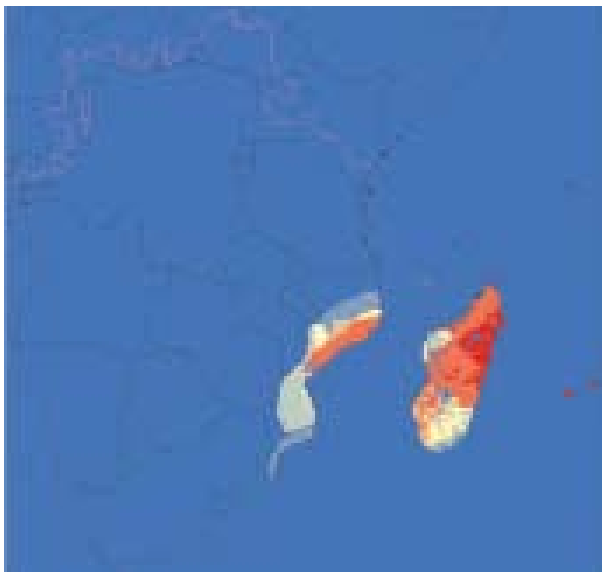

We obtained data on the incidence of cyclones from the Center for Hazards and Risk Research (Dilley et al. 2005). CHRR provide a Global Cyclone Hazard Frequency and Distribution grid. This is a 2.5 by 2.5 minute grid based on more than 1,600 storm tracks for the period 1 January 1980 through 31 December 2000 for the Atlantic, Pacific, and Indian Oceans that were assembled and modeled at UNEP/GRID-Geneva PreView. Post-modeling, the cells were divided into deciles, 10 classes consisting of approximately equal number of grid cells. The higher the value of the grid cell, the higher the decile ranking and the greater the frequency of the hazard relative to other cells. N.B. Areas of no data are not necessarily areas without hazard – a mask was used to exclude from analysis those areas that had a population density less than 5 persons per square kilometer and without significant agriculture.

We cropped the data to the analysis area. All cell values were reclassified to a scale of 1-9 using Jenks natural breaks method to be comparable with other layers (missing values were converted to zeros). This layer is shown in the figure with red areas representing exposed areas. Full detail in metadata.

web-links, sources, credits:
http://www.ldeo.columbia.edu/chrr/research/hotspots/coredata.html

Center for Hazards and Risk Research (CHRR); Center for International Earth Science Information Network (CIESIN), Columbia University; International Bank for Reconstruction and Development/The World Bank; United Nations Environment Programme Global Resource Information Database Geneva (UNEP/GRID-Geneva)

4.3.4 Risk of Floods

weighting * 2

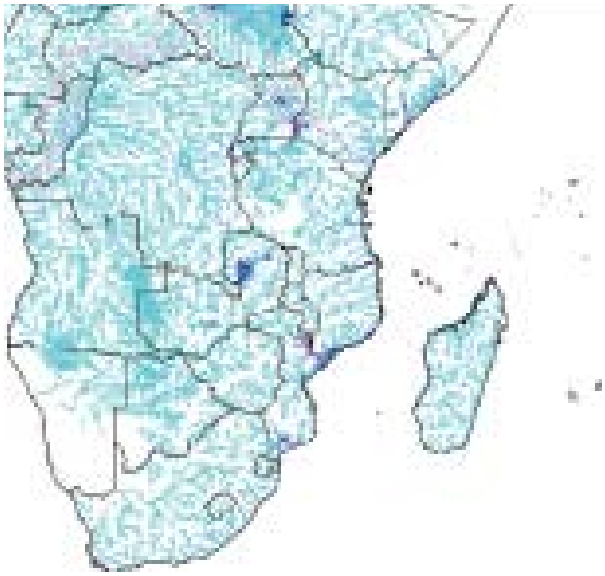

This dataset was generated as part of the Global Assessment Report on Disaster Risk Reduction (UNISDR, 2009). It includes an estimate of flood frequency. It is based on three sources: 1) A GIS modeling using a statistical estimation of peak-flow magnitude and a hydrological model using HydroSHEDS dataset and the Manning equation to estimate river stage for the calculated discharge value. 2) Observed flood from 1999 to 2007, obtained from the Dartmouth Flood Observatory (DFO). 3) The frequency was set using the frequency from UNEP/GRID-Europe PREVIEW flood dataset. In area where no information was available, it was set to 50 years returning period. Unit is expected average number of event per 100 years. This product was designed by UNEP/GRID-Europe for the Global Assessment Report on Risk Reduction (GAR). It was modeled using global data.

All cell values were reclassified to a scale of 1-9 using Jenks natural breaks method to be comparable with other layers (missing values were converted to zeros). This layer is shown in the figure with blue ranging to purple areas representing exposed areas. Full detail in metadata.

web-links, sources, credits:
http://preview.grid.unep.ch/

Global Risk Data Platform (PreventionWeb), World Bank, UNEP, UNDP, UNISDR. Credit: GIS processing UNEP/GRID-Europe, with key support from USGS EROS Data Center, Dartmouth Flood Observatory 2008.

4.3.5 Standardised Precipitation Index

weighting * 2

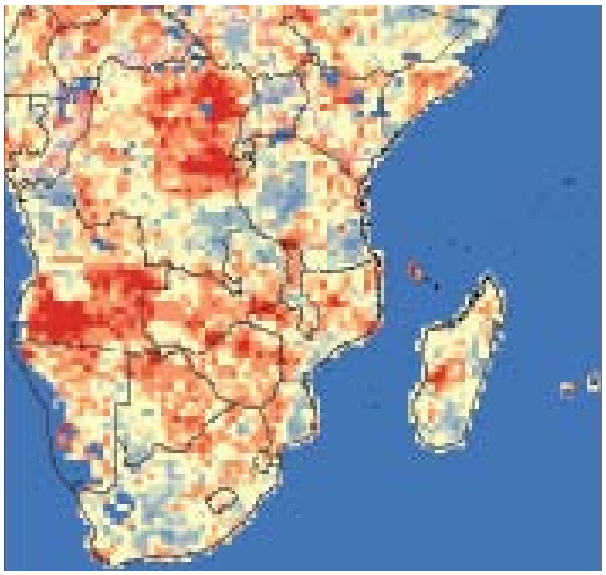

This dataset includes an estimate of Standardized Precipitation Index with a 6 month time interval to indicate areas susceptible to drought based on detailed temporal patterns in rainfall. It is based on two sources: 1) A global monthly gridded precipitation dataset obtained from the Global Precipitation Climatology Center (GPCC). 2) A GIS modeling of global Standardized Precipitation Index based on McKee et al. (1993) methodology. Unit is SPI index. This product was designed by IRI and CIESIN (Columbia University) for the Global Assessment Report on Risk Reduction (GAR). It was modeled using global data.

All cell values were reclassified to a scale of 1-9 using Jenks natural breaks method to be comparable with other layers (missing values were converted to zeros). This layer is shown in the figure with red areas representing exposed areas. Full detail in metadata.

web-links, sources, credits:
http://preview.grid.unep.ch/

Global Risk Data Platform (PreventionWeb), World Bank, UNEP, UNDP, UN/ISDR. Credit: IRI and CIESIN (Columbia University).

4.3.6 Fire frequency

weighting * 1

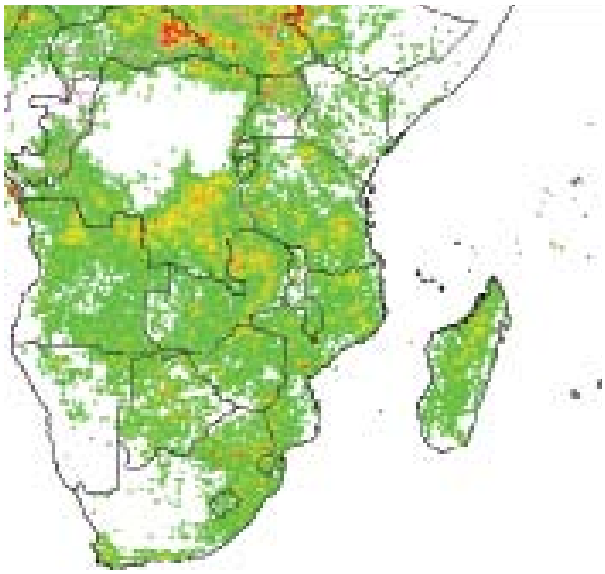

This dataset includes an estimate of fires events over the period 1997-2008. It is based on the modified algorithm 1 product of World Fire atlas (WFA, ESA-ESRIN) dataset. UNEP/GRID-Europe compiled the monthly data. This product was aggregated by UNEP/GRID-Europe for the Global Assessment Report on Risk Reduction. It was modeled using global data.

All cell values were reclassified to a scale of 1-9 using Jenks natural breaks method to be comparable with other layers (missing values were converted to zeros). This layer is shown in the figure with green ranging to red areas representing exposed areas. Full detail in metadata.

web-links, sources, credits:
http://preview.grid.unep.ch/

Global Risk Data Platform (PreventionWeb), World Bank, UNEP, UNDP, UN/ISDR. Credit: GIS processing World Fire atlas (ESA-ESRIN).

4.3.7 Disaster Events: Number of Events by Area

weighting * 1

To further identify areas where climate-related disasters may be anticipated in the future, we looked at the past record of where these disasters have occurred. We used data from EMDAT on the number of disaster events by country for all periods 1900 – 2009. We included those categories of disasters which we felt could be affected by climate change: droughts, extreme temperatures, floods, mass movements, storms.

Tabular data were linked by country to the national boundaries shapefile (Digital Chart of the World). We then standardised the number of events for each country by dividing that number by the area of the country. We then converted the polygon data into a floating point raster format (1km^2 resolution) and cropped to the analysis area. All cell values were reclassified to a scale of 1-9 using Jenks natural breaks method to be comparable with other layers (missing values were converted to zeros). This layer is shown in the figure with red areas representing exposed areas. Full detail in metadata.

web-links, sources, credits:
http://www.emdat.be/advanced-search

WHO Collaborating Centre for Research on the Epidemiology of Disasters (CRED): Emergency Events Database EM-DAT

4.3.8 Disaster Events: Numbers Affected per Population

weighting * 1

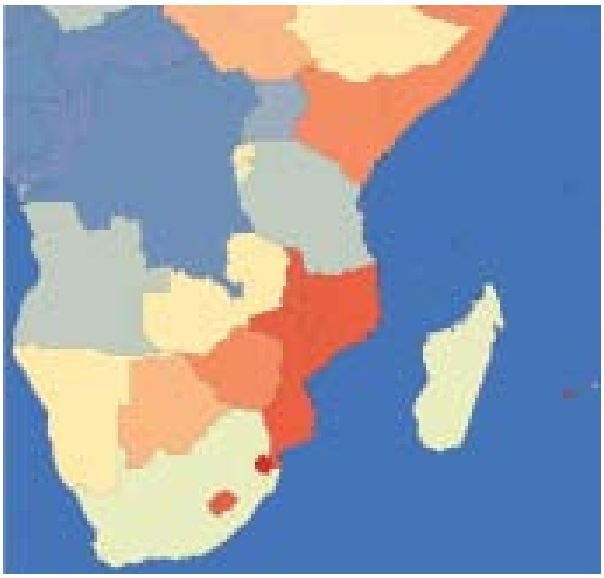

To further identify areas where climate-related disasters may be anticipated in the future, we looked at the past record of where people have been affected by these disasters. We used data from EMDAT on the number of people affected by disaster events by country for all periods 1900 – 2009. We included those categories of disasters which we felt could be affected by climate change: droughts, extreme temperatures, floods, mass movements, storms.

Tabular data were linked by country to the national boundaries shapefile (Digital Chart of the World). We then standardised the number of people affected by dividing that number by the population of the country. We then converted the polygon data on numbers affected per one thousand of population into a floating point raster format (1km^2 resolution) and cropped to the analysis area. All cell values were reclassified to a scale of 1-9 using Jenks natural breaks method to be comparable with other layers (missing values were converted to zeros). This layer is shown in the figure with red areas representing exposed areas. Full detail in metadata.

web-links, sources, credits:
http://www.emdat.be/advanced-search

WHO Collaborating Centre for Research on the Epidemiology of Disasters (CRED): Emergency Events Database EM-DAT

4.4 Layer overlays: status quo (2008)

4.4.1 Adaptive capacity summary layer 2008

We used the following combination of grid layers to perform a weighted overlay for the adaptive capacity summary layer shown below:

((A_pov_infra) * 2) + ((A_GDP_pc) * 3) + ((A_abovewt) * 3) + ((A_educ_ind) * 2) + ((A_health_exp) * 2) + (A_malaria) + (A_tsetse) + ((A_HIV_neg) * 2) + ((A_imp_water) * 3) + (A_cell_subs) + ((A_travelt) * 2) + ((A_nightlights) * 3) + ((A_agric_GDP) * 2) + (A_water_dis) + (A_irrigpot * 2) + (A_conflicts) + (A_governance * 2) + (A_forestres) + (A_biodiv * 2)

We inverted the values such that high values, shown in red here, represent incapacity for change.

Although we strived to access geographically detailed datasets, a number of the datasets for this category could only be acquired at the national scale. This is not considered to be a major drawback because we believe that the response of a community to adapt to potential climate stressors is likely to be strongly influenced by the nation's capacity.

It is clear from the adaptive capacity summary map that South Africa, closely followed by Namibia and Botswana, form a major block of socio-economically stronger countries in the south-west, while Mauritius also has a very high adaptive capacity. Lesotho, Swaziland and Zimbabwe are intermediate while the DRC, Zambia, Mozambique, Tanzania, Madagascar, Angola and Malawi all have weaker socio-economic conditions, and thus adaptive capacity to climate-related risk.

The high adaptive capacity of the south-west block is primarily a function of wealth and associated infrastructure availability, combined with stable government and peace. Angola, Zimbabwe and the small inland nations of Swaziland and Lesotho have higher values for GDP per capita than countries further north and east. Intense economic activity and extensive infrastructure are indicated by the night lights concentration, these extend up through Zimbabwe and through the copper belt in Zambia. There is good infrastructure access in South Africa and Zimbabwe and from the coastal ports inland; in the DRC access is evident along the rivers. The south-west block also shows the highest proportion of cellular telephone subscribers, although Zambia is unexpectedly high in this regard and it is well known that the cellular networks are well used throughout the continent. South Africa, Namibia, Botswana, Lesotho, Zimbabwe and Mauritius provide the best standards of education in the region. Apart from Zimbabwe, these countries also enjoy better governance and lack of conflict.

The south-west block scores high in health – these countries allocate a large portion of their GDP to health and have best access to improved water. Malawi and Zimbabwe also score unexpectedly high in this regard. Mozambique and DRC are poorest in terms of access to improved water. One of the few criteria which the south-west block achieve a high incapacity score for is the incidence of HIV which is highly prevalent in this region and along the transport corridors into Zimbabwe, Zambia, Mozambique and Malawi. Incidence of HIV and its debilitating effects on the population are far lower in Angola, DRC, Tanzania and Madagascar. The other strength of the north-west block (DRC, Angola) and Madagascar lies in its valuable forest resources which provide economic benefits and critical ecosystem services.

The south-west block extending into southern parts of Angola, Zambia, Zimbabwe and Mozambique, is largely free of tsetse flies which are vectors to significant livestock diseases. DRC and northern Angola are suitable for the greatest diversity of tsetse fly groups and species. South Africa (excluding the Lowveld), Lesotho, southern Botswana, southern Namibia and Zimbabwe are the only major regions of SADC that do not experience endemic malaria.

The less developed countries at lower latitudes show high reliance on agriculture's contribution to national GDP, which makes them more susceptible to climate risk. Whilst these countries currently do not tap into their often considerable water resources for irrigated crop production, high potential for the development of irrigation schemes exists across the region which could stabilise yields and boost productivity.

The recurring patterns outlined above are not, however, reflected in the distribution of high levels of biodiversity. Countries with the highest biodiversity (innate value and what needs to be protected i.e. what is rare and vulnerable) include Madagascar, Tanzania, South Africa, Zambia and Botswana, with smaller pockets in other countries. These resources, if managed sustainably, provide potential adaptive capacity.

RCCP Health and Food Security Risk Profile Mapping for Southern Africa
Adaptive Capacity
Phase 2: current conditions and recent history

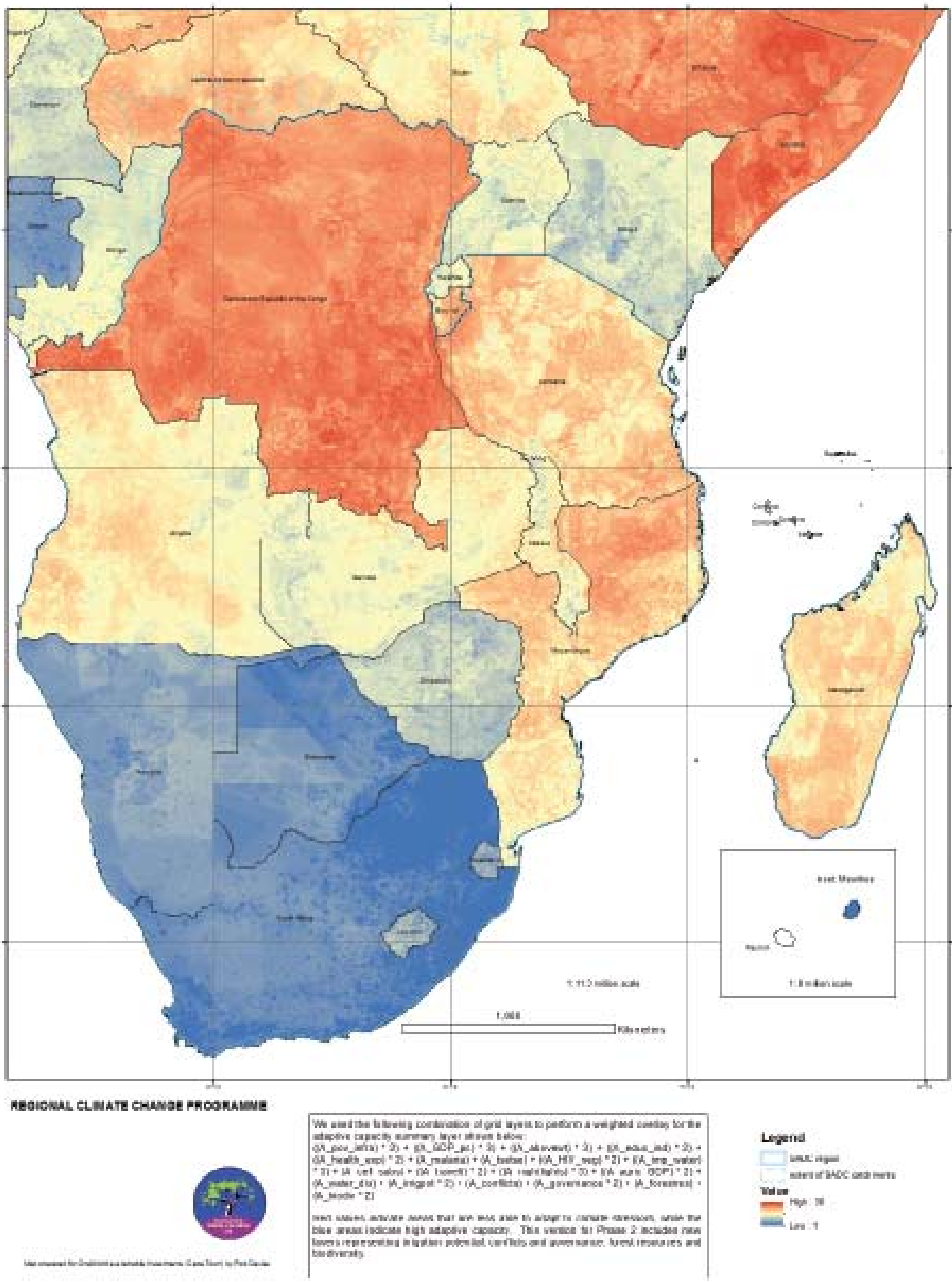

4.4.2 Sensitivity summary layer 2008

We used the following combination of grid layers to perform a weighted overlay for the sensitivity summary layer shown below:

((S_irrigated) * 3) + ((S_app_NPP) * 2) + ((S_rain_pp_crop) * 3) + ((S_popd_agric) * 2) + ((S_lgp) * 2) + ((S_avail_soilM) * 3) + ((S_soil_deg) * 2) + ((S_slope) * 2) + ((S_npp) * 2) + (S_agric_syst) + ((S_food_prod) * 1) + ((S_prot_cons) * 1) + ((S_diet_div) * 1) + ((S_waterwithd) * 2) + ((S_water_str) * 2) + (S_forestloss * 2)

Red values indicate environments that are most sensitive to climate stressors, while the blue areas indicate low sensitivity.

The regions of southern Africa that are revealed to be most sensitive to climate stressors follow, to a large degree, the Afro-montane belt, including the arid areas. This is in contrast to a stable, resilient region in the tropical Congo basin. Lesotho, Swaziland, Zimbabwe and Malawi emerge as the most sensitive countries to climate stressors, followed by South Africa, Tanzania and Zambia. The arid south-western corner of Madagascar is noticeably sensitive. There is a small dense patch showing environmental sensitivity near the border in northern Namibia. This is due to very high values here for density of people on agricultural land, low water supplies per capita on agricultural land and high appropriation of net primary productivity. Most of the network of these small patches and corridors of high sensitivity through central southern Africa can be attributed to the distribution of high human population density in centres and along the main transport routes. Wherever these high densities correspond to other environmental disadvantages such as soil degradation they appear most noticeably in the sensitivity map.

Northern and eastern Angola and northern DRC emerge as the least sensitive regions in southern Africa to climate stressors. Mauritius also has a very low value for sensitivity as measured this way. Some countries exhibit a very patchy distribution of sensitivity with areas of resilience in southern Tanzania, northern and central Mozambique, northern Zambia, and northern Madagascar. Protected areas are noticeable for low values of sensitivity on account of their low population density.

RCCP Health and Food Security Risk Profile Mapping for Southern Africa
Sensitivity
Phase 2: current conditions and recent history

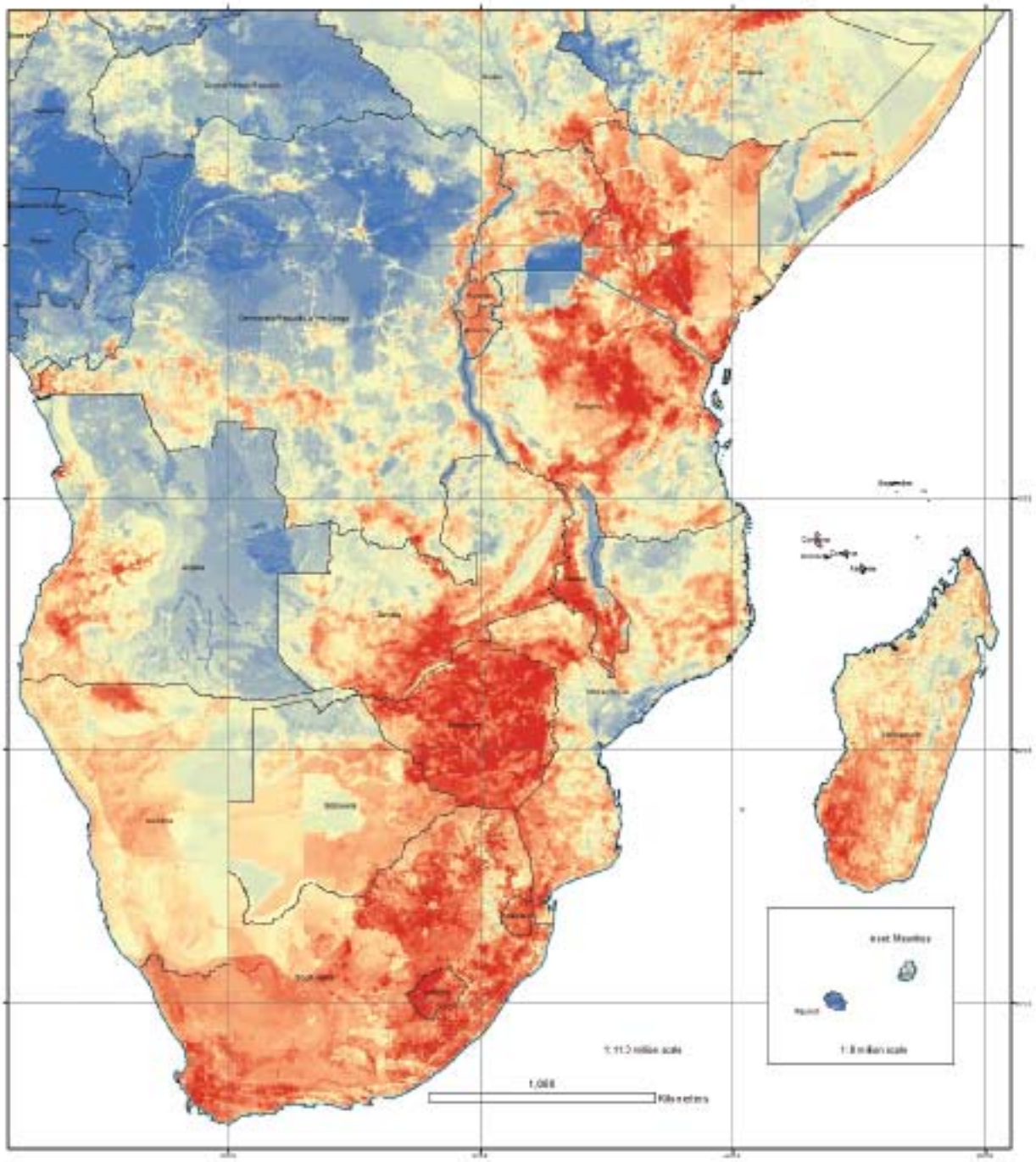

REGIONAL CLIMATE CHANGE PROGRAMME

Sensitivity: Red values indicate where people are most likely to be in need of help adapting to climate stressors, while the blue areas indicate patches of resilience. Calculated as:
(S_irrigated) * 0) + (S_app_hh*) * 2) + (S_rain_dp_crop * 3) + (S_popd_agric * 3) + (S_lgp * 2) + (S_avail_cattle * 3) + (S_soil_deg * 2) + (S_slope * 3) + (S_npp * 2) + (S_agric_dyst) + (S_road_prox * 1) + (S_prot_area * 1) + (S_dwt_dv * 1) + (S_waterwithd * 1) + (S_water_str * 2) + (S_forestloss * 2)
This version for Phase 2 includes a new term representing forest loss. See report (Phase 2) for further detail.

4.4.3 Exposure to climate risk summary layer 2008

We used the following combination of grid layers to perform a weighted overlay for the exposure to climate risk summary layer shown below:

((max2methsraincv) * 2) + ((E_mcv_monthly) * 2) + ((E_cyclones) * 2) + ((floodfreq) * 2) + ((SPI) * 2) + ((firefreq) * 1) + ((E_dis_event) * 1) + ((E_dis_affect) * 1)

Red values indicate areas that are most exposed to climate stressors, while the blue areas indicate low exposure.

The past and current experience of climate stress in southern Africa are presented in this category, including national data on historical natural disaster events that are climate-related and the numbers of people affected by these. Of great bearing is the variability of weather over southern Africa giving rise to droughts, floods and other extreme events.

Our summary layer for this category indicates the following states as being most at risk to climate stress: Madagascar, Mozambique, Mauritius, Malawi, Zimbabwe, Botswana, and parts of Namibia, Angola, Zambia and Swaziland. Thus, the greatest exposure to climate risk follows a broad latitudinal band (roughly between 12°S and 25°C). The map of exposure risk highlights the impact of cyclones and floods along the eastern sea board of southern Africa and on the island states. Cyclones hit Mauritius, Madagascar and Mozambique the hardest but are able to penetrate inland to southern Malawi, eastern Zimbabwe and Swaziland. Arid and semi-arid regions in the south-west are also exposed to climate risk mainly due to periodic droughts, but also risk of flash floods.

The least exposed regions to climate stress in southern Africa are DRC, north-eastern Angola, southern and eastern South Africa and (as with sensitivity) an area in southern Tanzania, western Tanzania, and, surprisingly, the south-eastern corner of Madagascar. One would expect the climate in the tropical lowlands, characterised by high rainfall and low rainfall variability, to be least exposed to climate stress.

RCCP Health and Food Security Risk Profile Mapping for Southern Africa
Exposure to Risk
Phase 2: current conditions and recent history

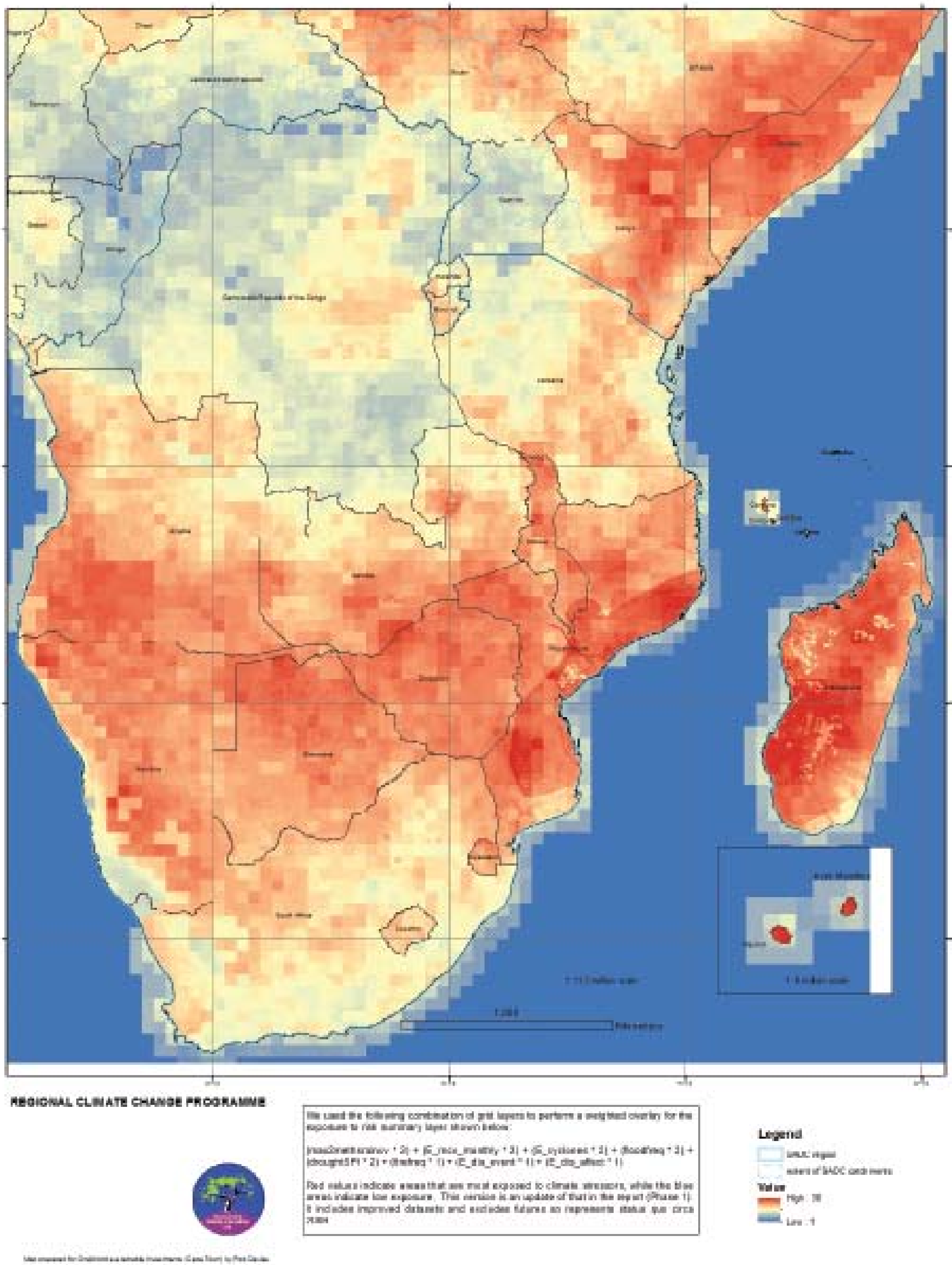

4.4.4 Problem areas (impact) overlay 2008

We derived the following layer as (sensitivity * 2) + exposure, thus giving sensitivity a higher weighting. The reason for this was that the 16 high quality sensitivity layers should receive a higher weighting than the eight slightly lower quality exposure layers.

Red values indicate 'problem area' (impact) while the blue areas indicate low impact.

This combined layer represents the current impact of climate stressors regardless of any local adaptive capacity. With sensitivity and exposure categories combined like this, the Afro-montane belt becomes very evident as an area of high impact in contrast to the Congo basin and other small patches.

Most of the eastern seaboard and islands, apart from an area north and south of the Tanzania-Mozambique border in the vicinity of Niassa, are highlighted as high impact areas; and most of the arid areas of south-western SADC are highlighted as high impact areas.

Zimbabwe appears to be the most highly impacted country on this map but actually, the smaller nations of Swaziland and Lesotho carry slightly higher overall scores for this combination. Malawi also carries a high score. All four of these countries score as highly vulnerable to the anticipated impact of climate stressors. At a sub-national level, parts of Madagascar, Mozambique, Zambia and Tanzania contained 'high impact' areas.

The stable, productive and humid ecosystems of the lowland tropics form a centre of resilience by contrast and this influence apparently extends into eastern Angola and adjoining lowland areas of Tanzania and Zambia. The larger patch of resilience in southern Tanzania and Niassa is the effect of lack of crowding in this region and more fertile soils (sensitivity category).

RCCP Health and Food Security Risk Profile Mapping for Southern Africa
Problem Areas (sensitivity + exposure)
Phase 2: 2050

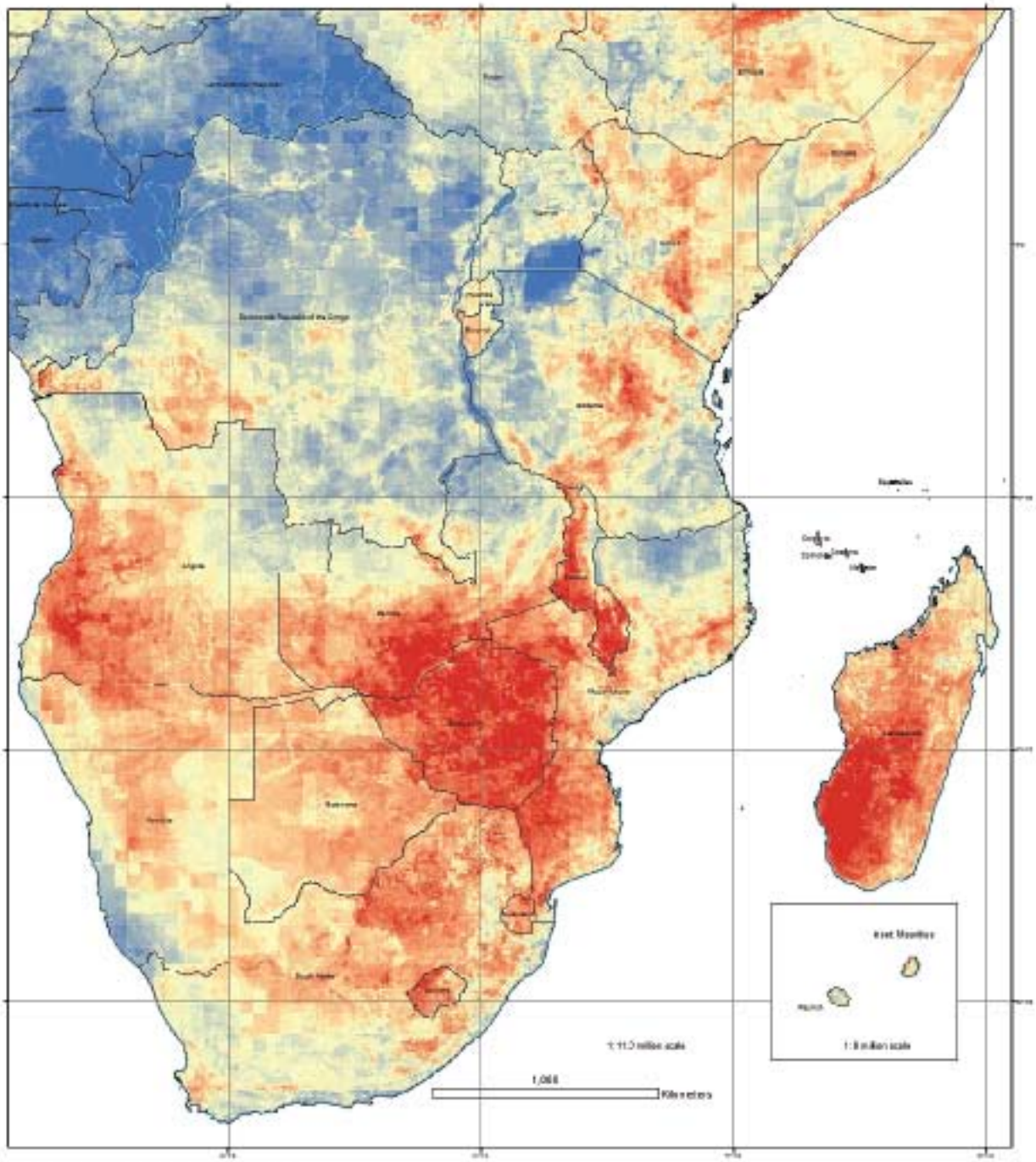

REGIONAL CLIMATE CHANGE PROGRAMME

Identified areas where people are likely to encounters problems from climate stressors by adding the layers for sensitivity and exposure. Red values indicate 'problem areas', while the blue areas indicate low sensitivity and exposure. See report (Phase 2) for further detail

4.4.5 Vulnerability Hotspots 2008

The final summary hotspot layer in the analysis is derived as (sensitivity * 2) + exposure + adaptability (thus problem areas + adaptability).

Red values indicate hotspots where people are most likely to be in need of help adapting to climate stressors, while the blue areas indicate patches of resilience.

Introducing the adaptive capacity factor changes the emphasis and distribution of the problem areas profoundly. Most of the data layers in the adaptive capacity category are from national data tables so the effect on this final hotspots layer is for abrupt change across the national boundaries.

The national order of priorities is thereby changed. The high impact areas across the arid countries of Namibia, South Africa and Botswana are no longer evident. These three countries, and Mauritius, have a greater capacity for dealing with problems. The implication is not that problems will not occur in these countries with climate stressors, but rather that other SADC countries may be expected to suffer more on account of their reduced capacity for adaptation.

Swaziland and Lesotho are still visible as hotspots but their representation as high impact areas is diminished by reasonably high adaptive capacity, as is that of Zimbabwe. These top three countries in terms of high climate impact are now displaced by Mozambique, Madagascar, Malawi, Zambia and Tanzania with adaptive capacity taken into account. Almost the entire country of Mozambique, except the far north and the floodplain area around Beira, now appears as a hotspot. In Tanzania, a very large hotspot occupies the centre of the country and spills through into highly populated areas of Kenya which share a river catchment. A hotspot is also evident in the semi-arid south-west of Angola.

The smaller impact areas in DRC are accentuated in this hotspot summary layer as a result of the poor adaptive capacity in this country.

RCCP Health and Food Security Risk Profile Mapping for Southern Africa
Hotspots: (sensitivity * 2) + exposure + adaptability
Phase 2: current conditions and recent history

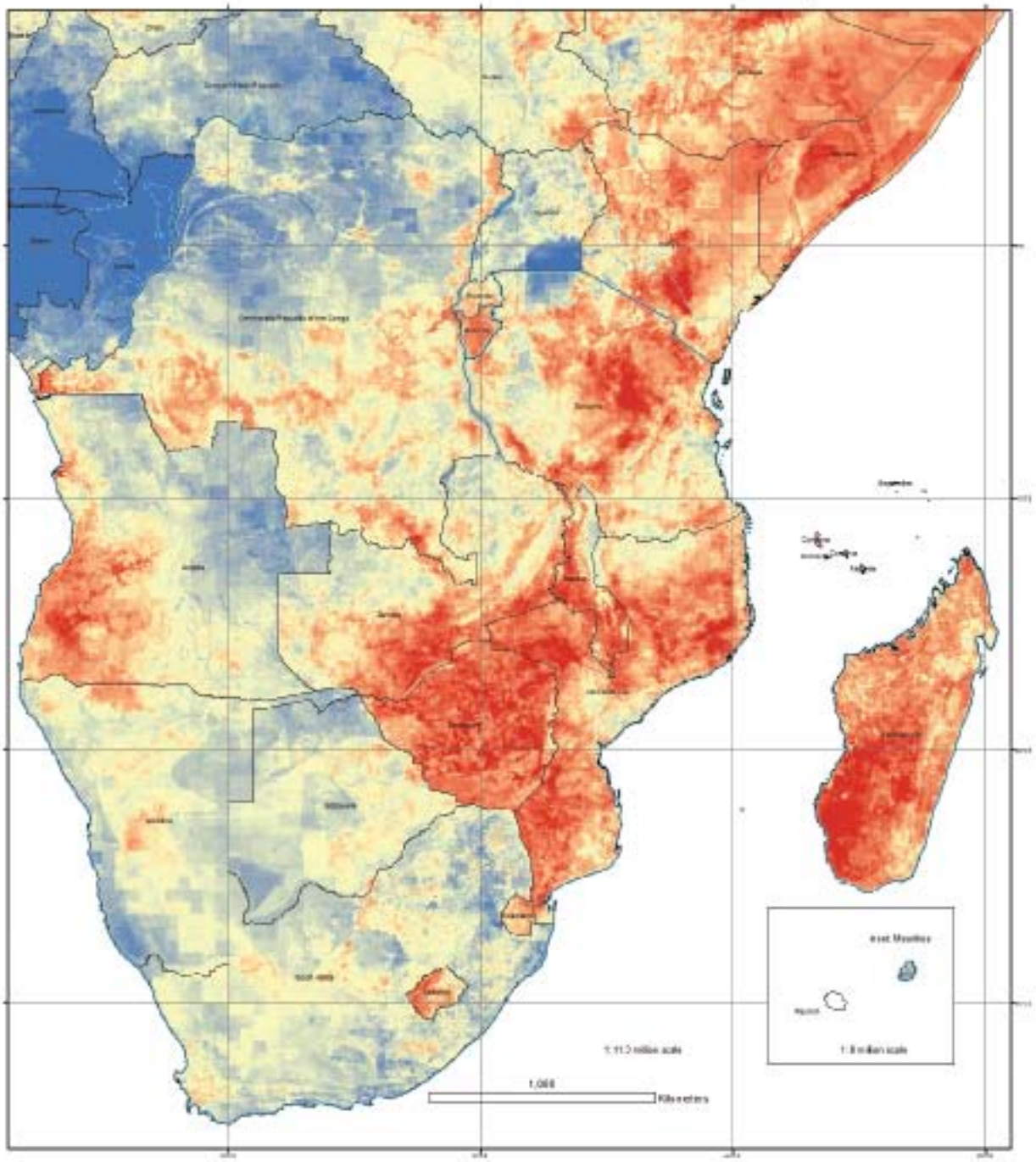

REGIONAL CLIMATE CHANGE PROGRAMME

Actual hotspots are derived : (sensitivity * 2) + exposure + adaptive capacity. Red values indicate 'hotspots' where people are most likely to be in need of help adapting to climate stressors, while the blue areas indicate patches of resilience. See report (Phase 2) for further detail.

Legend

4.4.6 Averaged problem areas (impact) and vulnerability hotspots 2008

The fine-resolution geographic data presented in the previous summary layers is highly patchy and granular. We aggregated the grids of the summary layers to a coarser resolution (10km^2), converted the raster data to point data and then carried out a kernel density analysis to provide the following

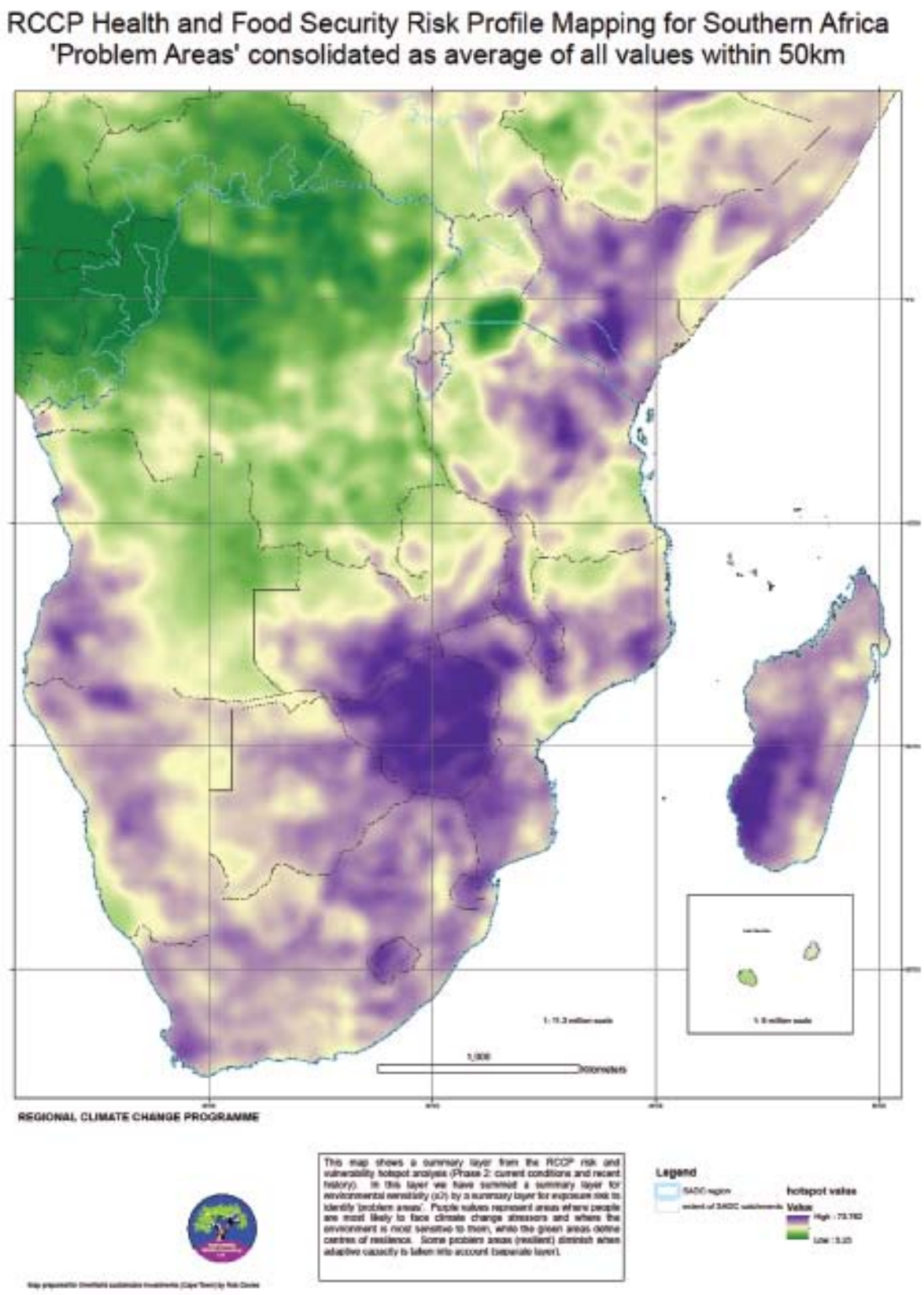

figures which help to clarify the patterns and identify the locations of obvious hotspots or centres of resilience. The first figure shows average values within a 50km radius of (sensitivity*2) + exposure values. From this figure, and from the following figure which shows the same treatment for hotspot values, we were able to identify and map the focal points for SADC and surrounds.

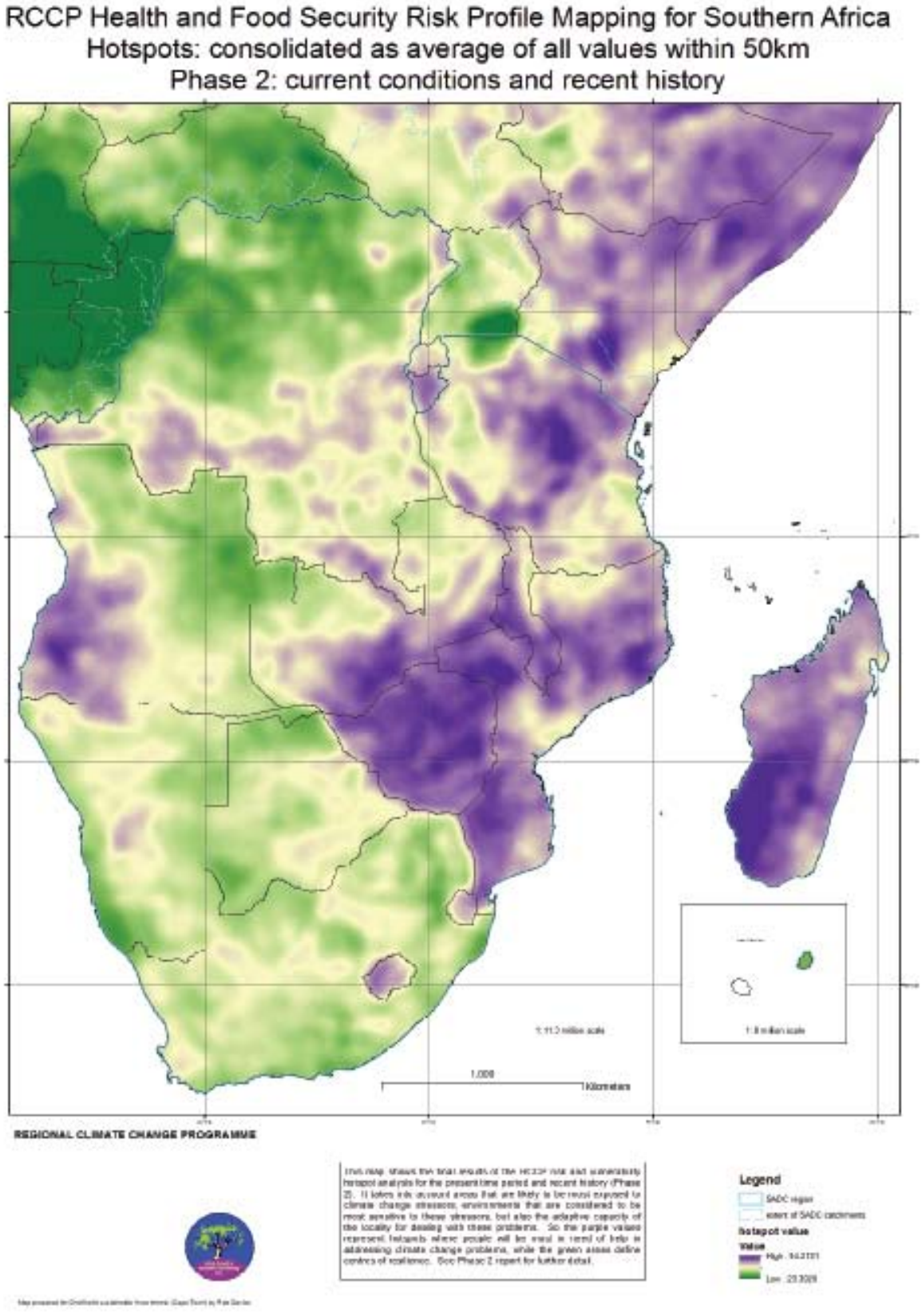

5. Future (2050) Risk and Vulnerability

How are these vulnerability hotspots likely to change over the next roughly 40 years, to 2050, under projected climate and population changes across southern Africa? For this analysis we took the approach that the Exposure category would be further developed to reflect the climatic and population futures for the region. For now, we make the assumption that current Adaptive Capacity and Sensitivity will remain the same over this time period. Further iterations of the mapping could conceivably analyse how these categories may change (e.g. through rapid socio-economic development of some countries) and in themselves become responsive to climate and population change, particularly the components of the Sensitivity category.

The following layers (for 2050) were added to the Exposure category (status quo). The assumption is that current exposure to climatic stressors will remain, but will be exacerbated by additional pressures arising from population growth, future climate change, resulting loss of cropland, and sea level rise.

5.1 Exposure category layers: future (2050)

5.1.1 Additional population density

weighting * 3

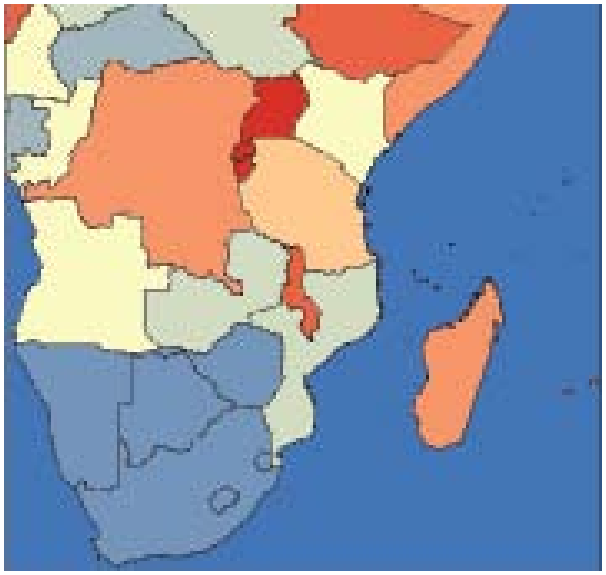

While much uncertainty still surrounds expected climate change for southern Africa in 40 years time, we can be more certain that the human population in this region is going to increase dramatically over this time period. We use the UNPD Population Division projections of population change which are based on current growth and detailed national cohort data. The report 'World Population to 2300' uses projections to 2050, together with historical population estimates back to 1950, from the *2002 Revision* of the official United Nations population projections, the eighteenth and latest such revision. Long-range projections are made by extrapolation of recent trends by country.

The report indicates that the population for the SADC region (Seychelles data not provided) may be expected to increase by 231 million between 2000 and 2050, to a total of 447 million. However, this expected increase in the human population of the region is not expected to be distributed evenly. The report documents that three African regions, East Africa, Middle Africa, and West Africa, will grow unusually fast in comparison to every other region through 2100, even though total fertility will be close to replacement by 2050. This is despite the prediction that by 2045-2050, life expectancy in Africa is projected to be 11 years shorter than in the next lowest region. In southern Africa a decline in life expectancy to a lower level than anywhere else is predicted through the influence of HIV, but life expectancy will rebound, rise quite rapidly, and overtake other African regions beyond 2050. The following table presents data for SADC countries from this report giving population size in thousands and an area estimate in km^2 (calculated using the continent in a Lambert Conformal Conic projection). The difference between 2000 data and the 2050 projection is expressed as an additional density that will need to be accommodated in persons/km^2.

We reclassified the additional density values onto a scale of 1 to 9 with highest values of additional density shown in red on the graphic. For SADC countries we can expect most population growth impact to occur in Mauritius and Malawi, followed by Madagascar and DRC, then Tanzania, then Angola. Mozambique and Zambia show intermediate impact. The southern block consisting South Africa, Namibia, Botswana, Zimbabwe, Lesotho and Swaziland, show very low or even negative impact of population growth linked to the demographic influence of HIV over the next four decades.

COUNTRY	AREA	1950	2000	2050	2000-2050 DIFFERENCE	ADDITIONAL DENSITY
Mauritius	1835	493	1186	1461	275	150
Malawi	106755	2881	11370	25949	14579	137
Madagascar	567389	4230	15970	46292	30322	53
Democratic Republic of the Congo	2029830	12184	48571	151644	103073	51
Tanzania	823245	7886	34837	69112	34275	42
Angola	1123160	4131	12386	43131	30745	27
Mozambique	738734	6442	17861	31275	13414	18
Zambia	680930	2440	10419	18528	8109	12
Namibia	817652	511	1894	2654	760	1
Zimbabwe	372137	2744	12650	12658	8	0
Botswana	572656	419	1725	1380	-345	-1
South Africa	1346610	13683	44000	40243	-3757	-3
Swaziland	18239	273	1044	948	-96	-5
Lesotho	33865	734	1785	1377	-408	-12

With the decline in water resources and rainfed agricultural production that is expected to accompany climate change in southern Africa over the next decades, nations which will need to accommodate a significantly larger density of people in 2050 will experience unfavourable change in the associated *per capita* water and food resources. We treat population growth as a highly significant future source of stress across the region and give it maximum weighting in the overlay analysis. Full detail in metadata.

web-links, sources, credits:
http://www.un.org/esa/population/publications/longrange2/WorldPop2300final.pdf

United Nations Department of Economic and Social Affairs/Population Division 9
World Population to 2300

5.1.2 1 in 10 year drought

weighting * 1

It is widely held that, in addition to overall warming and changes in rainfall amounts, there will be greater variability in climate and a greater frequency of more extreme climate events. In our exposure category we already include data layers on current geographic variability in climate (e.g. coefficient of variation of rainfall and drought indices). For the futures analysis we access a relevant projection on extreme drought events from a GCM which offers high resolution output and shows good representation of current climate: MIROC (high resolution), scenario A1b.

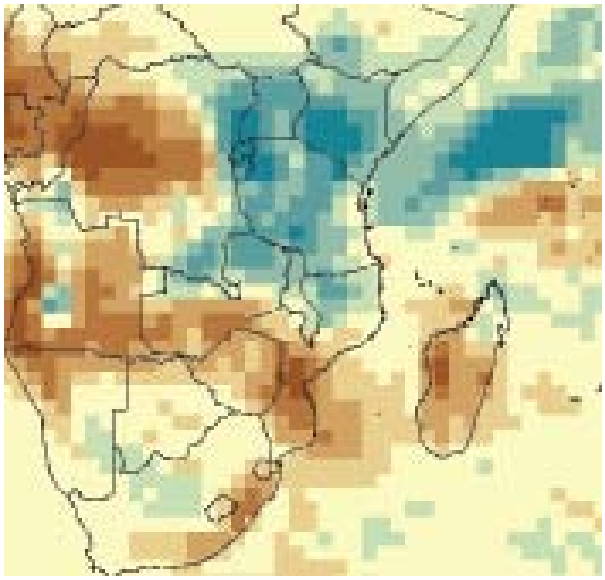

We use this model to extract comparative data on the 1 in 10 year drought value from two centuries: we compare 2000 -2100 with 1900-2000. We selected seasonal rainfall corresponding to the austral summer (November – March) as this is the principal food production period for southern Africa. A return value was obtained for each decade within the respective centuries which provides the extreme value for the minimum rainfall or 1 in 10 year drought event. We then compared these return values for the two time periods and the resulting difference is plotted in the graphic with brown areas representing worsening of the drought return levels over this century. There is broad correspondence between this pattern and the overall expected change in precipitation (5.1.3) but the current analysis represents an extreme

level of precipitation rather than a mean level. Intensification of drought in the DRC is apparent. All climate data were extracted as summarized geotiff files from the Climate Explorer website *http://climexp.knmi.nl*, under the advice and in consultation with Geert Jan van Oldenborgh (whose help is gratefully acknowledged). Full details on the method are provided in Shongwe et al. (2009). Full detail in metadata.

web-links, sources, credits:
http://climexp.knmi.nl/

5.1.3 GCM ensemble precipitation change

weighting * 3

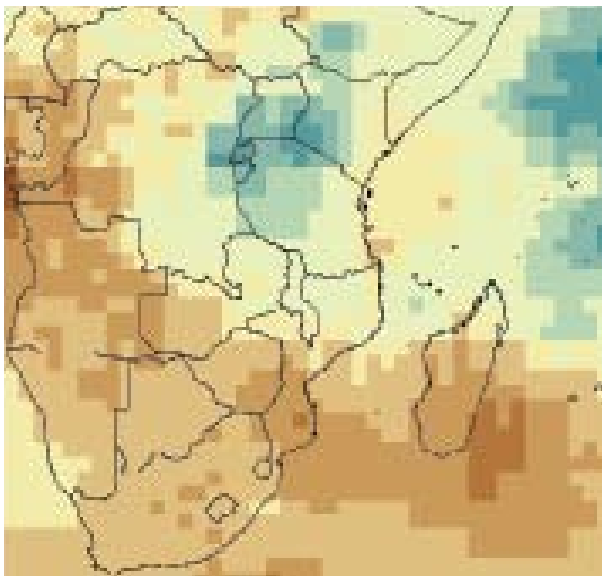

Convincing evidence for the anthropogenic role in climate change has arisen from convergence of projections of change obtained through independently-designed General Circulation Models or GCMs. The agreement amongst these models gives us reason to believe we do hold an understanding of the mechanics of climate at a coarse global scale at least, and that projections based upon notional changes in key parameters especially greenhouse gases can and should be taken seriously. Across Africa there is good agreement between many models on temperature increase. Precipitation change is associated with more variability or noise and thus uncertainty, and in certain regions models are unable to agree upon even the direction of change. For southern Africa, fortunately, the precipitation signal from these models is relatively strong and most models indicate forthcoming drying (based on total annual rainfall) out of southern Africa but wetting of highland areas of East Africa.

We chose to combine the rainfall projections from multiple GCMs. We took advice on which models and scenarios to combine from Dr Guy Midgley (SANBI, South Africa), Dr Carlo Buontempo (Senior Scientist, Meteorological Office Hadley Centre, UK) and Dr Geert Jan van Oldenborgh (Royal Netherlands Meteorological Institute KNMI), and others. We used the following GCMs: HADCM3, CSIRO, ECHAM5, CCCMA and MIROC (high resolution); and the SRES A1b futures scenario. All climate data were extracted as summarized geotiff files from the Climate Explorer website *http://climexp.knmi.nl*, under the advice and in consultation with Geert Jan van Oldenborgh (whose help is gratefully acknowledged). We computed a difference calculation for each model by comparing the GCM result for the period 2041 - 2060 with recent conditions for the period 1976 - 2005. Thus we use the 'delta' value for each model and then combined these difference values to obtain the mean value of change indicated by the ensemble of five models. Values were reclassified on a scale 1 to 9 with maximum values (brown in the graphic) relating to drying. We gave this layer a maximum weighting in the analysis. Full detail in metadata.

The following table presents a summary of the model results by SADC nation (ranked by values of drying in mm/day):

COUNTRY	DRYING
Angola	-0.20312600000
Madagascar	-0.18013400000
Zimbabwe	-0.17022600000
Botswana	-0.15135200000
South Africa	-0.15055400000
Lesotho	-0.14389500000
Namibia	-0.13811200000
Swaziland	-0.13399300000
Mozambique	-0.08743160000
Zambia	-0.05122210000
Mauritius	-0.03918820000
Democratic Republic of the Congo	0.00578718000
Malawi	0.07285900000
Tanzania	0.18695800000

web-links, sources, credits:
http://climexp.knmi.nl/

5.1.4 GCM ensemble temperature change

weighting * 3

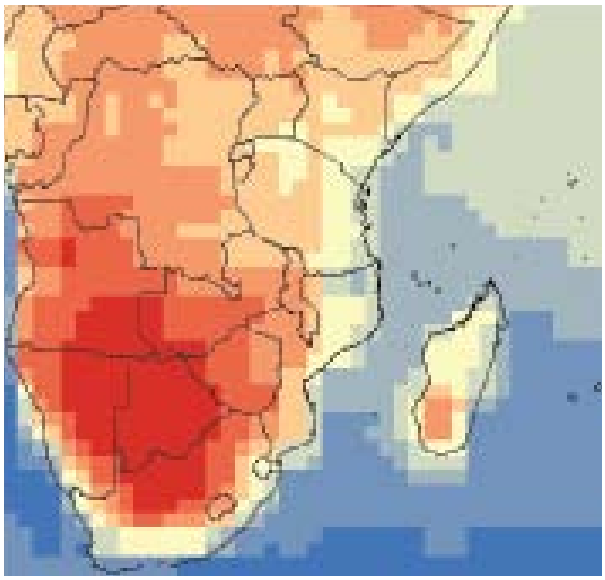

We used the same procedure as outlined in 5.1.3 above to compute change in annual near surface temperature from 1976-2005 to 2046-2060. We used an ensemble of five models (HADCM3, CSIRO, ECHAM5, CCCMA and MIROC (high resolution) and the SRES A1b scenario.

The results compare favourably to the plots from model ensembles in the IPCC AR4 QG1 report (available at *www.ipcc.ch*).

A clear warming is indicated by most models, especially for the arid interior surrounding the Kalahari region. Values were reclassified on a scale 1 to 9 with maximum values (red in the graphic) associated with most warming. We gave this layer a maximum weighting in the analysis. Full detail in metadata.

The following table presents a summary of the model results by SADC nation (ranked by values of warming in °C):

COUNTRY	WARMING
Botswana	2.60725000000
Zimbabwe	2.35082000000
Angola	2.32935000000
Namibia	2.29752000000
Zambia	2.29558000000
Lesotho	2.20575000000
Democratic Republic of the Congo	2.11589000000
South Africa	2.09945000000
Malawi	2.09515000000
Mozambique	1.93634000000
Tanzania	1.89729000000
Swaziland	1.87864000000
Madagascar	1.81991000000
Mauritius	1.29987000000

web-links, sources, credits:
http://climexp.knmi.nl/

5.1.5 Worldclim ensemble precipitation change

weighting * 1

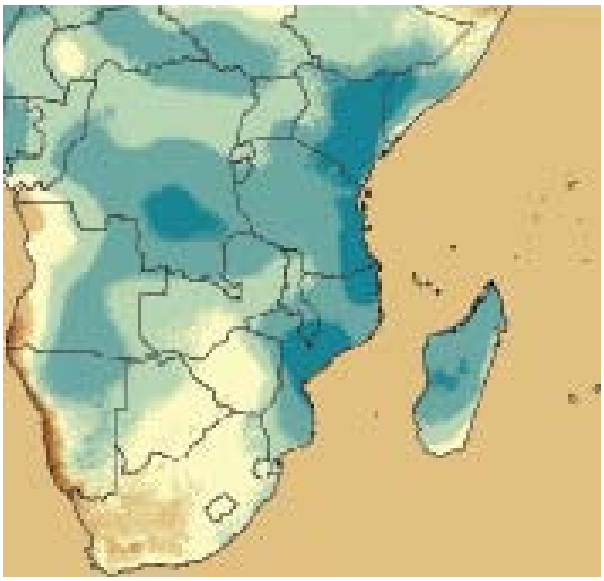

The General Circulation Models provide climate data at a global scale. The resolution of these models is coarse and they cannot provide fine-detail separation of e.g. mountainous areas in Africa such as the Rift Valley. Fortunately this fine resolution of detail is available in the Worldclim climate dataset which provides downscaled projections at 1km^2 from certain GCM runs. This downscaling is based upon excellent datasets e.g. the Shuttle Radar DEM, distance from the coast and other measures described in Hijmans et al. (2005). In a similar manner to the GCM analysis we obtained a measure of overall precipitation change across southern Africa at fine scale resolution from an ensemble of three models under the SRES A2a scenario (HADCM3, CCCMA and CSIRO). We expressed this measure of change in rainfall as a percentage of the current rainfall by grid cell. We cropped the data to the analysis area. All cell values were reclassified to a scale of 1-9 using Jenks natural breaks method to be comparable with other layers (missing values were converted to zeros). This layer is shown in the figure with brown areas representing drying. The influence of water body temperature, distance from the coast and altitude is apparent in this fine-scale output. The Worldclim datasets are very large and less manageable so we had to confine our analysis to data from just 2050 in comparison with current

precipitation conditions (Worldclim Bioclimatic variable number 12). Because this analysis is based upon a short time period, fewer models and because downscaling methods for the same regions have produced very dissimilar results, we include this layer in our analysis with a lower weighting. Full detail in metadata.

web-links, sources, credits:
http://www.worldclim.org/

5.1.6 Worldclim HADCM3 maximum temperature change

weighting * 1

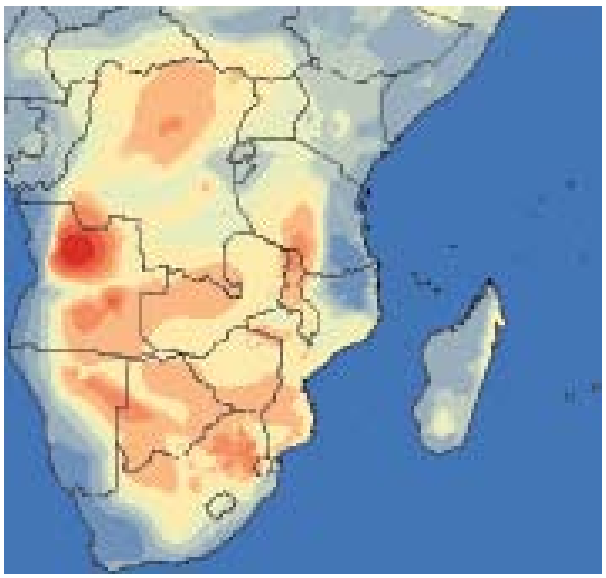

For temperature change at similar fine-scale resolution we use downscaled projections of maximum temperature from the HADCM3 A2a projections provided by Worldclim. We compare these values for 2050 with current conditions (Worldclim bioclimatic variable number 5).

We cropped the data to the analysis area. All cell values were reclassified to a scale of 1-9 using Jenks natural breaks method to be comparable with other layers (missing values were converted to zeros). This layer is shown in the figure with red areas representing warming. For reasons as given above, and in this case only a single model was used, we include this layer in our analysis with a lower weighting. Full detail in metadata.

web-links, sources, credits:
http://www.worldclim.org/

5.1.7 Loss of suitability for cropland

weighting * 2

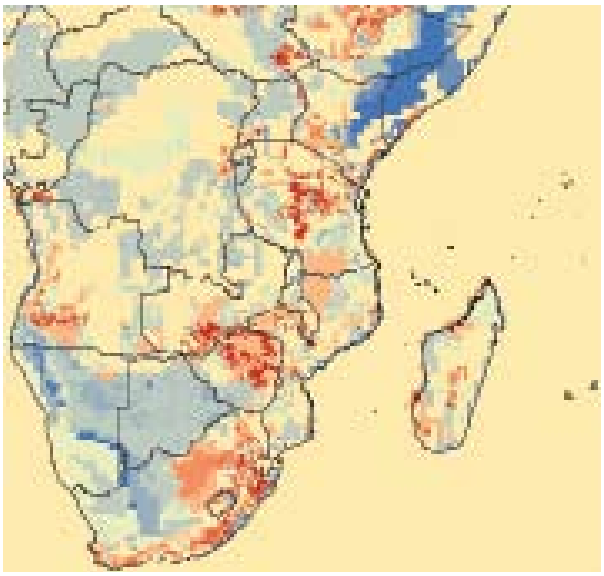

It is clear from the data layers presented above that certain large areas of southern Africa are likely to experience both reduction in rainfall and increase in temperature during the course of this century under the likely emissions scenarios. So a reduction in water input through reduced precipitation may be aggravated further by increases in evaporative loss through an increase in temperature. Future projection data on evapotranspiration rate were not immediately available to us. Instead we looked to a classification of climate zones called Holdridge Life Zones which takes account of temperature, precipitation and potential evapotranspiration. IIASA provides the global distribution of 38 classes of life zones in two datasets: one for current climatic conditions and a second for a doubling of CO_2.

We compared the current extent of cropland in Africa, provided by FGGD / IIASA (FAO 2007) with the current distribution of life zones to obtain an indication of density of cropland per km^2 of each life zone. We assume that cropland has been developed across Africa in the most suitable life zones and that the density indicators correspond to suitability indicators. We extrapolate the likely future density of cropland across Africa with the second life zones dataset based on doubling of CO_2, using these indicator measures. We then measure the difference between the overall density of cropland now with the projected density of cropland

under a doubling of CO_2 in order to obtain a data layer which reveals where cropland is likely to expand and where it is likely to contract under the influence of climate change. For the areas where cropland is expected to expand we multiplied the results by the proportion of each grid cell occupied by soils without constraints (PAGE dataset). Thus the dark blue areas on the graphic illustrate where cropland is likely to expand into areas with good soils. Orange areas on the graphic represent areas of likely cropland loss due to the expected shifts in the life zones. These data values were reclassified on a scale of 1 to 9 where 9 represented maximum cropland loss. Furthermore we added in values of nine (dark red on the graphic) for grid cells where loss of cropland was indicated in the study by ILRI which is based on changes in the length of the growing period (also accommodates both temperature and rainfall change).

We are very grateful to Drs Philip Thornton, Peter Jones and colleagues for allowing us to incorporate their findings into this analysis (ILRI 2006; Jones & Thornton 2009). There was good correspondence between the ILRI dataset and our life-zone analysis for SADC. The overall graphic illustrates how we may expect rainfed production of cereal crops to alter across southern Africa in the future. Certain current arid regions (notably outside SADC in the Horn of Africa) may be able to produce more food in the future while other areas, particularly Zimbabwe, central Tanzania, southern Zambia, southern Angola, the Highveld and South African escarpment areas may be forced to look to other methods of food production. Full detail in metadata.

web-links, sources, credits:
http://gcmd.nasa.gov/records/GCMD_GNV00005.html

Pilot Analysis of Global Ecosystems (PAGE): Agroecosystems Dataset *www.maweb.org*

5.1.8 Sea level rise

weighting * 2

To derive the risk of a sea level rise we used the Shuttle Radar Topography Mission DTED® Level 1 (3-arc second) Data. The resolution is 3 arc seconds (90 meters). The pixel value represents the elevation in meters. For the RCCP we used spatial analyst extension in ArcMAP to derive slope from this DEM.

We cropped the data to the analysis area and extracted all pixel values that were lower elevation than 12m.a.s.l. We ascribed the following pixel values on the basis of likelihood of projections for sea level rise: 0-1m value 9, 1-2m value 6, 2-6m value 3, 6-12m value 1. This put the layer on a scale comparable with other layers (missing values were converted to zeros). This layer is shown in the figure with red and yellow areas representing most exposed areas. Full detail in metadata.

web-links, sources, credits:
http://edcsns17.cr.usgs.gov/srtmdted/

U.S. Geological Survey Center for Earth Resource Observation and Science (EROS), National Aeronautics and Space Administration (NASA), National Geospatial-Intelligence Agency (NGA), ESRI

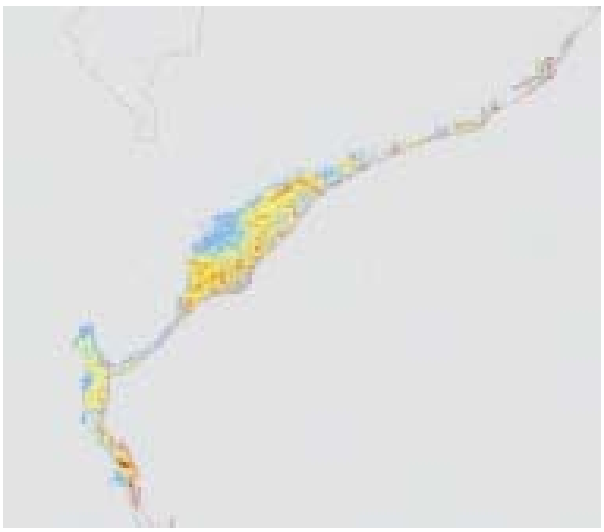

5.2 Layer overlays: future (2050)

5.2.1 Exposure to climate risk summary layer 2050

We used the following combination of grid layers to perform a weighted overlay for the Exposure summary layer shown below:

((max2methsraincv) * 2) + ((E_mcv_monthly) * 2) + ((E_cyclones) * 2) + ((floodfreq) * 2) + ((SPI) * 2) + ((firefreq) * 1) + ((E_dis_event) * 1) + ((E_dis_affect) * 1) + (E2_add_dens * 3) + (E2_GCM1in10drought * 1) + (E2_GCM_precipchange * 3) + (E2_GCM_tempchange * 3) + (E2_WCmaxtempchange * 1) + (E2_WCprecipchange * 1) + (E2_cropchange * 2) + (E2_searisk * 2)

Red values indicate areas that are most exposed to climate stressors, while the blue areas indicate low exposure.

The summary layer shows a central band of future high exposure across the sub-tropics (southern Angola, southern Zambia, Zimbabwe, central and southern Mozambique, Malawi and Madagascar), and adjacent broad bands of medium high exposure extending from about 12°S (northern Zambia, northern Mozambique) to central South Africa and Lesotho (about 30°S), and also into northern Angola and the DRC. The least exposed regions in southern Africa are the southern, western and coastal regions of South Africa, the Namib Desert of coastal southern Namibia, northern Mozambique and northern Zambia, eastern and north-western Tanzania, and south-eastern DRC.

RCCP Health and Food Security Risk Profile Mapping for Southern Africa
Exposure to Risk
Phase 2: 2050

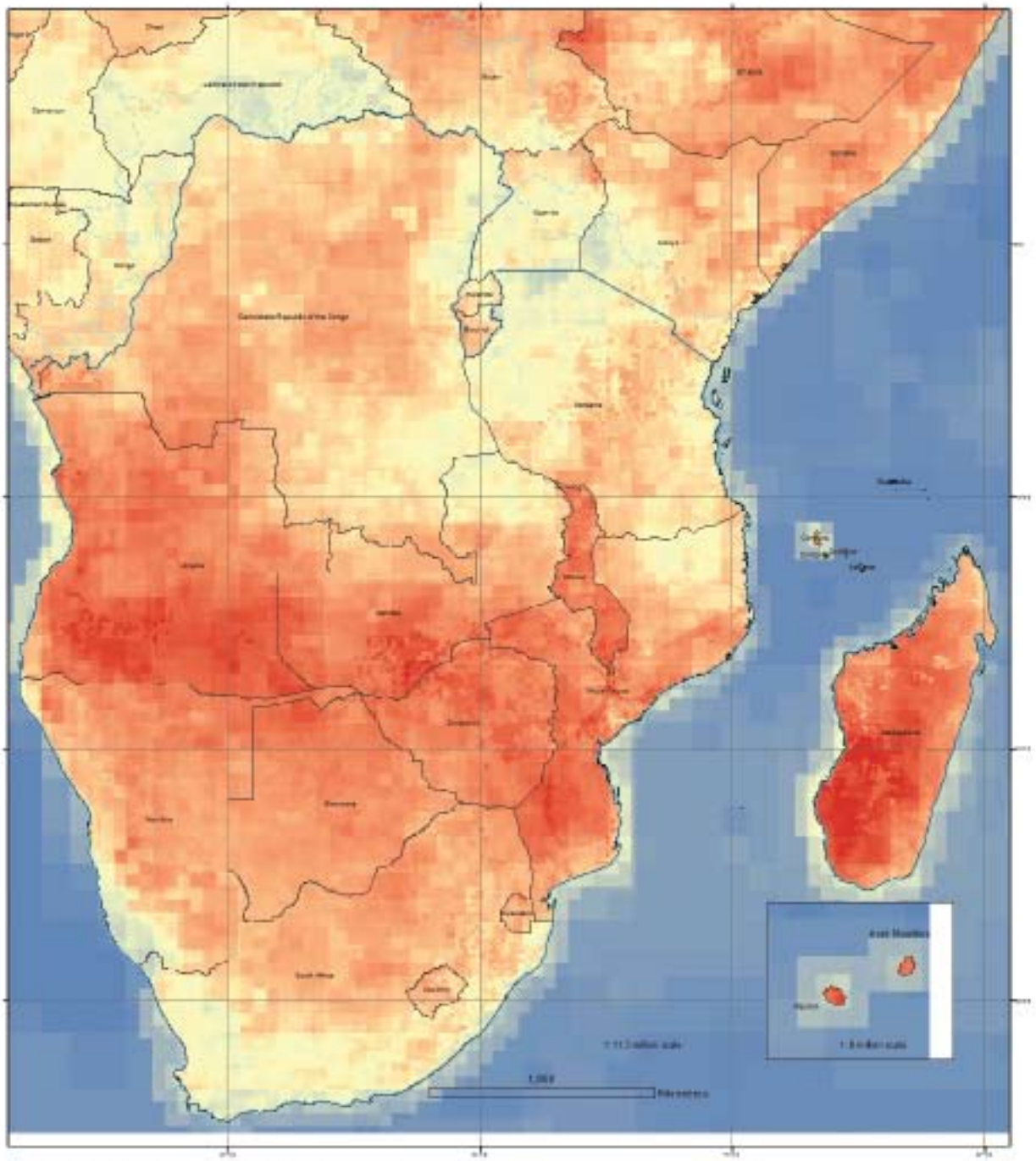

5.2.2 Problem areas (impact) 2050

We derived the following layer as (sensitivity + exposure). The Exposure category was in this case given equal weighting to the Sensitivity category, since the two categories now contain almost equal numbers of layers of equally high quality and importance.

Red values indicate 'problem areas' (impact) while the blue areas indicate low impact.

The inclusion of climate and population futures leads to a broadening and intensification of problem areas in southern and central Angola extending into northern Namibia and western Zambia, as well as south-western Madagascar. The countries most highly impacted are Zimbabwe, Malawi, Lesotho, Swaziland, and substantial portions of Zambia, Mozambique, Madagascar and Angola.

Lower impacts emerged in the southern and coastal areas of South Africa, the southern Namib desert, in addition to currently less impacted areas of northern Mozambique / southern Tanzania, north-western Tanzania, northern Zambia, north-eastern Angola and large parts of the DRC.

RCCP Health and Food Security Risk Profile Mapping for Southern Africa
Problem Areas (sensitivity + exposure)
Phase 2: 2050

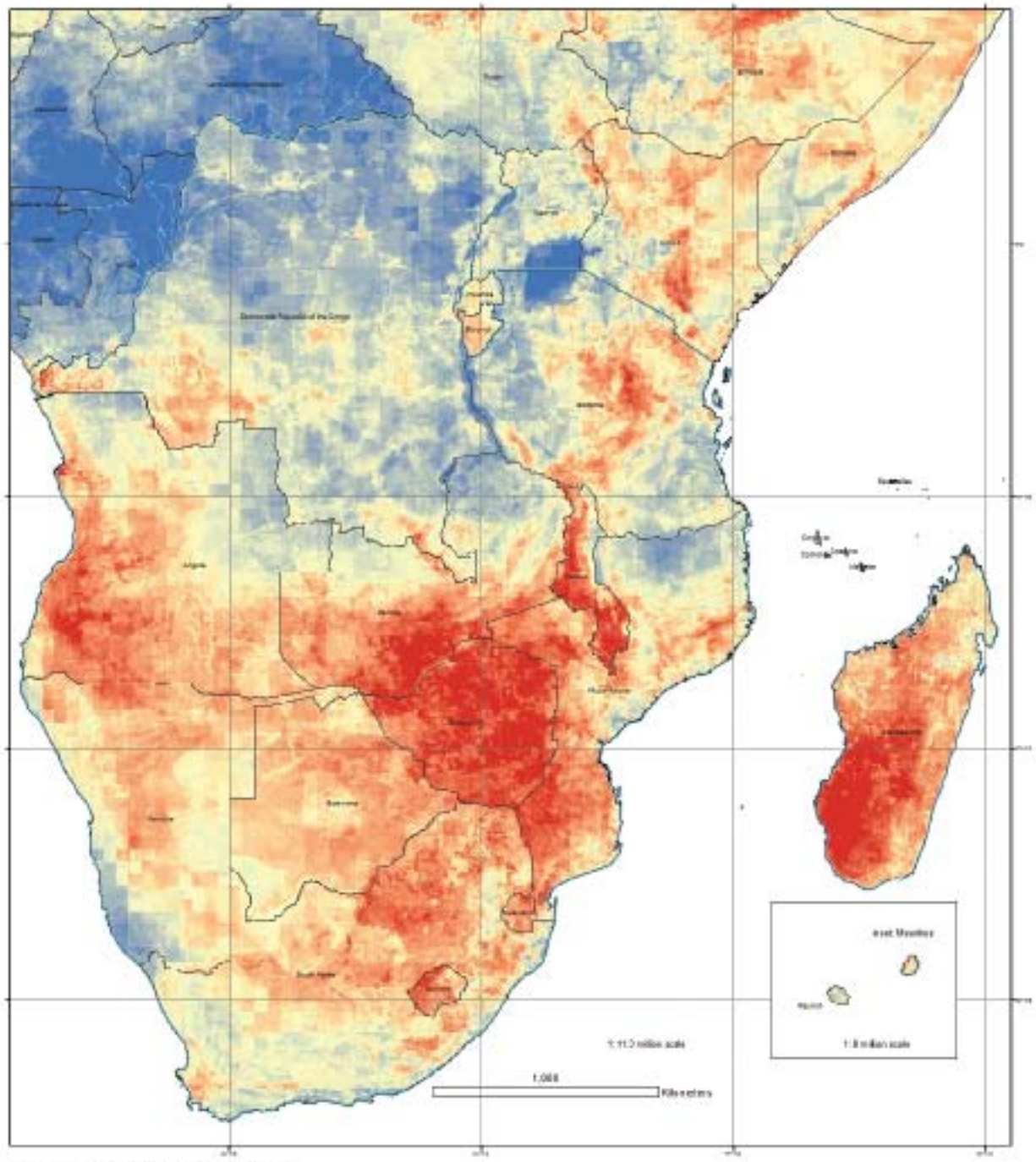

REGIONAL CLIMATE CHANGE PROGRAMME

5.2.3 Vulnerability Hotspots 2050

The final summary hotspot layer in the analysis is derived as (sensitivity + exposure + adaptability), thus (problem areas + adaptability).

Red values indicate hotspots where people are most likely to be in need of help adapting to climate stressors, while the blue areas indicate patches of resilience.

Large extensions in future hotspots are evident across southern and central Angola, and large parts of southern and western DRC (the north-western parts of southern Africa), owing to the lower adaptive capacity of these regions combined with greater climate exposure. The central-eastern regions (southern Zambia, Zimbabwe, Malawi, southern and central Mozambique, Madagascar) remain as hotspots, and the north-eastern hotspot regions (northern Mozambique, Tanzania) become less intensive.

RCCP Health and Food Security Risk Profile Mapping for Southern Africa
Hotspots: (sensitivity + exposure + adaptability)
Phase 2: 2050

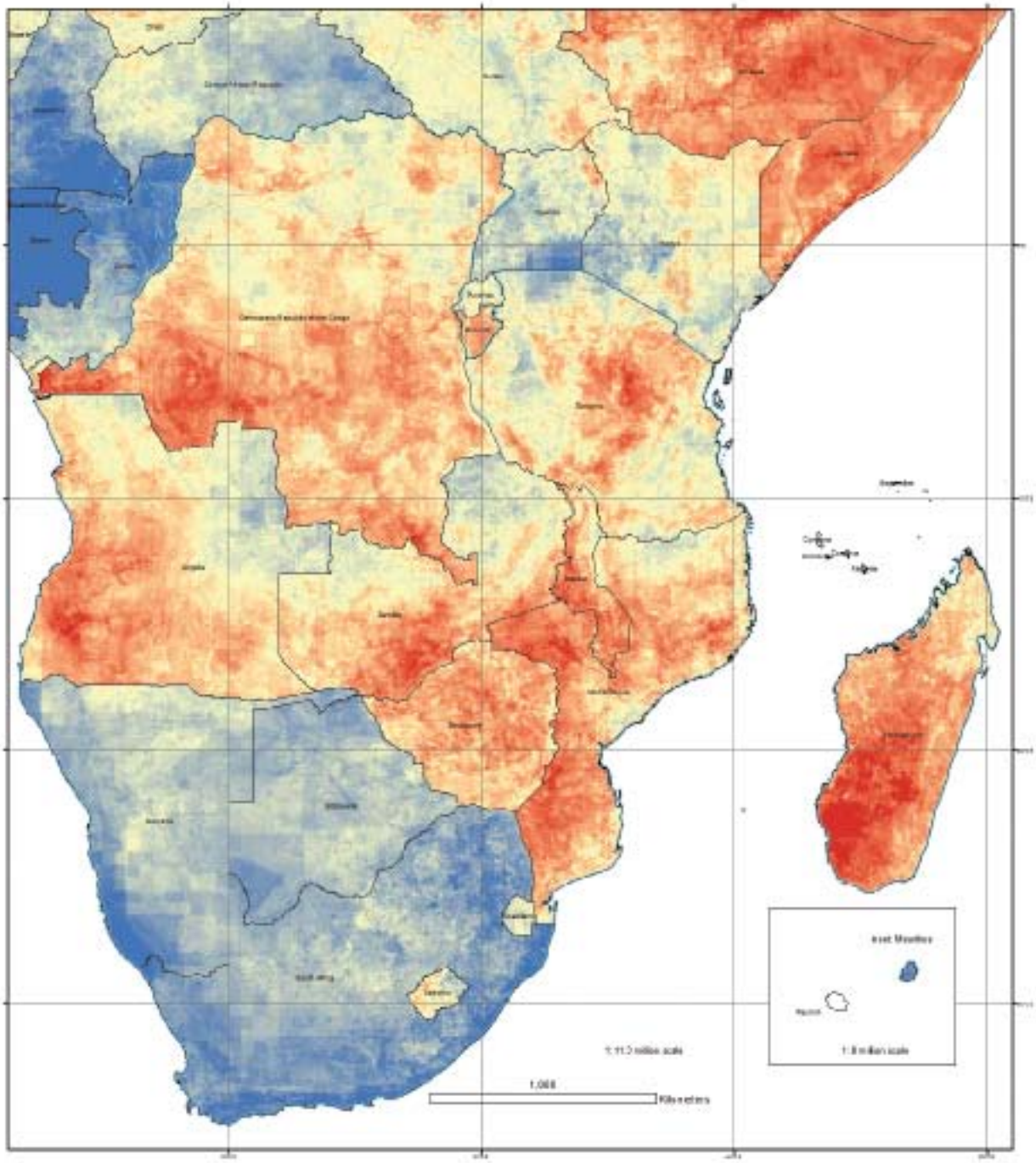

REGIONAL CLIMATE CHANGE PROGRAMME

5.2.4 Averaged problem areas (impact) and vulnerability hotspots 2050

We aggregated the grids of the summary layers to a coarser resolution (10km^2), converted the raster data to point data and then carried out a kernel density analysis to provide the following figures which help to clarify the patterns and identify the locations of obvious hotspots or centres of resilience. The first figure shows average values within a 50km radius of (exposure + sensitivity) values. From this figure, and from the following figure which shows the same treatment for hotspot values, we were able to identify and map the focal points in SADC and surrounds.

In summary, five major clusters of vulnerability 'hotspots' emerge in southern Africa (depicted by the orange circles in the hotspot map below). These are (1) central Tanzania; (2) a large area

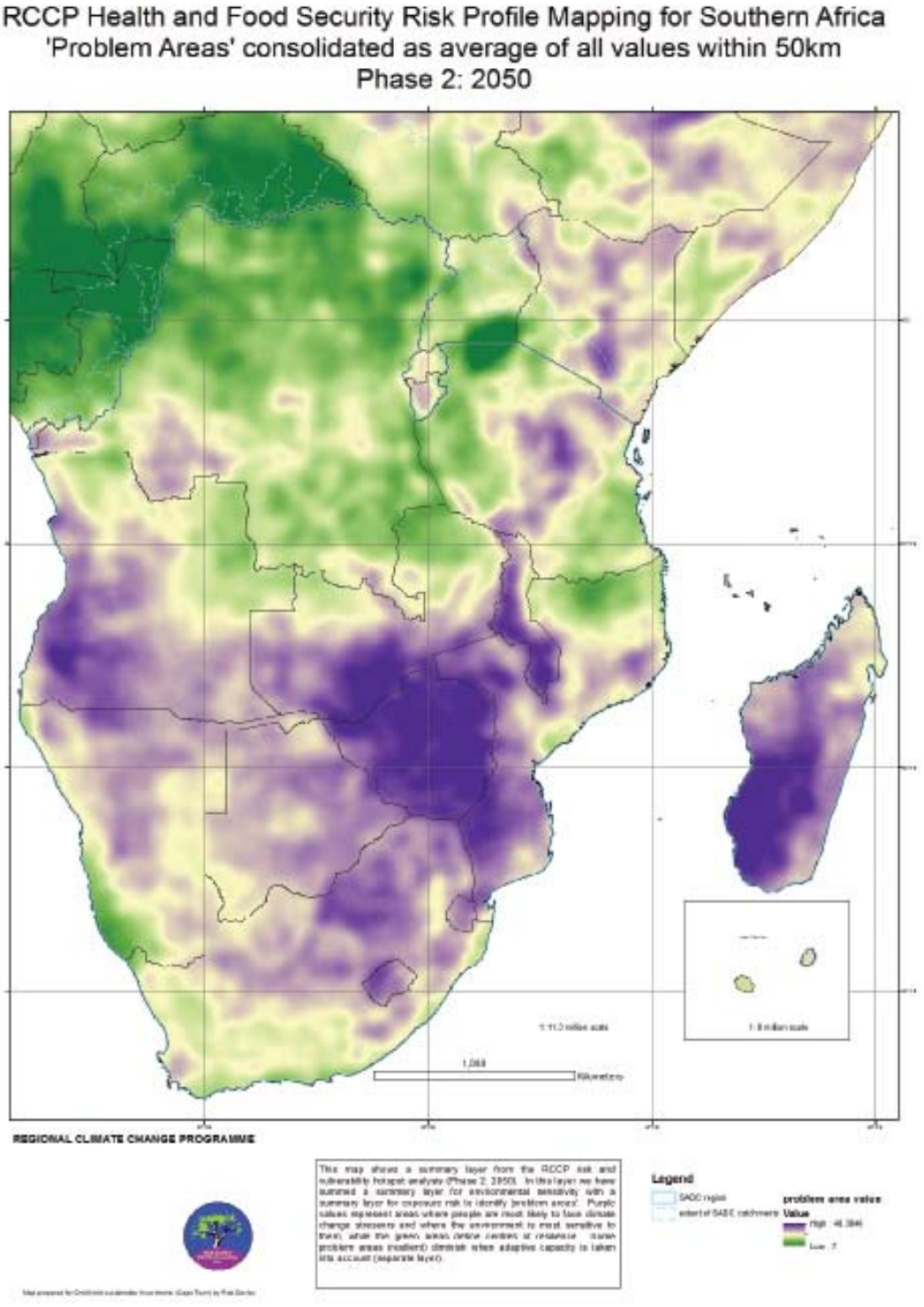

incorporating southern and central Mozambique, Malawi, Zimbabwe and southern Zambia; (3) most of Madagascar; (4) southern and north-western Angola; (5) southern and particularly western DRC. Centres of resilience are identified for the northern Congo Basin, north-eastern Angola, northern Zambia, north-western and south-eastern Tanzania, and northern Mozambique. The south-west block (South Africa, Botswana, Namibia) and Mauritius are less vulnerable on account of their higher adaptive capacity, at a national level. This is also the case, to a smaller degree, for Lesotho and Swaziland. This does not diminish the fact that highly vulnerable communities also exist in these regions, who will be in need of assistance in dealing with increased climate-related risk brought about by climate change.

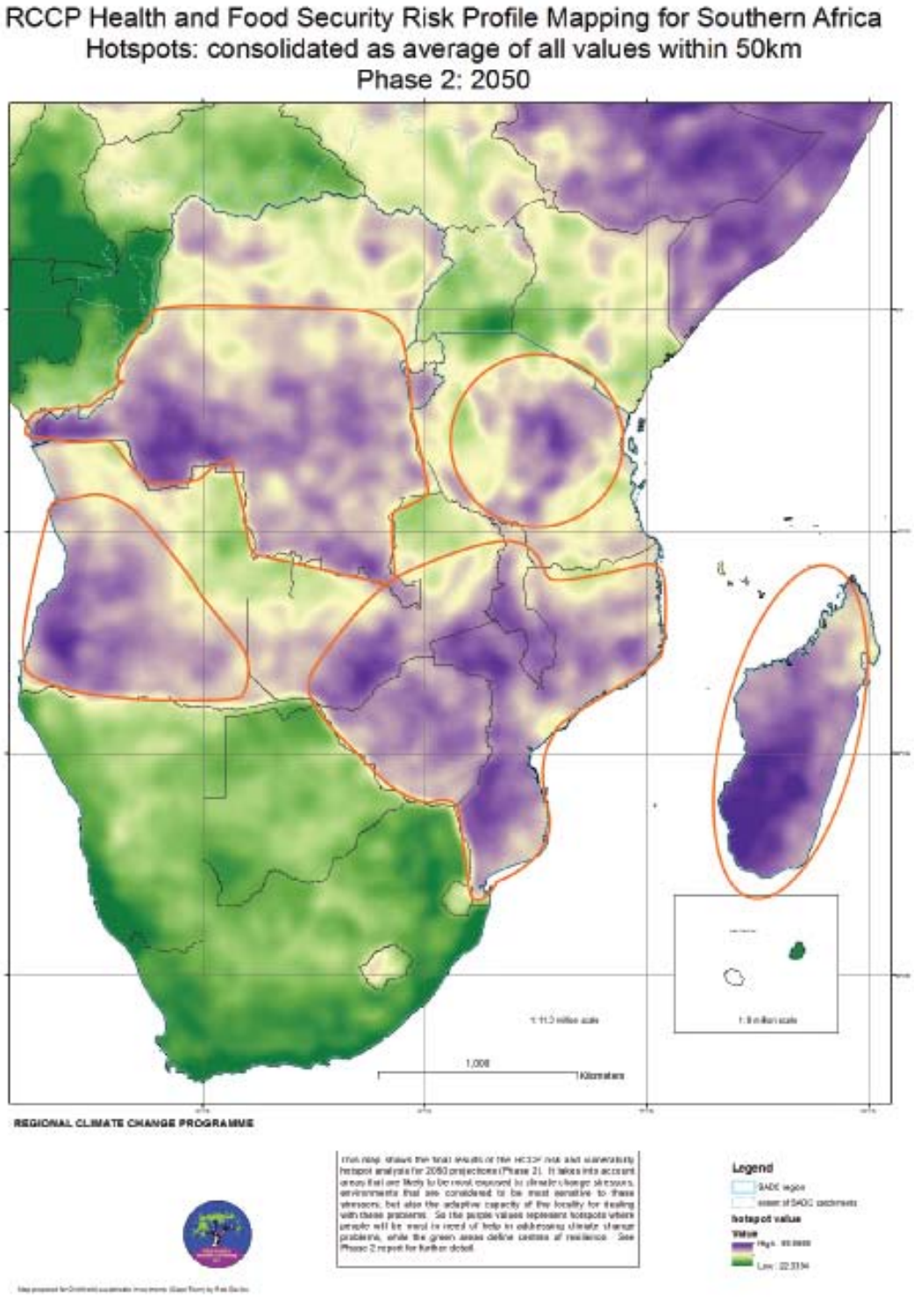

6. Shifts between current and future hotspots

6.1 Exposure to climate risk summary layer

The following provides a comparison between the exposure category for current (2008) and future (2050) conditions:

STATUS QUO (2008)	FUTURE (2050)
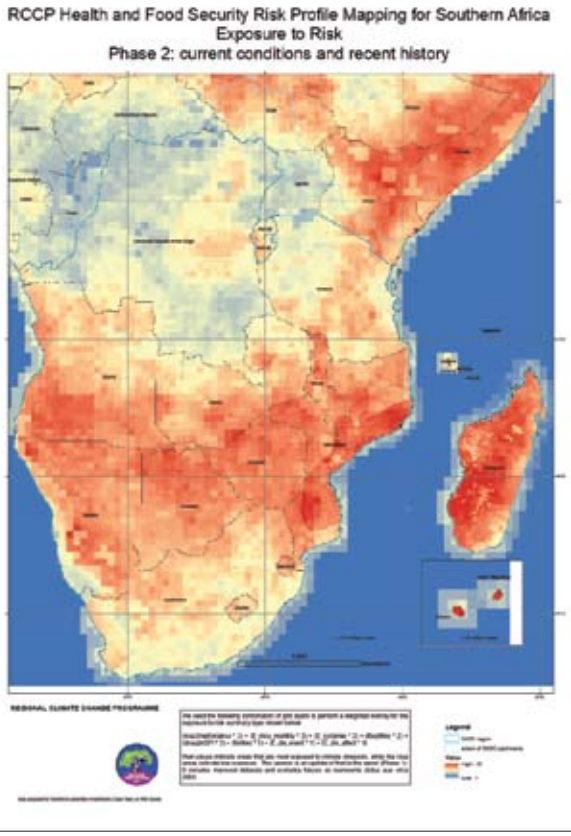	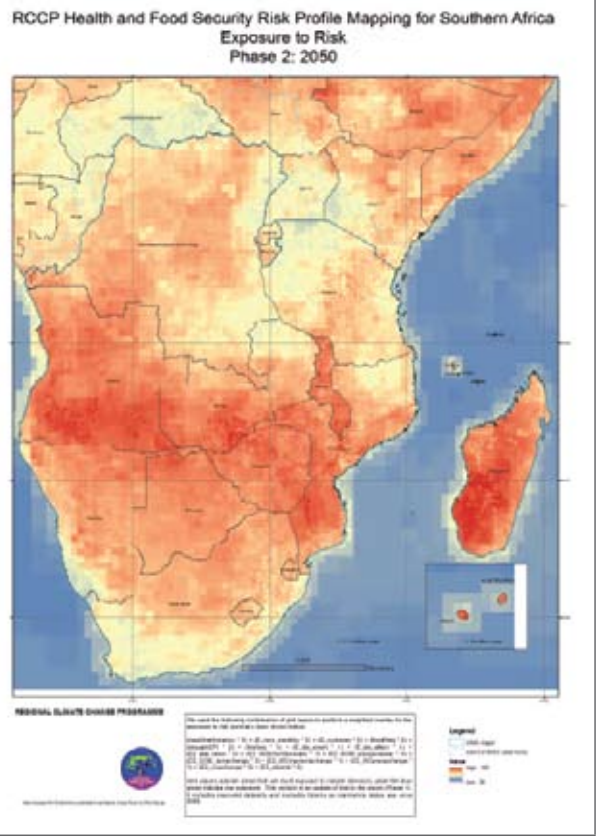

To further analyse the above comparison, we have computed the shift between exposure to risk under current conditions and exposure to risk projected for 2050. The amelioration of climate-related risk in northern Mozambique / southern Tanzania can be partially attributed to the GCM-based rainfall projections which consistently show increasing annual rainfall over East Africa.

Areas of worsening impact include southern Malawi, the Highveld of South Africa, south-eastern Madagascar, southern and western Zambia, and extensive areas within Angola and DRC. Malawi, Madagascar and DRC are expected to have high population growth rates over the next few decades, resulting in increasing pressure on water resources and agricultural land. Increasing risk of drought, decreased annual rainfall projections and significant warming across western DRC, Angola, and south/west Zambia partially account for the results for these parts of southern Africa.

RCCP Health and Food Security Risk Profile Mapping for Southern Africa
Change in Exposure to Risk from current to 2050

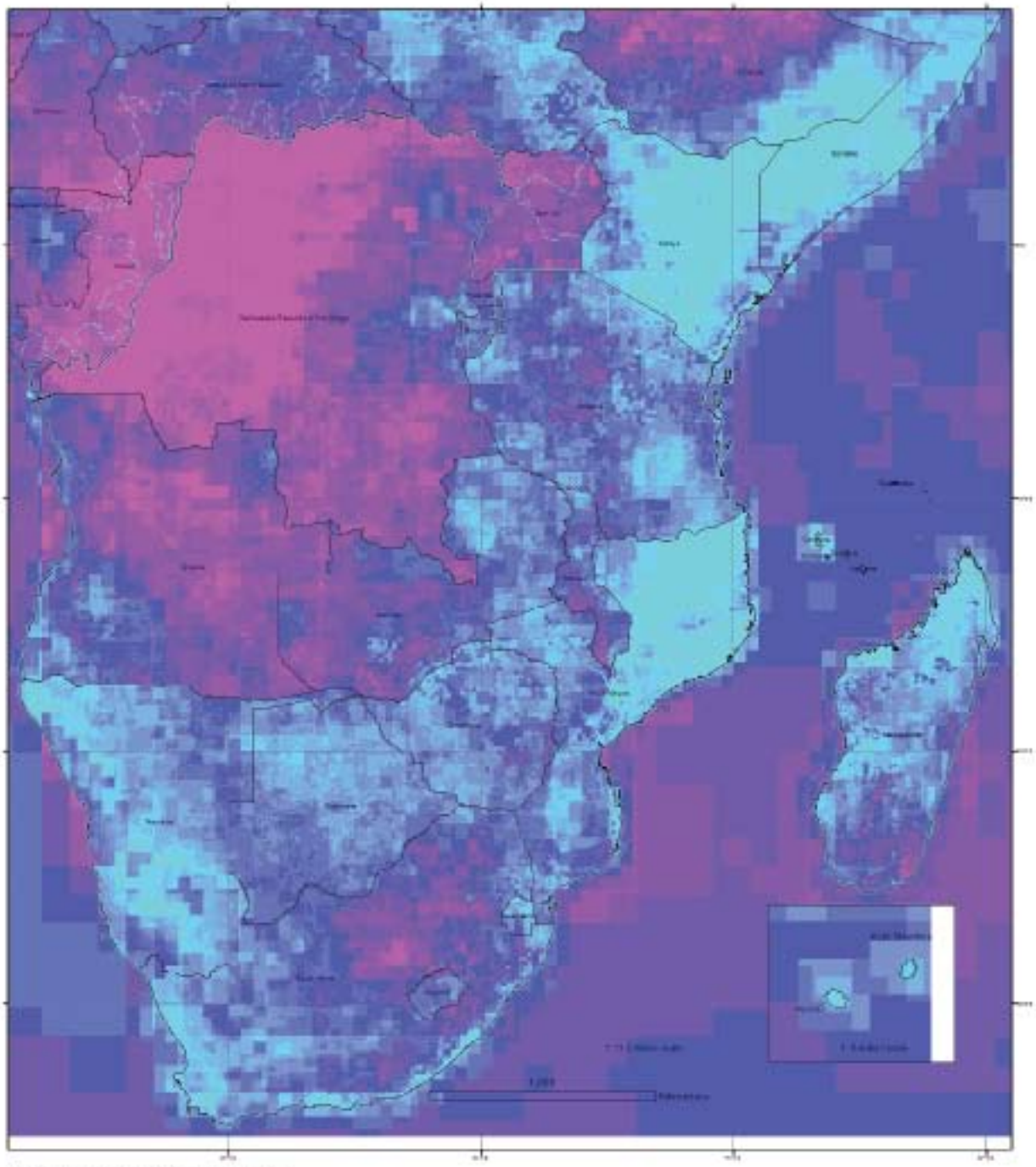

6.2 Problem areas (impact) overlay

The following provides a comparison between the problem areas (impacts) for current (2008) and future (2050) conditions. We re-computed the status quo (2008) map using (sensitivity + exposure) for better comparison with the future (2050) map, where exposure was given the same weighting and sensitivity.

STATUS QUO (2008)	FUTURE (2050)
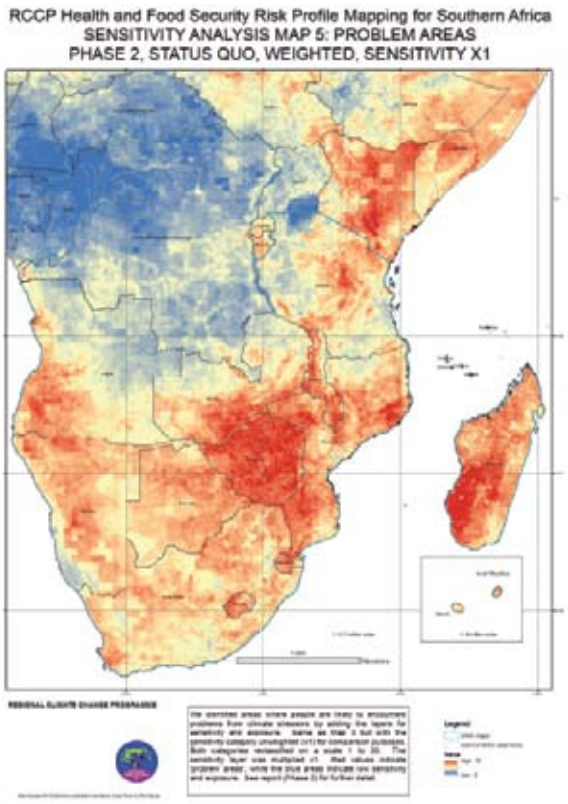	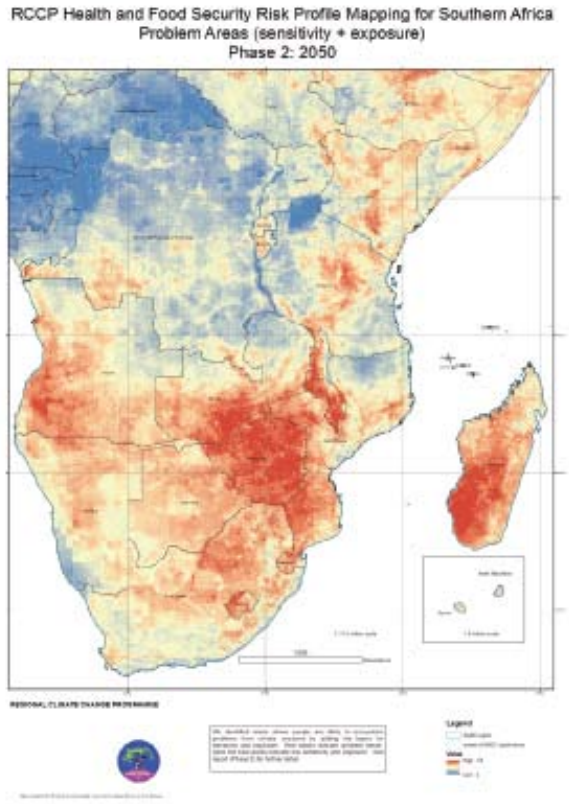

The patterns of projected impact remain similar, with the exception of higher impact areas emerging across southern Angola and western DRC. There is an intensification of problem areas (impact) over the South African Highveld, southern and western Zambia, Malawi and south-western Madagascar. Reductions in intensity are seen in northern Mozambique, central Tanzania and south-western South Africa.

6.3 HOTSPOTS OVERLAY

The following provides a comparison between the hotspot areas for current (2008) and future (2050) conditions:

STATUS QUO (2008)	FUTURE (2050)
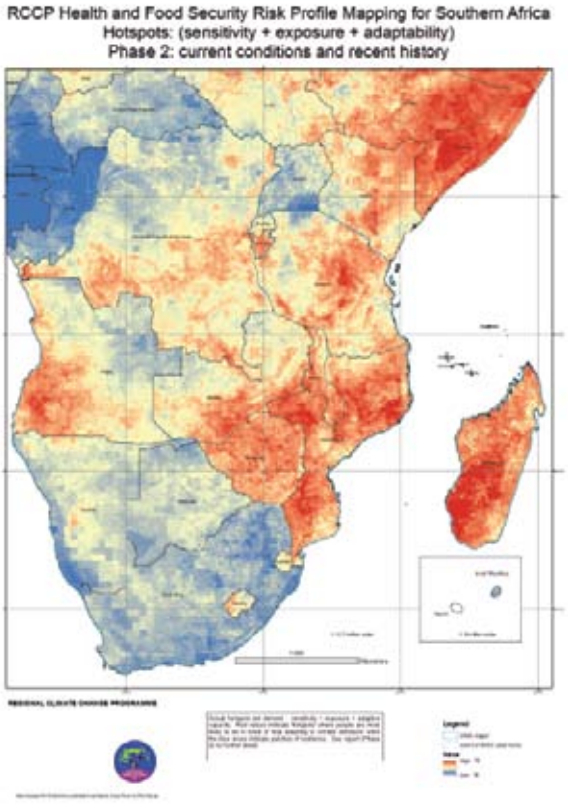	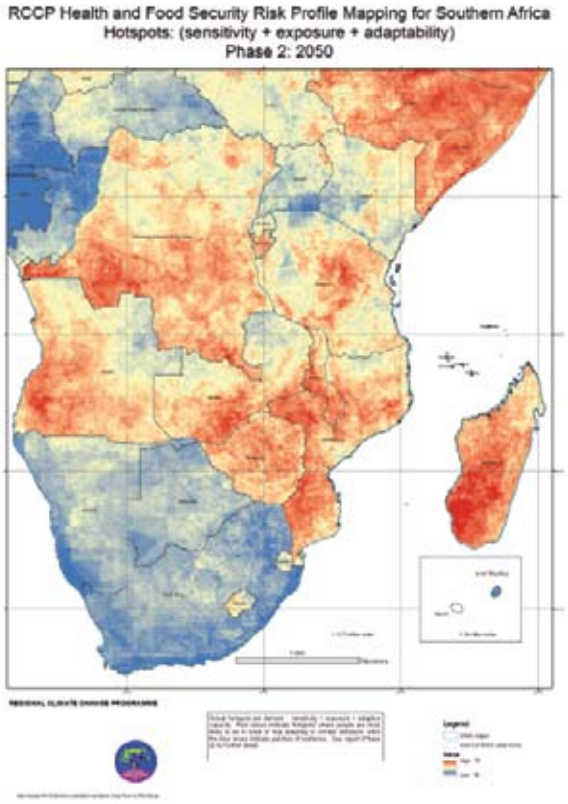

New and intensive vulnerability hotspots emerge over large parts of the DRC and Angola, as well as Madagascar. These countries share the combination of increased exposure to climate risk and thus new and intensified problem areas, and weaker adaptive capacity. Countries such as Zambia, South Africa and Malawi also show intensification of problem areas, but their better adaptive capacity results in little change to this 'hotspot' outcome.

7. Sensitivity analysis

7.1 Rationale and methods

Through the course of the mapping project for the RCCP we have noticed similar recurring geographic patterns of hotspots across SADC despite radically differing combinations of component data layers and methods. This indicates that the findings of the weighted overlay models are robust. But we wanted to examine this more systematically in a sensitivity analysis. To do this we chose to look at 'problem areas' across SADC which are a combination of the exposure and sensitivity categories rather than 'hotspots' which also include the adaptive capacity category. We took this decision because exposure and sensitivity data layers represent potential environmental problems rather than the resources that people have available to them. We wanted to know where the problem areas were across the whole of SADC and how these varied in a sensitivity analysis without the rather subjective assumptions associated with applying the adaptive capacity layers which has the effect of masking the problem areas in certain countries.

For our sensitivity analysis we test the influence of introducing or removing data layers on the identification of problem areas, and of changing the weightings of both the overall categories and the individual component data layers. Identification of the problem areas and also the centres of resilience are carried out by simple visual comparison of the output problem area maps. Just as a reminder, component data layers within each category are summed after being multiplied by their respective weighting factors and the resultant summary layer for each category is then reclassified on a scale 1 to 30 before combination with and without an overall weighting score for the category to produce the problem area map.

Early on in the mapping project we experienced limited numbers and quality of exposure layers. Whereas we had many sensitivity layers which showed excellent geographic representation of the parameters. Accordingly, we began by issuing a greater overall weighting to the sensitivity category. At the end of Phase 1 however we managed to access superior quality exposure layers and at the beginning of Phase 2 we introduced a new series of data layers to represent future exposure to climate stressors. This brought the number and quality of the exposure layers to a level comparable to the sensitivity layers and consequently there was no need to accord the additional weighting to the overall sensitivity category. So the first major division to our sensitivity analysis is the overall weighting to the sensitivity category. The second major comparison of problem areas is enabled by introducing future projected exposure layers in Phase 2. We complete the analysis by comparing the effects of varying the individual data layer weighting values and by removing entire subsets of data layers from each category. These are highly radical changes to the input variables for the weighted overlay model but if the same geographic patterns persist in the output maps in spite of these changes then we can be confident that our identification of problem areas is highly robust.

Problem Area (Impact) maps were generated in the following ways:

MAP 1: EARLY PHASE 1, STATUS QUO, WEIGHTED LAYERS, SENSITIVITY X2

This was an early version in Phase 1 (2009) of the RCCP mapping: 15 sensitivity layers plus 8 exposure layers. We identified areas where people are likely to encounters problems from climate stressors by multiplying the layers for sensitivity and exposure. The sensitivity layer was multiplied x2 prior to combination. See report (Phase 1, 2009) for further detail.

MAP 2: PHASE 1 IMPROVED, STATUS QUO, WEIGHTED LAYERS, SENSITIVITY X2

As above, we identified areas where people are likely to encounters problems from climate stressors by multiplying the layers for sensitivity and exposure. Exposure layers for Phase 1 (status quo) were improved by access to new layers from Global Risk Data Platform. The sensitivity layer was multiplied x2 prior to combination. See report (Phase 1 improved, 2010) for further detail.

MAP 3: PHASE 2, STATUS QUO, WEIGHTED LAYERS, SENSITIVITY X2

In Phase 2 (this map and subsequent maps), we identified areas where people are likely to encounters problems from climate stressors by adding the layers for sensitivity

and exposure. Exposure layers for Phase 2 (status quo) were largely unchanged from Phase 1. One additional sensitivity layer (forest loss, 4.2.16 this report) was incorporated. The sensitivity layer was multiplied x2 prior to combination.

MAP 4: PHASE 2, 2050, WEIGHTED LAYERS, SENSITIVITY X2

Eight new layers were incorporated into the exposure category of Phase 2 to account for climate and population stressors projected for 2050 (see 5.1 this report). The sensitivity layer was multiplied x2 prior to combination.

MAP 5: PHASE 2, STATUS QUO, WEIGHTED LAYERS, SENSITIVITY X1

Same as Map 3 but with the sensitivity category unweighted (x1).

MAP 6: PHASE 2, 2050, WEIGHTED LAYERS, SENSITIVITY X1

Same as Map 4 but with the sensitivity category unweighted (x1).

MAP 7: PHASE 2, 2050, UNWEIGHTED LAYERS, SENSITIVITY X1

This analysis shows projected exposure in 2050 with all data layers weighted equally. The sensitivity category was not given additional weighting (X1).

MAP 8: PHASE 2, 2050, ONLY WEIGHT >1 LAYERS, SENSITIVITY X1

In this analysis for projected exposure in 2050 we only included data layers that were weighted *2 or *3. Four exposure layers and four sensitivity layers are dropped. The sensitivity category was not given additional weighting (X1).

MAP 9: PHASE 2, 2050, ONLY WEIGHT >2 LAYERS, SENSITIVITY X1

In this analysis for projected exposure in 2050 we only included data layers that were weighted *3. Thirteen exposure layers and thirteen sensitivity layers are dropped leaving only three of each remaining. The sensitivity category was not given additional weighting (X1).

We produce a total of nine output maps shown in the figures below. Output maps 1-4 represent combinations where the overall sensitivity is weighted X2. Output maps 5-9 are each produced with no additional weighting given to the overall sensitivity category. The first four outputs largely represent developments in the early phase of the mapping project while the remaining outputs concern developments and improvements in the latter stages. Status quo maps are compared with projected future maps in both of these groupings.

In each map, red values indicate 'problem areas' or high impact, while the blue areas indicate low impact.

7.2 Results and Discussion

Across the nine iterations performed, the broad pattern of climate impact remains remarkably similar. Substantial changes only emerge in Map 9. In considering all 9 output maps, the following problem areas are recognisable throughout despite the radical differences in method: southern Madagascar; most of Malawi except adjoining the lake; the Highveld of South Africa; Lesotho and Swaziland; southern Mozambique; patches in central Tanzania; southern Zambia; south-western Angola, extending into northern Namibia; western DRC; southern DRC notably the 'tail' extending between northern and southern Zambia; the neighbourhood of the Orange River through South Africa. The following problem areas are recognisable on all but the final map: Zimbabwe; the South African escarpment; Cape Town environs.

The following centres of resilience are recognisable throughout: southern Namib Desert; northern Mozambique, extending into southern Tanzania; northern Zambia; eastern DRC (particularly in the north); western Tanzania. The following centres of resilience are visible on all but the final map: north-eastern Angola, extending somewhat into western Zambia. There is recurring evidence of small centres of resilience in north-eastern Madagascar and in the vicinity of Beira on the Mozambique coast.

Clearly the addition of improved exposure layers and future exposure layers during the course of Phase 1 and early Phase 2, represented by Maps 1-5, has little influence on the identification of problem areas across SADC. Map 5 is our final output map from Phase 2 representing status quo, and map 6 is our final output map representing 2050. The greater influence accorded to future exposure layers in map 6 (no additional weighting to the sensitivity category) reveals the first really noticeable differences when compared to Map 5 (status quo) and these differences are expected: an amelioration of problem areas in East Africa owing to expected additional annual precipitation in 2050; and a worsening of problem areas across the central subtropical belt. Nevertheless, the problem areas and centres of resilience identified above remain although their respective size and influence may have changed.

In Map 7 we removed all individual weighting of the component data layers. This leads to greater influence of national data sets, which we generally gave lower weightings to, so some of the countries, particularly Zimbabwe, Swaziland and Lesotho, appear 'blocked out' with greater impact. But again the overall pattern is similar to Map 6 despite the drastic treatment of removing all weightings. In Maps 8 and 9 we strip out large subsets of the component data layers. The four least important

Map 1:
Early Phase 1, Status Quo Weighted, Sensitivity X2

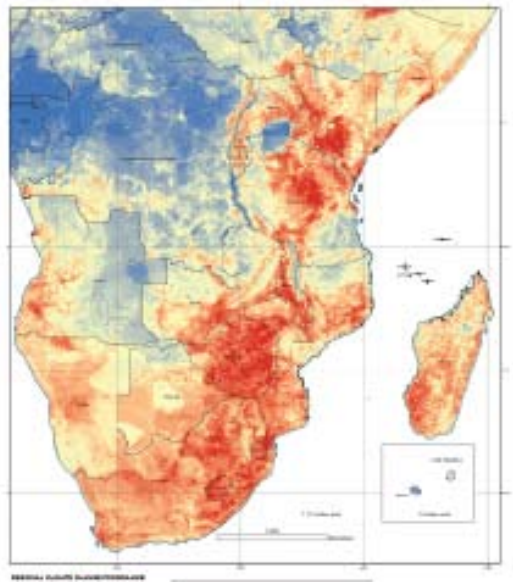

Map 3:
Phase 2, Status Quo, Weighted, Sensitivity X2

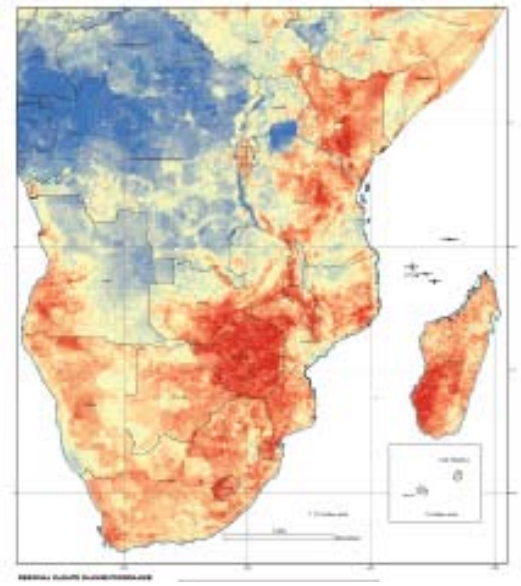

Map 2:
Phase 1 Improved, Status Quo, Weighted, Sensitivity X2

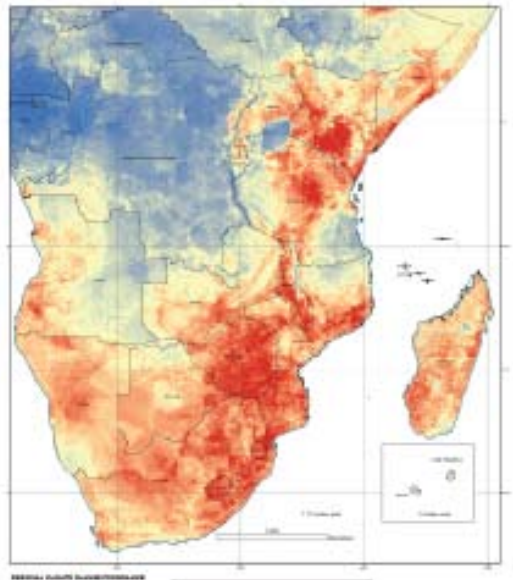

Map 4:
Phase 2, 2050, Weighted, Sensitivity X2

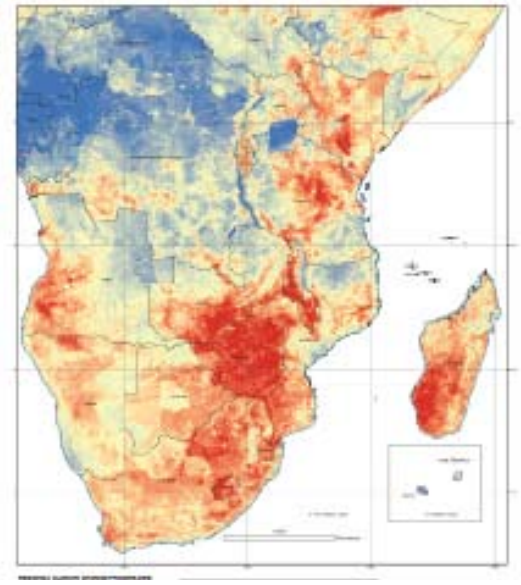

data layers are removed in Map 8, while in Map 9 the 13 least important data layers are removed leaving only three data layers in each category. It is only by removing three quarters of the component data layers that we obtain a noticeably different emphasis in Map 9, but this skeleton of a model still reveals many of the problem areas and centres of resilience outlined above.

We conclude from the sensitivity analysis that the patterns of problem areas and centres of resilience revealed by weighted overlay models for status quo in Map 5 and for 2050 in Map 6 are persistent and robust and can withstand significant alteration of the component layers and methods of combination.

Map 5:
Phase 2, Status Quo, Weighted, Sensitivity X1

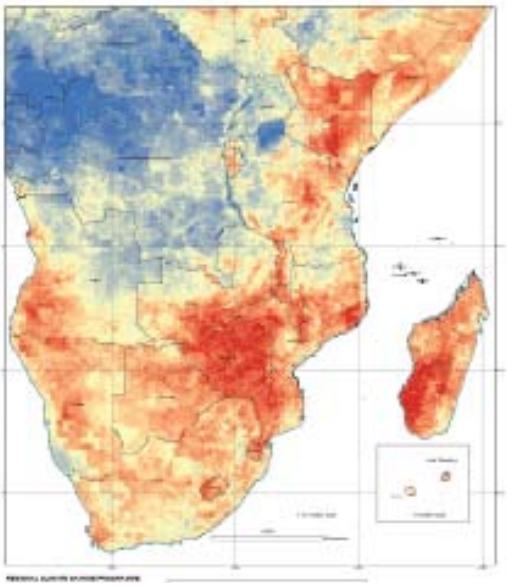

Map 6:
Phase 2, 2050, Weighted, Sensitivity X1

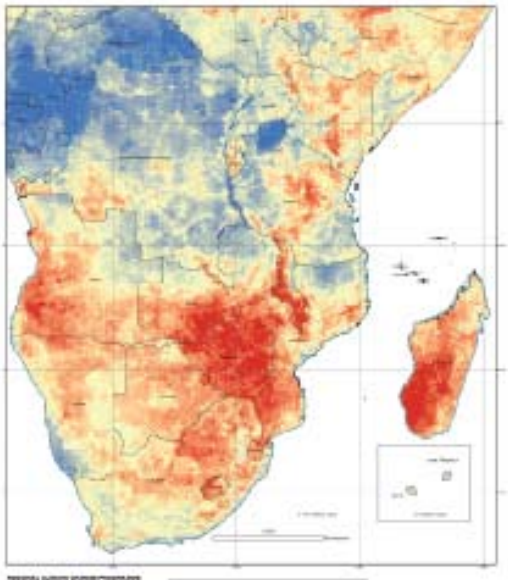

Map 7:
Phase 2, 2050, Unweighted, Sensitivity X1

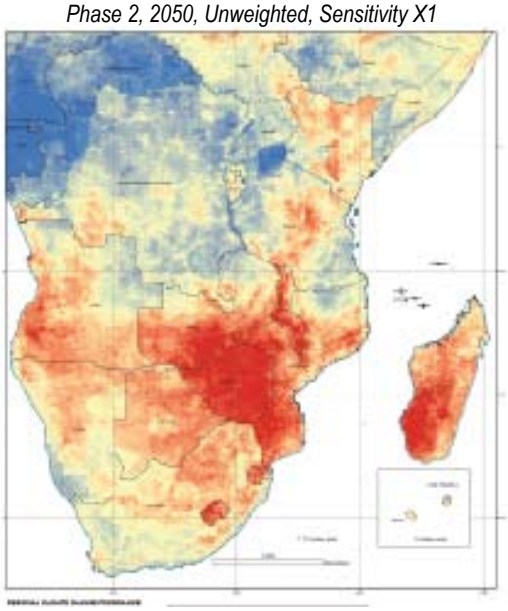

Map 8:
Phase 2, 2050, Only Weight ➤ 1 Layers, Sensitivity X1

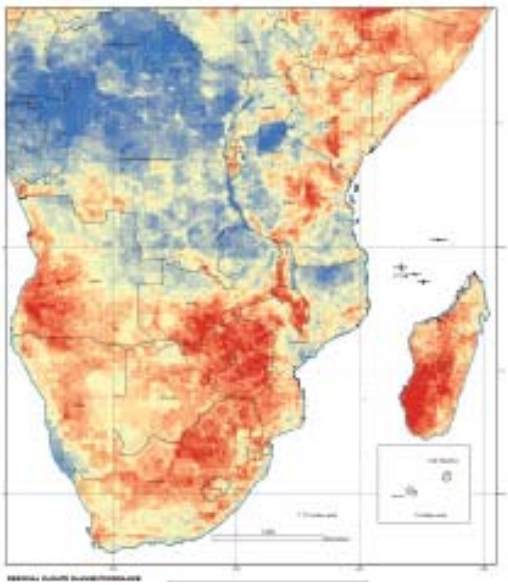

Map 9:
Phase 2, 2050, Only Weight ➤ 2 Layers, Sensitivity X1

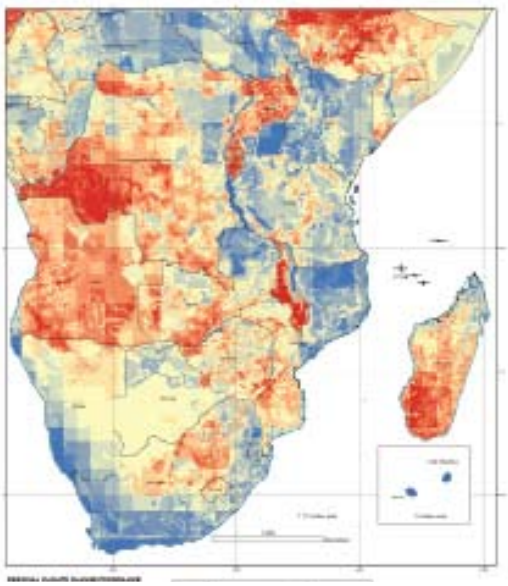

8. References

CIESIN. 2005. Poverty Mapping Project: Global Subnational Prevalence of Child Malnutrition. GIS Dataset. CIESIN, Columbia University, New York.

Dilley, M., Chen, R.S., Deichmann, U., Lerner-Lam, A.L., Arnold, M., Agwe, J., Buys, P., Kjekstad, O., Lyon, B. & Yetman, G. 2005. Natural Disaster Hotspots: A Global Risk Analysis. Digital Data Publication. Disaster Risk Management Series No. 5. The World Bank, Washington, D.C.

Doll, C.N.H., Muller, J.-P. & Elvidge, C.D. 2000. Night-time imagery as a tool for global mapping of socio-economic parameters and greenhouse gas emissions. Ambio 29: 157–162.

Elvidge, C.D., Sutton, P.C., Ghosh, T., Tuttle, B.T., Baugh, K.E., Bhaduri, B. & Bright, E. 2009. A global poverty map derived from satellite data. Computers & Geosciences 35: 1652–1660.

Eriyagama, N., Smakhtin, V. & Gamage, N. 2009. Mapping Drought Patterns and Impacts: a global perspective. Columbo, Sri Lanka: International Water Management Institute. (IWMI Research Report 133). 31pp.

FAO. 2007. Module 5 "Land use patterns and land cover" of Food Insecurity, Poverty and Environment Global GIS Database (FGGD).

FAO and IIASA. 2007. Mapping biophysical factors that influence agricultural production and rural vulnerability. Food and Agriculture Organisation of the United Nations, Rome. 96 pp.

Galster, S., Burgess, N.D., Fjeldsa, J., Hansen, L.A. & Rahbek, c. 2007. One degree resolution databases of the distribution of mammals in Sub-Saharan Africa. On-line data source: Zoological Museum, University of Copenhagen, Denmark.

Hansen, L.A., Burgess, N.D., Fjeldsa, J. & Rahbek, C. 2007b. One degree resolution databases of the distribution of amphibians in Sub-Saharan Africa. On-line source: Zoological Museum, University of Copenhagen, Denmark.

Hansen, L.A., Fjeldsa, J., Burgess, N.D. & Rahbek, C. 2007. One degree resolution databases of the distribution of birds in Sub-Saharan Africa. On-line source: Zoological Museum, University of Copenhagen, Denmark.

Hansen, M., Stehman, S. & Potapov, P. 2010. Quantification of global gross forest cover loss. Proceedings of the National Academy of Sciences of the U.S.A.

Hay, S.I., Okiro, E.A., Gething, P.W., Patil, A.P., Tatem, A.J., et al. 2010. Estimating the Global Clinical Burden of Plasmodium falciparum Malaria in 2007. PLoSMed 7(6): e1000290. doi:10.1371/journal.pmed.1000290.

Hijmans, R.J., Cameron, S.E., Parra, J.L., Jones, P.G. & Jarvis, A. 2005. Very high resolution interpolated climate surfaces for global land areas. International Journal of Climatology 25: 1965-1978. Hulme, M., Doherty, R., Ngara, T., New, M. & Lister, D. 2001. African Climate Change: 1900-2100. Climate Research 17: 145-168.

ILRI. 2006. Mapping climate vulnerability and poverty in Africa. Report to the Department for International Development, ILRI, PO Box 30709, Nairobi 00100, Kenya. 200pp.

Imhoff, M.L., Bounoua, L., Ricketts, T., Loucks, C., Harriss, R. & Lawrence, W.T. 2004. Global patterns in human consumption of net primary production. Nature 429, 24 June 2004: 870-873.

IPCC. 2007a. Africa. In: Climate Change 2007: Impacts, Adaptation and Vulnerability. Contribution of Working Group II to the Fourth Assessment Report of the Intergovernmental Panel on Climate Change [Boko, M., I. Niang, A. Nyong, C. Vogel, A. Githeko, M. Medany, B. Osman-Elasha, R. Tabo and P. Yanda, (eds.)]. Cambridge University Press, Cambridge, UK, 433-467.

IPCC. 2007b. Appendix 1: Glossary. In: Climate Change 2007: Impacts, Adaptation and Vulnerability. Contribution of Working Group II to the Fourth Assessment Report of the Intergovernmental Panel on Climate Change. M.L. Parry, O.F. Canziani, J.P. Palutikof, P.J. van der Linden and C.E. Hanson (eds.). Cambridge University Press, Cambridge, UK.

IPCC, 2007c. Summary for Policymakers. In: Climate Change 2007: The Physical Science Basis. Contribution of Working Group I to the Fourth Assessment Report of the Intergovernmental Panel on Climate Change [Solomon, S., D. Qin, M. Manning, Z. Chen, M. Marquis, K.B. Averyt, M.Tignor and H.L. Miller (eds.)]. Cambridge University Press, Cambridge, United Kingdom and New York, NY, USA.

James, A.N., Green, M.J.B. & Paine, J.R. 1999. A Global Review of Protected Area Budgets and Staff. WCMC Biodiversity Series No. 10. World Conservation Monitoring Centre, Cambridge. 39pp.

Jones, P.G. & Thornton, P.K. 2009. Croppers to livestock keepers: livelihood transitions to 2050 in Africa due to climate changes. Environmental Science and Policy 12: 427-437.

Lieth, H. 1972. Modelling the primary productivity of the earth. Nature and resources. UNESCO, VIII, 2:5-10.

McKee, T.B., Doesken, N.J. & Kleist, J. 1993. The Relationship of Drought Frequency and Duration to Time Scales. Proc. 8th Conf. on Appl. Clim. 17-22. Jan 1993, Anaheim, CA 179-184.

Nelson, A. 2008. Accessibility Model and Population Estimates. Background paper for the World Bank's World Development Report 2009.

Oldeman, L.R., Hakkeling, R.T.A. & Sombroek, W.G. 1990. World Map of the Status of Human-Induced Soil Degradation; Explanatory Note. ISRIC and UNEP in cooperation with the Winand Staring Centre, ISSS, FAO and ITC. 27 pp.

OneWorld Sustainable Investments 2009. Regional Climate Change Programme: Southern Africa. Programme Memorandum for the Department for International Development CNTR 200607514. OneWorld Sustainable Investments, Cape Town.

Raleigh, Clionadh & Håvard Hegre. 2005. Introducing ACLED: An Armed Conflict Location and Event Dataset. Paper presented to the conference on 'Disaggregating the Study of Civil War and Transnational Violence', University of California Institute of Global Conflict and Cooperation, San Diego, CA, 7–8 March.

Rasmussen, J.B., Hansen, L.A., Burgess, N.D., Fjeldsa, J. & Rahbek, C. 2007. One degree resolution databases of the distribution of snakes in Sub-Saharan Africa. On-line data source: Zoological Museum, University of Copenhagen, Denmark.

Scharlemann, J.P.W., Kapos, V., Campbell, A., Lysenko, I., Burgess, N.D., Hansen, M.C., Gibss, H.K., Dickson, B. & Miles, L. 2010. Securing tropical forest carbon: the contribution of protected areas to REDD. Fauna & Flora International, Oryx 44(3): 352-357.

Shongwe, M.E., van Oldenborgh, G.J. & van den Hurk, B.J.J.M. 2009. Projected Changes in Mean and Extreme Precipitation in Africa under Global Warming. Part I: Southern Africa. J. Climate 22: 3819 – 3837.

Sutton, P.C., Elvidge, C.D. & Ghosh, T. 2007. Estimation of gross domestic product at subnational scales using night time satellite imagery. International Journal of Ecological Economics and Statistics, 507: 5-21.

United Nations Development Program. 2007. Human Development Report 2007/2008. UNDP, New York, 399pp.

UNISDR. 2009. Risk and poverty in a changing climate. 2009 Global Assessment Report on disaster risk reduction. United Nations International Strategy for Disaster Reduction Secretariat. Geneva, Switzerland.

Vörösmarty, C.J., Douglas, E.M., Green, P.A. & Revenga, C. 2005. Geospatial indicators of emerging water stress: An application to Africa. Ambio 34 (3): 230-236.

World Bank. 2006. World Development Indicators 2006. Washington D.C.

World Bank. 2007. World Development Indicators 2007. Washington D.C.

TECHNICAL REPORTS NO. 1

FUNDED BY

RCCP

UKaid
from the Department for International Development

Sida

oneWORLD
We build resilient futures